DIAGNOSING CHANGES IN THE NORTH ATLANTIC CIRCULATION USING A VERTICAL SECTION MODEL

JIE XU

DIAGNOSING CHANGES IN THE NORTH ATLANTIC CIRCULATION USING A VERTICAL SECTION MODEL

BY

JIE XU

A Thesis submitted to the School of Graduate
Studies in partial fulfillment of the
requirements for the degree of
Master of Science

Department of Physics
Memorial University of Newfoundland

June, 1992

St. John's Newfoundland

ISBN 0-315-78090-8

Abstract

A two-dimensional vertical section model is described. The model takes density data along a section as input and calculates the velocity through the section referenced to the bottom. We have used it to analyse changes in the circulation of the North Atlantic by taking as input the objectively analysed density data of Levitus(1982,1989) for the climatological annual mean and for the pentads 1955-59 and 1970-74.

Sections along 55.5^oW, 64.5^oW, 54.5^oN and 23.5^oN have been considered and estimates of the poleward heat transport through 54.5^oN and 23.5^oN have been made. Ekman transports are calculated using the Hellerman and Rosenstein(1983) wind stress field and wind stress analysed by da Silva and Levitus for the period 1945-1989. At 54.5^oN, mass balance is achieved by combining with the absolute transport calculations of Greatbatch et al.(1991), giving values for the poleward heat transport of $0.6PW$, $0.7PW$ and $0.5PW$ for the climatological annual mean and the pentads 1955-59 and 1970-74, respectively. The estimated error is $\pm 0.2PW$. These values compare well with previous estimates obtained using surface heat flux calculations and suggest that the poleward heat transport in 1970-74 may have been marginally less than in 1955-59. We have performed a similar calculation for 23.5^oN, this time by requiring mass balance through the section assuming that the northward transport and flow temperature of the

Florida Current was the same in each pentad and equal to the climatological annual mean value, an assumption we believe to be justified. The calculated heat transports are $1.2PW$, $1.0PW$ and $0.8PW$ for the climatological annual mean and the pentads 1955-59 and 1970-74, respectively, with an error of $\pm 0.3PW$. The climatological value agrees with previous estimates at this latitude and there is again the suggestion that the 1970-74 value is less than the others, particularly in comparison with the climatological annual mean. Along $54.5°N$, the reduced heat transport in 1970-74 is attributed to a deeper North Atlantic Current and a warmer return flow in the Labrador Sea. Along $23.5°N$, on the other hand, the southward flow over the interior of the North Atlantic is more surface confined in 1970-74 than in the climatological case.

Other results concern the vertical distribution of the absolute transport changes diagnosed by Greatbatch et al.(1991). Along $55.5°W$, the transport of the Gulf Stream referenced to the bottom was some $30Sv$ less in 1970-74 than in 1955-59, a change comparable in magnitude to that found by Greatbatch et al.(1991). However, the maximum change found by Greatbatch et al. is displaced to the south of that referenced to the bottom, indicating the importance of changes in bottom velocity. Greatbatch et al. also considered a case in which the density below 1500 m is assumed to have remained unchanged between the pentads, and diagnosed a transport change for the Gulf Stream of over $20Sv$. On the other hand, the change in transport referenced to and above 1500m is only $7Sv$, in-

dicating that even in this case, changes in bottom velocity play an important role. There is a suggestion in the model results that in the 1970-74 pentad, the northern recirculation gyre of the Gulf Stream was weaker than in both 1955-59 and the climatological case.

Acknowledgements

I could not possibly name all those who have contributed to my understanding of oceanography, but several mentors deserve special mention: Richard Greatbatch, Brad deYoung, Alex Hay and Kevin Lamb, from whom I learned not only oceanography but scientific discipline.

Richard Greatbatch and Brad deYoung guided me through graduate school, providing support and encouragemant at crucial juncture. Especially Richard Greatbatch patiently reviewed my early cumbersome manuscript for many times which resulted in numerous important revisions.

I am also grateful to Syd Levitus for providing his density fields, to Arlindo Moraes da Silva for providing us with the da Silva and Levitus wind stress fields, and to Andrew Weaver for his encouragement on first hearing of our heat transport results. Ying Ren provided assistance with the graphics, Allan Goulding helped in dealing with computer problems and Gus Fanning helped in providing wind stress data.

This work has been carried out with support from the Networks of Centres of Excellence program of the Natural Science and Engineering Research Council of Canada through the Ocean Production Enhancement Network (OPEN). Support from the NSERC Collobarative Research Initiative Programme in support of Canadian university activities in the World Ocean Circulation Experiment

(WOCE) is also acknowledged.

Finally, I would like to thank my parents and my brother for their support and encouragement.

Contents

List of Figures

List of Tables

Chapter 1

Introduction

The North Atlantic has been subjected to intensive study and most of its general circulation patterns have been discovered. The salient feature is the two gyres, one is the subtropical gyre, which is anticyclonic (clockwise in the northern hemisphere), another is the subpolar gyre, which is cyclonic (anticlockwise in the northern hemisphere).

A schematic chart of the surface current is shown in Fig. 1.1, following that presented by Sverdrup et al (1942) and discussed by Stommel (1965). A clockwise gyre can be easily identified and is conventionally called the subtropical gyre. It starts with the North Equatorial Current. As this current flows to the west, it is joined from the south by the South Equatorial Current, part of which crosses the equator into the North Atlantic. The combined flow splits into two parts when it reaches the Caribbean Islands. One, which flows on the north side is

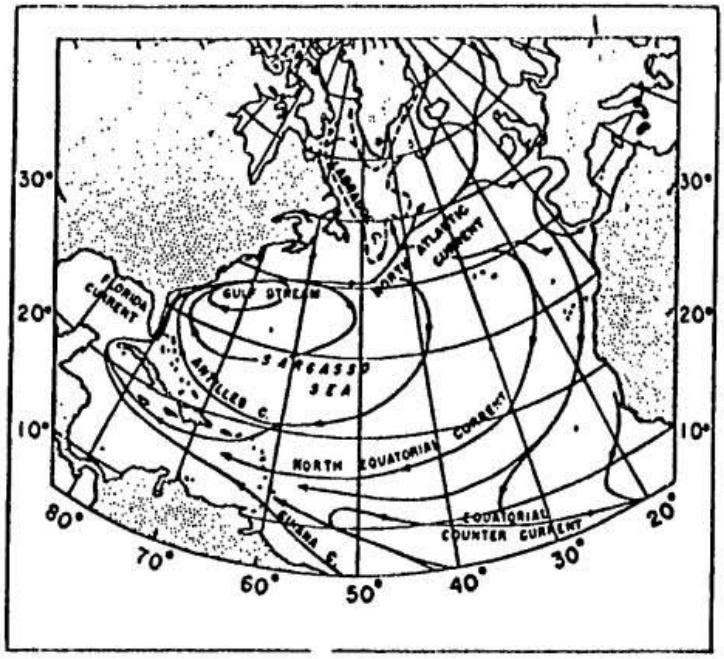

Figure 1.1: *Chart showing the chief features of the surface-water circulation of the North Atlantic circulation, according to Sverdrup et al (1942, fig. 187).*

called Antilles Current, whereas another flows on the south side into the Gulf of Mexico and, from there, escapes between Florida and Cuba to become the Florida Current. The Florida Current meets the Antilles Current off the coast of Florida to become the Gulf Stream and the combined current continues to flow north-east alongshore until it reaches about Cape Hatteras, where the current breaks away from the North American coast. The Gulf Stream then flows north-east towards the tail of Grand Banks of Newfoundland at about $40°N$, $50°W$. From there, part of the flow turns southward to close the gyre system, whereas the other part continues to go northeast, which is called the North Atlantic Current. This current also divides as it flows northeast, with part of the North Atlantic Current flowing between Scotland and Iceland to join the circulation of the Norwegian,

Greenland and Arctic Seas, part turning south past Spain and North Africa to complete the subtropical gyre and to feed into the North Equatorial Current, and with the remainder flowing westward on the southern side of Iceland, in what is called the Irminger Current. Off the southern coast of Greenland, this current is joined by the East Greenland Current. The circuit of the gyre is completed to the west by a branch of the Labrador Current (probably offshore from the shelf break).

This shallow circulation in the North Atlantic is primarily wind-driven in most regions and has been studied and interpreted by numerous authors. Sverdrup (1947) showed how the main features of the equatorial surface currents could be attributed to the wind as a driving agent. In 1948, Stommel explained the westward intensification of the wind-driven circulation. Combining most previous work, Munk (1950) obtained analytic expressions which qualitatively described the main features of the wind-driven circulation in terms of the observed wind field.

Although wind driving probably dominates the shallow circulation, to about 800 m or so, the effects of density changes, in driving what is called the 'thermohaline' circulation, is also very important, playing the dominant role in the deep circulation. For the North Atlantic, when warm salty water spreads into the northern North Atlantic, it is cooled by both sensible and latent heat loss. This cooled salty water sinks to the deep ocean, forming the North Atlantic

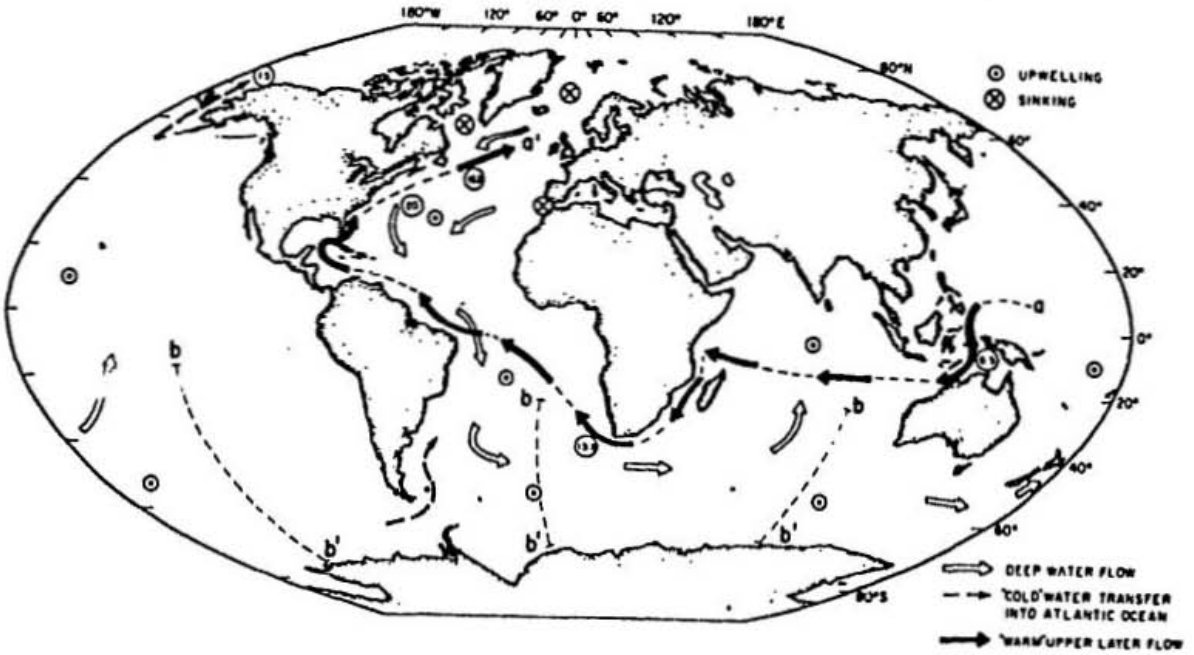

Figure 1.2: *Chart showing the global stucture of the thermohaline circulation cell associated with NADW production. The circled values are volume flux in Sverdrup which are expected for uniform upwelling of the NADW with a production rate of 20 Sverdrup. Adapted from Gordon, 1986, Fig. 2a.*

Deep Water (NADW). The NADW from the two northern sites (Labrador Sea and the Greenland Sea - Norwegian Sea overflow) moves southward within the deep layer, in what is called the Deep Western Boundary Undercurrent, while the warm salty upper layer water is drawn into the northern North Atlantic, forming the general pattern of the thermohaline circulation. As NADW moves southward, it gradually rises over most of the middle and low latitude areas of North Atlantic. Gordon (1986) pointed out that NADW may spread and upwell throughout the Atlantic Ocean and is exported to the Indian and Pacific Oceans by the Antarctic Circumpolar Current, returning water to the upper layer within the Antarctic region and into the thermocline (fig. 1.2). The upper layer water then returns to the Atlantic Ocean from two possible routes - Drake Passage from the Pacific or the south of Africa from the Indian Ocean, closing an extraordinary loop after a journey through the world ocean. Because of the difficulty of making measurements in the deep water, the thermohaline circulation is much less well known and less well described dynamically than the upper-layer circulation. However, the thermohaline circulation is now being given widespread attention by oceanographers due to its possible important role in generating variability on time scales of decades to thousands of years (e.g. Gordon, Zebiak and Bryan, 1992) and in transfering heat in north-south direction.

It has long been known that incoming solar energy exceeds outgoing infrared energy at low latitudes while the reverse is true at high latitudes. However, the

heat surplus at low latitudes and the heat deficit at high latitudes have been brought into balance, thanks to the poleward heat transfer in the atmosphere and ocean. Although the mechanisms for this heat transport have been studied for over a century, the relative importance of sea and air as the predominant heat transfer medium had been discussed throughout the period. In 1856, M.F.Maury expressed the view that the sea was primarily responsible for maintaining the global energy balance. Later in 1933, Bjerknes, Solberg and Bergeron (1933) regarded the contributions of sea and stratosphere as negligible and assigned the leading role in transferring heat to the troposphere. In recent years, the work of VonderHaar and Oort, 1973, and Oort and VonderHaar, 1976, indicated that the ocean carries more heat than was previously suspected, and thus stimulated much recent interest in the subject of meridional heat flux by the ocean. It is, therefore, of interest to estimate the poleward heat transport through various sections in North Atlantic.

Historically, there are several methods for calculating ocean heat transport. The traditional method, i.e. the surface heat balance method, is to examine air-sea exchanges of all types of heat energy to calculate the local sources and sinks, and then integrate over an entire polar cap extending from the pole to a fixed latitude to obtain the poleward heat flux necessary to maintain equilibrium. More recently, calculations have been made by the so called direct method, using knowledge of heat content and mass transport by the ocean (e.g., Bryan, 1962

and Hall and Bryden, 1982). In the past, the direct method has been the least used yet has also been given more and more attention. It is this method we have used to estimate heat transport through various sections in the North Atlantic. The details will be elaborated later.

Our knowledge of the interannual variability in the large-scale circulation of the North Atlantic is much more limited than the general picture of the circulation given earlier. Only in recent years has the magnitude and importance of this variability come to be appreciated (Gordon, Zebiak and Bryan, 1992). For example, in recent series of papers, Levitus (1989a,b,c,1990) has shown that the thermohaline structure of the North Atlantic underwent some remarkable changes between the two pentads 1955 - 1959 and 1970 - 1974. He found that, on constant-depth surfaces, the subtropical gyre(500-1300m) of the North Atlantic was colder and fresher during 1970-1974 compared to 1955-1959, with characteristic magnitudes of temperature and salinity decreases of order of several tenths of a degree centigrade and $0.025 - 0.10\ ^{0}/_{00}$, respectively. At intermediate depths the eastern portion of the subpolar gyre was also colder and fresher during the 1970-1974 pentad whereas the western portion of the subpolar gyre exhibited higher temperatures and salinities during 1970-1974 compared to 1955-1959, with characteristic magnitudes of temperature and salinity changes similar to those observed in the subtropical gyre (fig. 1.3). In the tropics, there were increases in temperature and salinity, yet with magnitudes smaller than those in the subtropical and subpolar

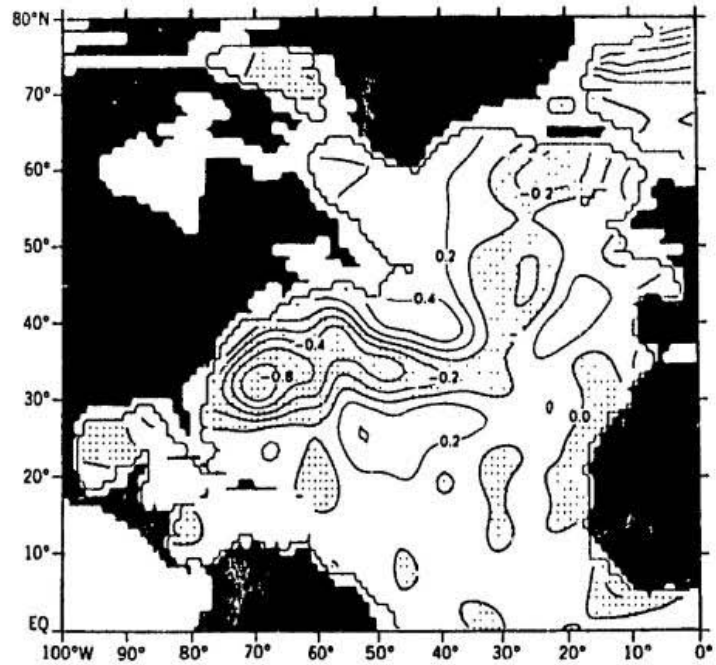

Temperature difference (in degrees Celsius) for 1970–1974 minus 1955–1959 at 1000-m depth. Dot shading indicates negative values.

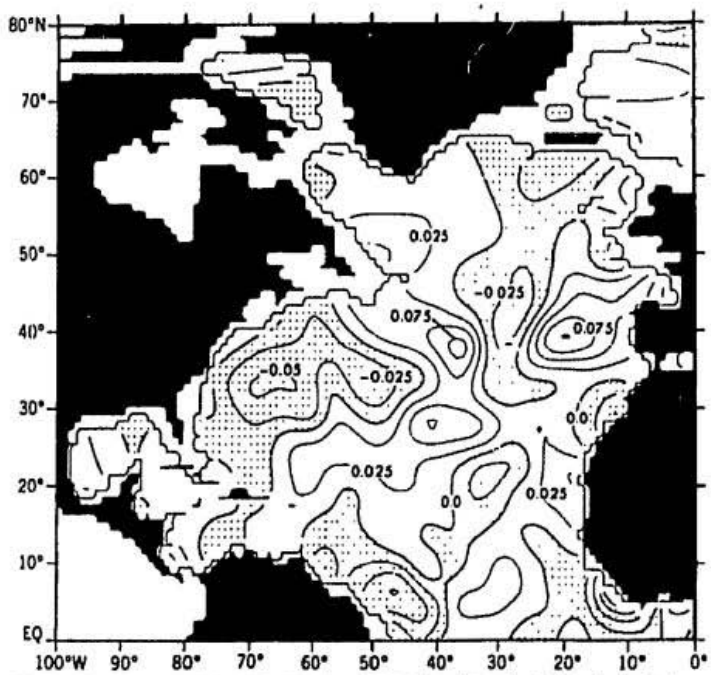

Salinity difference (per mil) for 1970–1974 minus 1955–1959 at 1000-m depth. Dot shading indicates negative values.

Figure 1.3: *Temperature (in degrees Celsius) and salinity (per mil) differences for 1970-1974 minus 1955-1959 at 500-m depth, according to Levitus (1989c, fig. 7, 8)*

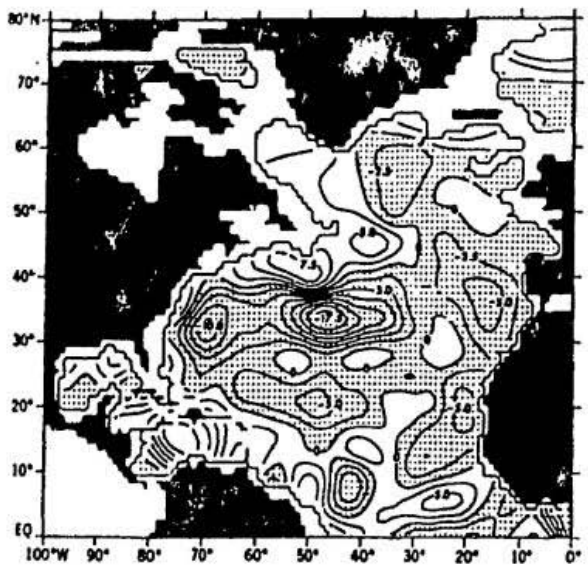

Figure 1.4: *Steric sea level differences in units of dynamic centimeters (1 dynam = 1000 $cm^2 s^{-2}$) for 1970-1974 minus 1955-1959 for the 0- to 1500-m depth interval, according to Levitus (1990, fig. 4).*

gyres. Comparing 1970-74 with 1955-59, potential density surfaces were found to have risen in the subtropical gyre, which is consistent with the relatively large changes in temperature and salinity on constant-depth surfaces in the subtropical gyre. Upward displacements of approximately 25m occurred for surfaces below the 26.9 $kg\ m^{-3}$ potential density surface. Maximum displacements of any surfaces were approximately 175m, which occurred for the 26.5 $kg\ m^{-3}$ potential density surface. In contrast to the shoaling which occurred in the subtropics. isopycnals in the western portion of the subpolar gyre, immediately to the north of the Gulf Stream and south of Atlantic Canada, increased in depth by as much as 100m. These changes suggest a substantial weakening of the Gulf Stream during 1970-1974 compared to 1955-1959.

A calculation of interpentadal variability of the steric sea level and geopotential thickness of the North Atlantic Ocean also reveals large changes. The geopotential thickness is defined as the vertical distance between two isobaric surfaces and depends on the density of the water in between. For two isobaric surfaces p_2 (upper) and p_1 (lower), the geopotential thickness is:

$$\Phi_2 - \Phi_1 = -\int_{p_1}^{p_2} \alpha dp \tag{1.1}$$

where α is the specific volume ($\alpha = 1/\rho$). If the upper surface is the free surface, then the departure in this thickness from a standard reference thickness is called the steric sea level. Levitus showed that, comparing 1970-1974 to 1955-1959 for the 0- to 1500-m depth interval, steric sea level underwent substantial changes (fig. 1.4). The steric sea level decreased by up to 17.5 dyn cm in the east central portion of the subtropical gyre, whereas in the western part of this gyre, differences are of the order of 10.0 dyn cm. The eastern boundary of the Atlantic Ocean exhibited sea level decreases on the order of several centimeters(5 dyn cm) between the 1970-1974 and 1955-1959 pentads. However, in the western subpolar gyre(north of the Gulf Stream and south of Atlantic Canada) steric sea level increased by an amount up to 7.5 dyn cm.

Further work has been carried out by Greatbatch et al.(1991). These authors attempted an inference of the change in volume transport between the pentads using diagnostic calculations of the circulation in the North Atlantic, following the diagnostic model of Mellor et al.(1982). The model calculates transport

from specified density and wind stress fields by integrating westwards along f/H contours from the eastern boundary, where a condition of no transport normal to the boundary is applied. Here f is the Coriolis parameter and H is the depth of the ocean. The model is arranged on a $1^0 \times 1^0$ grid for the North Atlantic Ocean using realistic bottom topography, wind forcing and density data. The density data used in the calculations were that of Levitus(1982,1989a,b,c:1990) and the wind stress was derived from the Comprehensive Ocean Atmosphere Data Set (COADS) by da Silva(1991). They studied three basic cases: the climatological mean state and the pentads 1955-1959 and 1970-1974. From their results, they showed that the transport of the diagnosed Gulf Stream is some 30 Sv less for the 1970-1974 pentad than for the 1955-1959 pentad, 20 Sv of which being due to a dramatic decrease in the strength of the diagnosed subtropical gyre (fig. 1.5). This 30 Sv change is roughly one-third of the total climatological mean transport through 55^oW estimated by Richardson (1985). Although roughly half this transport change was attributed to density changes in water below 1500m depth and, as such, may not be reliable, even a change of 15-20 Sv is significant. Wind stress was found to play very little role in the calculation of the transport change between the pentads. Almost all the information was contained in the density field.

Given the large changes in the thermohaline structure at the North Atlantic between 1955-1959 pentad and 1970-1974 pentad, it is clearly of interest to ex-

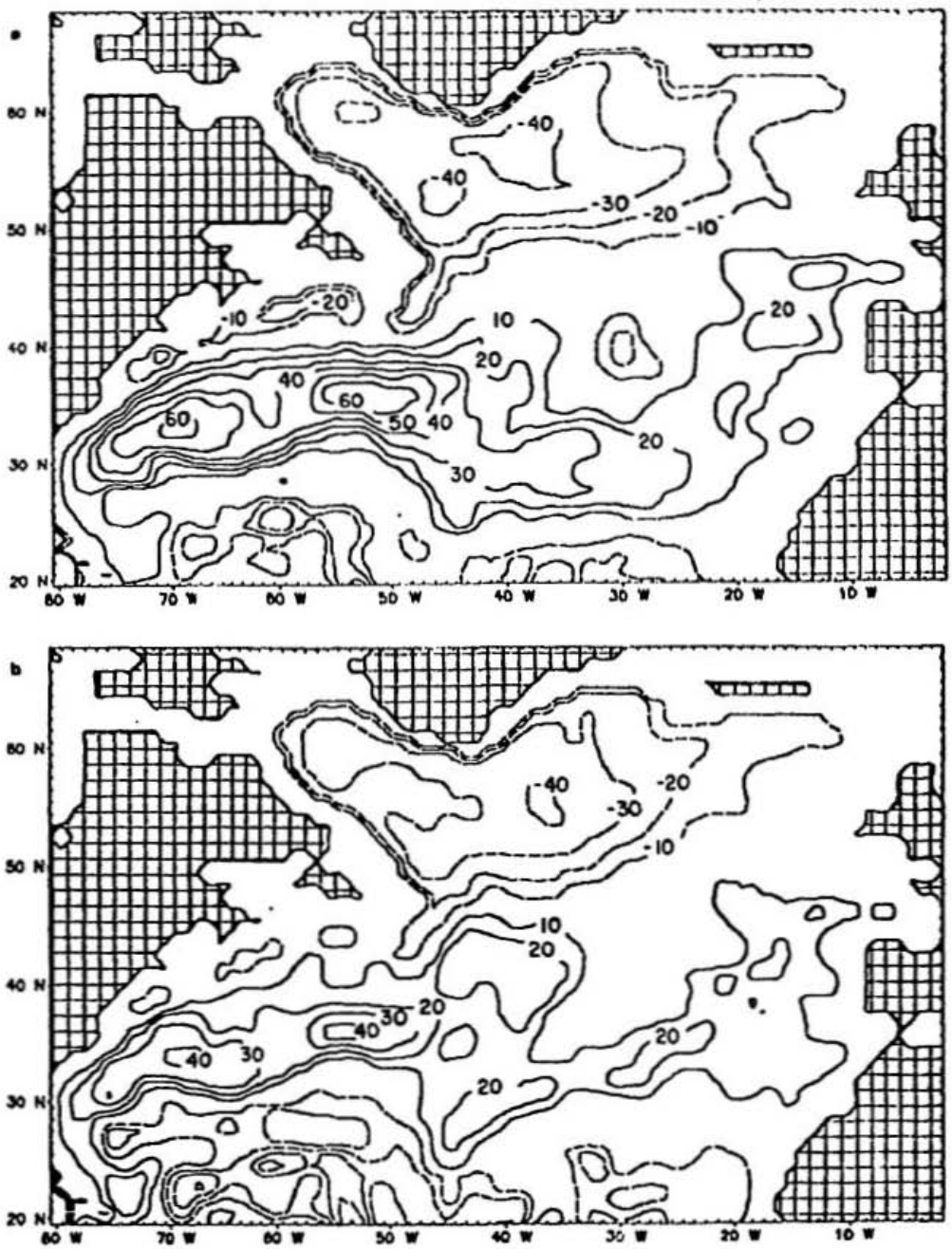

Figure 1.5: *Transport streamfunction calculated using (a) 1955-1959 wind and density data (b) 1970-1974 wind and density data, according to Greatbatch et al.(1991, fig. 9). The contour interval is 10 Sv and the zero contour is not drawn. Dashed contours indicate negative values; solid contours, positive values.*

amine the vertical structure of the transport change diagnosed by Greatbatch et al.(1991). For example, how much of the transport change takes place referenced to the bottom or referenced to some assumed level of no motion, as in the calculations of Worthington(1976,1977) ? How much did the poleward heat transport change between the pentads? The question arises as to whether or not these changes are fundamentally wind-driven or whether they arise as a result of changes in the thermohaline circulation of the North Atlantic. Recently, Weaver and Sarachik(1991) have shown that the Bryan-Cox ocean general circulation model (Bryan, 1969; Cox, 1984) exhibits decadal time scale oscillations in its thermohaline circulation when run in an idealised ocean basin using 'mixed' boundary conditions, corresponding to having a fixed atmospheric state. A decadal variation in the poleward heat transport is a feature of their results. If such variations occur in reality, they could be expected to have an effect on the overlying atmosphere and this could, in turn, feed back to the ocean. Indeed, decadal oscillations in both globally averaged and Northern Hemisphere averaged surface air temperature have been noted (Ghil and Vautard, 1991). Viewed together, these results suggest that decadal oscillations may be a feature of the coupled-ocean atmosphere system, as originally suggested by Bjerknes(1964), and are therefore of considerable interest from the point of view of climate variability.

In this thesis, we develop a two dimensional, density-stratified model to study the development of currents, volume transport, heat transport and sea level across

a section of either latitude or longitude in order to try and answer some of the questions posed above. The model is a generalization of the standard geostrophic velocity computation. It takes density data on a vertical section as input and calculates the velocity field through the section referenced to the bottom. Sections along $55.5^{o}W$, $23.5^{o}N$ and $54.5^{o}N$ have been considered and calculations of the poleward heat transport through $23.5^{o}N$ and $54.5^{o}N$ have been made, using data for the climatological annual mean and for the pentads 1955-59 and 1970-74 from Levitus(1982; 1989a,b,c). At $54.5^{o}N$, the non-zero bottom velocities required to achieve mass balance are obtained using the absolute transport calculations of Greatbatch et al.(1991) and at $23.5^{o}N$ using data from the Florida Straits (Niiler and Richardson,1973; Larsen, 1992). In addition to the Hellerman and Rosenstein(1983) wind stress field (used in the climatological annual mean case to estimate the Ekman transport), wind stress fields analysed by da Silva and Levitus (personal communication) are used.

The plan of this thesis is as follows. In chapter 2 we describe the model and its formulation. In chapter 3 we present diagnostic results obtained using the objectively analysed density data of Levitus(1982,1989a,b,c,1990). Finally, chapter 4 provides a summary and discussion.

Chapter 2

The Model

In this chapter we derive the basic equations of the model and discuss their validity. The methods for calculating volume transport, heat transport and sea level are also presented.

2.1 The Governing Equations

The model is a two-dimensional vertical section model. It assumes an infinite extent perpendicular to the section with no variability along that direction. We include vertical mixing of momentum and bottom friction in the model formulation in order to show that in a two-dimensional setting, it is natural to calculate the velocity through the section referenced to the bottom. This is a simple generalisation of the steric sea level method described by Csanady(1979). It should be noted, however, that there is no significant difference between model-calculated

velocities through the section and geostrophic velocities calculated referenced to the bottom.

We shall consider two cases : one in which the section is along a line of longitude and the other in which it is along a line of latitude. In the case of a line of longitude, the equations governing the model are

$$-fv = \frac{\partial \tau^{xz}}{\partial z} \tag{2.1}$$

$$fu = -\frac{1}{a\rho_0}\frac{\partial p}{\partial \phi} + \frac{\partial \tau^{yz}}{\partial z} \tag{2.2}$$

$$0 = -\frac{\partial p}{\partial z} - g\rho \tag{2.3}$$

$$\frac{1}{a\cos\phi}\frac{\partial}{\partial \phi}\left\{v\cos\phi\right\} + \frac{\partial w}{\partial z} = 0 \tag{2.4}$$

whereas along a line of latitude, the equations are

$$-fv = -\frac{1}{a\rho_0\cos\phi}\frac{\partial p}{\partial \lambda} + \frac{\partial \tau^{xz}}{\partial z} \tag{2.5}$$

$$fu = \frac{\partial \tau^{yz}}{\partial z} \tag{2.6}$$

$$0 = -\frac{\partial p}{\partial z} - g\rho \tag{2.7}$$

$$\frac{1}{a\cos\phi}\frac{\partial u}{\partial \lambda}+\frac{\partial w}{\partial z}=0 \tag{2.8}$$

Here λ is longitude, ϕ is latitude, z is the vertical coordinate measured upwards with $z = 0$ at the sea surface and $z = -H$ at the ocean bottom; $H = H(\lambda, \phi)$ is the depth of the ocean; u, v, and w are the velocities in the λ, ϕ and z directions, respectively; a is the radius of the earth; ρ_0 is a representative value for the density of sea water; p is the pressure; ρ is the specified density; (τ^{xz}, τ^{yz}) are turbulent Reynold's stresses and g is the acceleration due to gravity.

Among the two sets of equations, (2.1), (2.2), (2.5) and (2.6) are the horizontal momentum equations, (2.3) and (2.7) are the hydrostatic equation, and (2.4) and (2.8) are the continuity equations. In the horizontal momentum equations ((2.1), (2.2) and (2.5), (2.6)), the balance is between the Coriolis force, the horizontal pressure gradient force and the vertical mixing of momentum.

It should be noted that the local time-derivative, non-linear advection and horizontal Reynolds stress gradient terms have been omitted from the momentum equations (2.1), (2.2), (2.5) and (2.6). This means that we are working with the minimum set of equations consistent with the assumption that the dominant balance is geostrophy, but which also include vertical mixing.

The problem of parameterization of bottom stress in terms of the properties of mean flow has often been discussed. Usually, the bottom stress can be fairly accurately determined from a quadratic drag law involving the actual near-

bottom velocity - the velocity above a thin wall layer. For a steady state or long-time-scale model, where many high frequency flows have been averaged, the parameterization of bottom stress may be shown to reduce to a linear formula, i.e. the shear stress equals a constant (of the dimension of velocity) times the near-bottom velocity (see Csanady, 1982). In this thesis, a parameterization of bottom stress in terms of bottom velocity, using a linear stress law, is used, i.e.

$$\frac{(\tau_b^{xz}, \tau_b^{yz})}{\rho_0} = r(u_b, v_b) \tag{2.9}$$

where $(\tau_b^{xz}, \tau_b^{yz})$ is the bottom stress, $(u_b, v_b) = (u, v)$ evaluated at bottom $z = -H$ and r is the (linear) bottom friction coefficient.

When assuming zero surface wind stress, for both sets of equations, the boundary conditions at the sea surface ($z = 0$) and ocean bottom ($z = -H$) are

$$(\tau_s^{xz}, \tau_s^{yz}) = (0, 0) \tag{2.10}$$

and

$$(\tau_b^{xz}, \tau_b^{yz}) = r(u_b, v_b) \tag{2.11}$$

respectively. Here $(\tau_s^{xz}, \tau_s^{yz})$ is the surface stress.

The rigid-lid approximation at $z = 0$ and the kinematic condition at $z = -H$ give,

$$w = 0 \qquad at \quad z = 0$$

$$w = -(uH_x + vH_y) \qquad at \;\; z = -H \tag{2.12}$$

We shall now work with the equations (2.5)-(2.8), i.e. a section along a line of latitude. Similar results are valid for the system (2.1)-(2.4). Let us begin by vertically integrating (2.8) using (2.12) to give

$$\frac{\partial U}{\partial \lambda} = 0$$

where

$$(U, V) = \left(\int_{-H}^{0} u dz, \int_{-H}^{0} v dz \right)$$

is the vertically integrated volume transport. It follows that if either the eastern or western boundary is a coastline, as will always be the case in this thesis, then

$$U = 0 \tag{2.13}$$

We can also vertically integrate (2.6) using (2.10), (2.11) and (2.13) to obtain

$$u_b = 0 \tag{2.14}$$

where u_b is the velocity through the section at the bottom.

Similarly, in the case of the section along a line of longitude (eqns.(2.1)-(2.4)),

$$V = 0 \tag{2.15}$$

(provided there is a coastline at one end of the section) and hence

$$u_b = 0 \tag{2.16}$$

Equations (2.14) and (2.16) show that the assumption of no variations perpendicular to the section leads naturally to the conclusion that velocities should be referenced to the bottom. Of course in reality, bottom velocities are unlikely to be zero. To allow for non-zero bottom velocities, variations in the direction perpendicular to the section must be considered; e.g. by using a model formulated in three-dimensions, such as that of Mellor et al.(1982). In chapter 3, results from our two-dimensional, vertical-section model will be combined with the diagnostic calculations of Greatbatch et al.(1991) in order to estimate transport associated with non-zero bottom velocities. It should be noted that our model is very similar to that of Csanady(1979) which was used by him to calculate steric sea level in the Mid-Atlantic Bight, Scotian Shelf and Grand Banks regions of the eastern seaboard of North America. The only difference is in the parameterisation of the bottom friction which in the case of Csanady was in terms of either bottom geostrophic velocity (the case most similar to ours) or vertically averaged velocity.

The set of equations have been closed and, next, we move on to the algorithm of solution.

2.2 The Method of Solution

The solution procedure is similar to that used by Lynch et al.(1992) and Greatbatch and Goulding(1992) and requires the use of a simple parameterisa-

tion for the vertical mixing of momentum. To do this, we shall use a uniform vertical eddy viscosity coefficient. It should be noted, however, that this is not important for the results we present since the calculated velocities do not differ significantly from geostrophic velocities referenced to the bottom. We first separate the pressure term p into two parts, one due to surface pressure and another due to the non-uniform density of the fluid column, using (2.3)/(2.7) by writing

$$p = p_s + p' \tag{2.17}$$

where

$$p' = -g\int_z^0 \rho dz \tag{2.18}$$

and p_s is the pressure at $z = 0$. We then write the momentum equations((2.1), (2.2), (2.5), (2.6)) in the form

$$ifq - \frac{\partial}{\partial z}\left\{\nu\frac{\partial q}{\partial z}\right\} = R + G \tag{2.19}$$

where $i = \sqrt{-1}$ and $q = u + iv$. In the case of (2.1) and (2.2),

$$R = -\frac{i}{a\rho_0}\frac{\partial p'}{\partial \phi} \tag{2.20}$$

and

$$G = -\frac{i}{a\rho_0}\frac{\partial p_s}{\partial \phi} \tag{2.21}$$

In the case of (2.5) and (2.6)

$$R = -\frac{1}{a\rho_0 \cos\phi}\frac{\partial p'}{\partial \lambda} \tag{2.22}$$

and

$$G = -\frac{1}{a\rho_0 \cos\phi}\frac{\partial p_s}{\partial \lambda} \tag{2.23}$$

with surface and bottom boundary conditions

$$\begin{aligned} \nu q_z &= 0 \qquad at \;\; z = 0 \\ \nu q_z &= rq \qquad at \;\; z = -H \end{aligned} \tag{2.24}$$

where both R and G are complex. G is that part of the horizontal pressure gradient due to the gradient of pressure at $z = 0$. R is that part which arises from the density stratification.

We now follow a procedure similar to that used by Lynch et al. (1992) and define q_1 and q_2 by:

$$\begin{aligned} if q_1 &= R + (\nu q_{1z})_z \\ \nu q_{1z} &= 0 \qquad at \;\; z = 0 \\ \nu q_{1z} &= r q_1 \qquad at \;\; z = -H \end{aligned} \tag{2.25}$$

and

$$if q_2 = 1 + (\nu q_{2z})_z$$

$$\nu q_{2z} = 0 \quad at \quad z = 0 \tag{2.26}$$

$$\nu q_{2z} = r q_2 \qquad at \quad z = -H$$

It should be noted that, given the density field, R can be calculated using (2.18) and either (2.20) or (2.22), from which it follows that both q_1 and q_2 are known quantities that can easily be calculated.

Since G is independent of the vertical coordinate, and since (2.19) is a linear equation, q can be written in terms of q_1 and q_2 as

$$q = q_1 + G q_2 \tag{2.27}$$

where q_1 is the solution to (2.19) with forcing R and Gq_2 is the solution with forcing G. The problem is now to determine the unknown G.

To do this, we begin by vertically averaging equation (2.27) to give

$$\bar{q} = \bar{q}_1 + G\bar{q}_2 \tag{2.28}$$

where an overbar indicates vertical average. Using (2.13) or (2.15), whichever appropriate, it now follows that G can be expressed in terms of q_1, q_2 and the vertically averaged flow through the section. For example, if the section is along a line of latitude (equations (2.5)-(2.8)),

$$G = \left\{(0, \bar{v}) - \bar{q}_1\right\} / \bar{q}_2 \tag{2.29}$$

where

$$(\bar{u}, \bar{v}) = \frac{1}{H}\left(\int_{-H}^{0} u dz, \int_{-H}^{0} v dz\right)$$

is the vertically averaged velocity. Substituting into (2.27) then gives

$$q = q_1 + \frac{q_2}{\bar{q}_2}\left\{(0, \bar{v}) - \bar{q}_1\right\} \tag{2.30}$$

Evaluating (2.30) at $z = -H$ now gives an expression for the bottom velocity, $q_b = (u_b, v_b)$, and hence the bottom stress, $(\tau_b^x, \tau_b^y)/\rho_0 = r(u_b, v_b)$, in terms of the known quantities q_1, q_2 and the unknown $\bar{v}$. In the case of a line of latitude,

$$v_b = Im(q_b) = v_1 + u_2\bar{v} \tag{2.31}$$

where u_1, u_2, v_1, v_2 are all real and given by,

$$\begin{aligned} u_1 + iv_1 &= (q_1 - q_2\bar{q}_1/\bar{q}_2)_b \\ u_2 + iv_2 &= q_{2b}/\bar{q}_2 \end{aligned} \tag{2.32}$$

and the subscript "b" denotes evaluation at $z = -H$.

We now use (2.14) to set $v_b = 0$. $\bar{v}$ can now be calculated from (2.31),

$$\bar{v} = -\frac{v_1}{u_2} \tag{2.33}$$

Subsequently, G can be obtained by eqn (2.29) and then substitute into (2.27) to obtain the velocity field (u, v).

Similarly for a section along a line of longitude, $V = 0$ and, as above, we obtain

$$u_b = Real(q_b) = u_1 + u_2\bar{u} \tag{2.34}$$

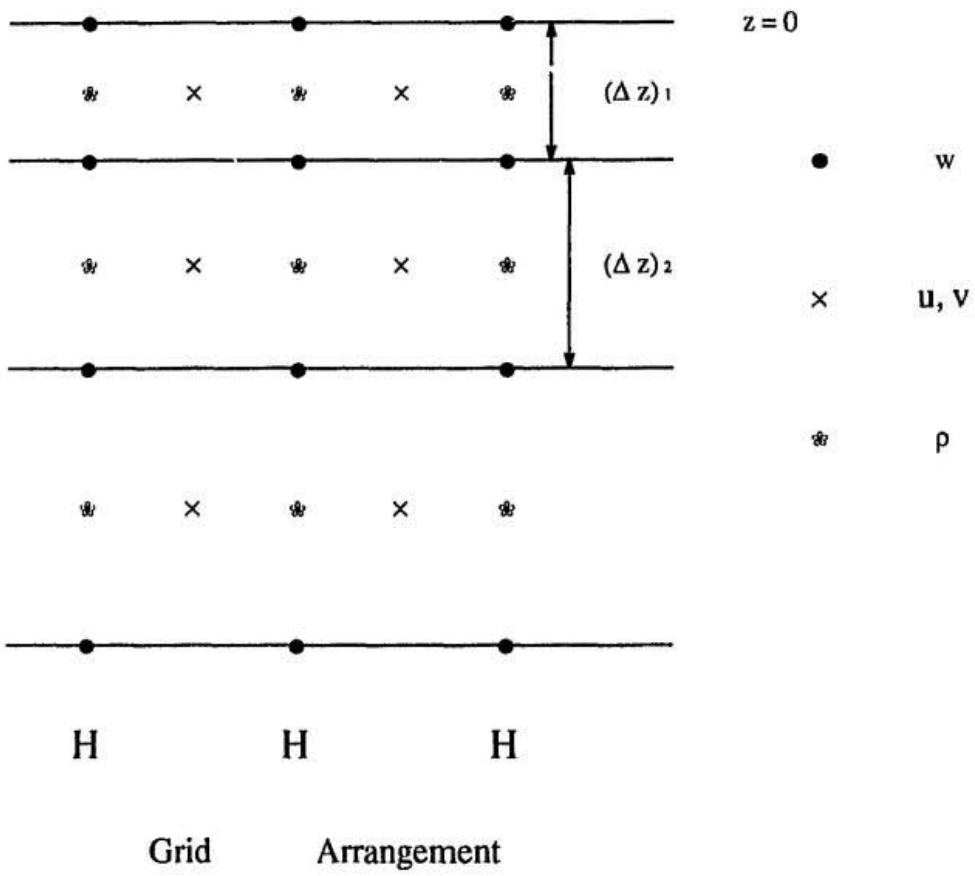

Figure 2.1: *Grid Arrangement*

and, putting $u_b = 0$ from (2.16), we obtain,

$$\bar{u} = -\frac{u_1}{u_2} \tag{2.35}$$

To solve q_1 and q_2 (and hence (u, v)), a finite difference scheme employing centred-differencing is used. The grid arrangement of the dependent variables u, v, w and ρ is shown in Fig. 2.1. In the horizontal, the w, ρ, and H are stored in the same grid point, with the u, v point stored in between. In the vertical, only w is stored at the edge of each z level, whereas u, v, *and* ρ are stored at the middle point of each z level. When values of H at (u, v) is needed for the calculation of

velocity field, two point averaging is employed. In all the calculations, uniform grid spacing is used in both the horizontal and vertical directions.

The total velocity field has now been solved. We can, therefore, further derive the volume transport, heat transport(provided the potential temperature field is known) and steric sea level, which will be elaborated in next section.

2.3 The Calculation of Volume Transport, Heat Transport and Steric Sea Level

It is straightforward to calculate the volume transport through the section. In case of a line of latitude, the volume transport $M(\lambda)$ is given by

$$M(\lambda) = \int_{\lambda_e}^{\lambda} \int_{-H}^{0} v dz \; a \cos\phi d\lambda \tag{2.36}$$

where λ_e is the longitude at the eastern boundary. The integration of z is from $-H$ to 0, i.e. from the bottom to the surface. The integration of λ is from eastern boundary. Integrating the volume transport from the eastern boundary to western boundary gives the total volume transport through the section.

Similarly, volume transport through a section of longitude $M(\phi)$ is given by,

$$M(\phi) = -\int_{\phi_n}^{\phi} \int_{-H}^{0} u dz \; a d\phi \tag{2.37}$$

where ϕ_n is the latitude at the northern boundary. The integration of ϕ is from

northern boundary. Integrating the volume transport from northern boundary to southern boundary gives the total volume transport through the section.

Taking u and v in (2.36) and (2.37) to be the velocity calculated by our model, M will be the (geostrophic) transport referenced to the bottom that is associated with the density field. We shall call this transport M_T. When we discuss the mass balance for a section of latitude, we shall also estimate the Ekman transport (M_{EK}) through the section due to the surface wind stress and the transport associated with non-zero bottom velocity (M_B). Therefore the absolute volume transport M is split into three parts,

$$M = M_T + M_B + M_{EK} \tag{2.38}$$

with

$$M_{EK} = -\int_{\lambda_e}^{\lambda_w} \frac{\tau_\lambda}{\rho f} a cos\phi dz d\lambda \tag{2.39}$$

and

$$M_B = \int_{\lambda_e}^{\lambda_w} v_b \int_{-H}^{0} a cos\phi dz d\lambda \tag{2.40}$$

where v_b is the non-zero bottom velocity and τ_λ is the eastward (in the case of a line of latitude) component of the surface wind stress.

The Ekman transport (M_{EK}) is estimated using the Hellerman and Rosenstein(1983) wind stress field (used in the climatological annual mean cases) as well as the wind stress fields analysed by da Silva and Levitus (used in the two pentad cases and in the climatological annual mean cases). The volume transport asso-

ciated with non-zero bottom velocity (M_B) is calculated by substracting the M_T and M_{EK} from the absolute volume transport. At 54.5^oN, this absolute volume transport is obtained using the transport calculations of Greatbatch et al.(1991) and at 23.5^oN using data from the Florida Straits (Niiler and Richardson,1973; Larsen, 1992).

In order to calculate the heat transport through a section, we need to know the potential temperature as well as the velocity field. Potential temperature θ is defined to be the temperature of sea water raised adiabatically and isentropically to the ocean surface, i.e. to a reference pressure of 1 atm. Given the *in situ* temperature and salinity field from Levitus data, the potential temperature can be calculated according to Bryden's(1973) empirical polynomial,

$$\begin{aligned}\theta(P,T,S) &= T - P(3.6504\times10^{-4} + 8.3198\times10^{-5}T - 5.4065\times10^{-7}T^2 \\ &\quad +4.0274\times10^{-9}T^3) - P(S-35)(1.7439\times10^{-5} \\ &\quad -2.9778\times10^{-7}T) - P^2(8.9309\times10^{-7} - 3.1628\times10^{-8}T \\ &\quad +2.1987\times10^{-10}T^2) + 4.1057\times10^{-9}(S-35)P^2 \\ &\quad -P^3(-1.6056\times10^{-10} + 5.0484\times10^{-12}T) \qquad (2.41)\end{aligned}$$

where $\theta(P,T,S)$ is in ^{0}C as a function of salinity S ($30 < S < 40$), temperature T (in ^{0}C with $2 < T < 30$, and pressure P (in bars and $0 < P < 1000$).

Strictly speaking, heat transport can only be calculated for a section through which there is zero net mass transport (Montgomery, 1974; Bryan, 1982), for,

otherwise, the results will depend on the units chosen for temperature. However, it is convenient to define the heat transport function $HT(\lambda)$ as

$$HT(\lambda) = -\int_{\lambda_e}^{\lambda}\int_{-H}^{0} \rho c_p v\theta dz \; a\cos\phi d\lambda \tag{2.42}$$

where ρ is the density, c_p is the specific heat at constant pressure, v is the absolute velocity through the section, and θ is the potential temperature in degree Celsius. ρc_p can be assumed to have a uniform value of $0.00409 PW^{o}C^{-1}Sv^{-1}$ within the limits of the present calculation. Integrating from the eastern boundary to the western boundary gives the poleward heatflux through the east-west section.

Since our model calculates the velocity field referenced to the bottom, it is convenient to split HT into three parts, as we did for the volume transport.

$$HT = HT_T + HT_B + HT_{EK} \tag{2.43}$$

HT_T is the thermocline part of the heat transport given by

$$HT_T(\lambda) = -\int_{\lambda_e}^{\lambda}\int_{-H}^{0} \rho c_p v_T \theta a cos\phi dz d\lambda \tag{2.44}$$

where v_T is the velocity field referenced to the bottom and calculated by our model. HT_B is that part of the heat transport associated with the bottom velocity v_b and is given by

$$HT_B(\lambda) = -\int_{\lambda_e}^{\lambda} v_b \int_{-H}^{0} \rho c_p \theta a cos\phi dz d\lambda \tag{2.45}$$

and HT_{EK} is the heat transport associated with the wind-driven Ekman trans-

port and is given by

$$HT_{EK}(\lambda) = \int_{\lambda_e}^{\lambda} c_p \frac{\tau_\lambda}{f} \theta_S a \cos\phi \, dz \, d\lambda \tag{2.46}$$

where θ_S is the sea surface temperature and τ_λ is the eastward (in the case of a line of latitude) component of the surface wind stress. It should be noted that this decomposition is different from that followed by most previous authors (e.g. Bryan, 1962, 1982; Hall and Bryden, 1982; Molinari et al, 1990), but is the most natural to use with our model. However, it has the disadvantage that the individual parts, i.e. HT_T, HT_B and HT_{EK} (but not their sum, when integrated all the way across the basin), depend on the units used for potential temperature. Since in this case we use $^\circ C$, this is equivalent to assuming a return flow for each component at $0^\circ C$ (difficulties in defining the temperature of the return flow and hence in defining exactly what is meant by each component of the heat transport are discussed in Bryden, Roemmich and Church, 1991).

The steric sea level can also be calculated. Usually, the technique of computing dynamic height suffers from some limitations, particularly in regions of variable bottom topography. Often, a level of no motion is assumed and the velocities are calculated referenced to this depth. Clearly, problems arise if the ocean is shallower that the depth of the assumed level of no motion. Helland-Hansen (1934) suggested a method which extends isopycnals horizontally under the bottom of the ocean from their point of intersection with the slope. This corresponds to assuming that the geostrophic velocity at the bottom is always zero

and is equivalent to the method of Csanady(1979). Since our model calculates the velocity referenced to the bottom, we can use the model to calculate steric sea level in regions of quite general bottom topography. We shall usually take the level of no motion to be at the greatest depth on the section. Calculations referenced to 1500m will also be presented for comparison with Levitus(1990). With this in mind, we calculate the dynamic height by integrating G (see eqn.(2.21) and (2.23)) using the relation

$$p_s = g\rho_0\eta \tag{2.47}$$

where η is the upwards displacement of sea level from some reference level. As discussed earlier, the integration starts at the point of greatest depth. The sea level at this point is obtained by vertically integrating the hydrostatic equation. Assuming $p = 0$ at $z = -H$, we have

$$\eta_0 = -\int_{-H}^{0} \frac{(\rho - \rho_0)}{\rho_0} dz \tag{2.48}$$

Here the reference density ρ_0 is chosen so that the sea level is not far from zero. After acquiring η_0, we use eqn.(2.21) and (2.23) to integrate towards the coast and hence, the whole sea level field can be constructed. Of special interest is the comparison of sea level changes between the 1950s and 1970s.

2.4 Data

The hydrographic data set used in this thesis is the data compiled and analysed by Levitus (1982). His results were based on the data which were obtained from the National Oceanographic Data Center (NODC), Washington, D. C., and represent all the data available in the oceanographic station data file (SDF) as of the first quarter of 1978. The SDF file contained about 500,000 hydrographic casts consisting mainly of Nansen casts along with several thousand conductivity and salinity-temperature-depth casts.

The objectively analysed data are available at 1^{o} resolution in both latitude and longitude and at the standard levels from surface to sea floor, i.e. at the depths of 0, 10, 20, 30, 50, 75, 100, 125, 150, 200, 250, 300, 400, 500, 600, 700, 800, 900, 1000, 1100, 1200, 1300, 1400, 1500, 1750, 2000, 2500, 3000, 3500, 4000, 4500, 5000, 5500 metres. As claimed by Levitus, the objective analysis procedure substantially smooths out features with wavelengths of less than several hundred kilometers. A detailed description of data sources, quality control, and the objective analysis procedure for constructing the data field is given by Levitus (1982).

In this model, the input density data of Levitus(1982, 1989a,b,c) is transfered to the model grid by means of linear interpolation. It is worth noting that sometimes the input density and bathymetry data do not always match. In particular, it sometimes happens that the bathymetry data indicate that the water depth is

less than that indicated by the density data, in which case, density data below the depth indicated by the bathymetry data are discarded. The other possibility is that the bathymetry data indicate a depth greater than does the density data. In such cases, density data are created by extending isopycnals horizontally, as in the method of Helland-Hansen(1934). This procedure is also carried out whenever density data is required below the bottom in order the calculate the velocity field. Grid points at which extrapolated density data meet from two sides are dealt with by calculating the velocity using density data from one side only. This approach ensures that the impact of the extrapolation precedure on the velocity field is kept to a minimum (it should be noted that extending isopycnals horizontally ensures that the velocity at the ocean bottom is always zero).

As noted earlier, when calculating the Ekman part of volume transport and heat transport, we shall use the Hellerman and Rosenstein(1983) wind stress field (used in the climatological annual mean case to estimate the Ekman transport), and the wind stress fields analysed by da Silva and Levitus (personal communication). The da Silva and Levitus wind stress fields are derived from COADS data by analysing each individual ship observation, making a correction for the Beaufort Scale (Kaufeld, 1981; da Silva, Young and Levitus, 1992) and an adjustment for anemometer height to 10m (Cardone et al., 1990; da Silva, Young and Levitus, 1992). Details can be found elsewhere, although a preliminary comparison,

using different wind stress climatologies to drive a numerical model, can be found in Fanning et al.(1992). It is these wind stress fields we use for the two pentads. We shall also show the effect of using da Silva and Levitus's climatology, rather than that of Hellerman and Rosenstein, in the climatological case.

In all the model runs to be described we use a uniform vertical eddy viscosity coefficient of $\nu = 0.001 m^2 s^{-1}$ and a bottom friction coefficient of $r = 0.001 m s^{-1}$. (Both values are quoted as being reasonable by Csanady (1982).) It follows that except very near the equator, the Ekman layer depth $\sqrt{\nu/f}$ is less than 10m and is only $3m$ at $45^o N$. Since the diagnosed velocity through the section is geostrophic everywhere except within an Ekman layer depth of the top and bottom, it follows that these velocities, as calculated by the model are geostrophic almost everywhere (departures from geostrophy will also occur in regions where the geostrophic velocity varies in the vertical on a scale of order the Ekman layer depth; there are no such regions in our analyses). The model will be used to diagnose the velocity field from the known density field, with the results being shown in the following chapter.

Chapter 3

The Model Results

We applied the model to four sections - two sections through 55°W and 65°W longitude and two sections through 24°N and 54°N latitude (fig. 3.1).

3.1 Section through 55°W and 65°W longitude

We use these two sections to study the velocity structure and transport, particularly that of the Gulf Stream. The Gulf Stream is of central importance to the general circulation of North Atlantic and a great deal of attention has long been given to the understanding of the Stream's mean velocity structure and transport (e.g. Stommel, 1965). But because of the swiftness and variability of the current, it is difficult to obtain direct long-term measurements. According to the review of the North Atlantic circulation by Worthington(1976), the average transport of Florida Current(off Florida) is 30 Sv(with variations from 15 to 38

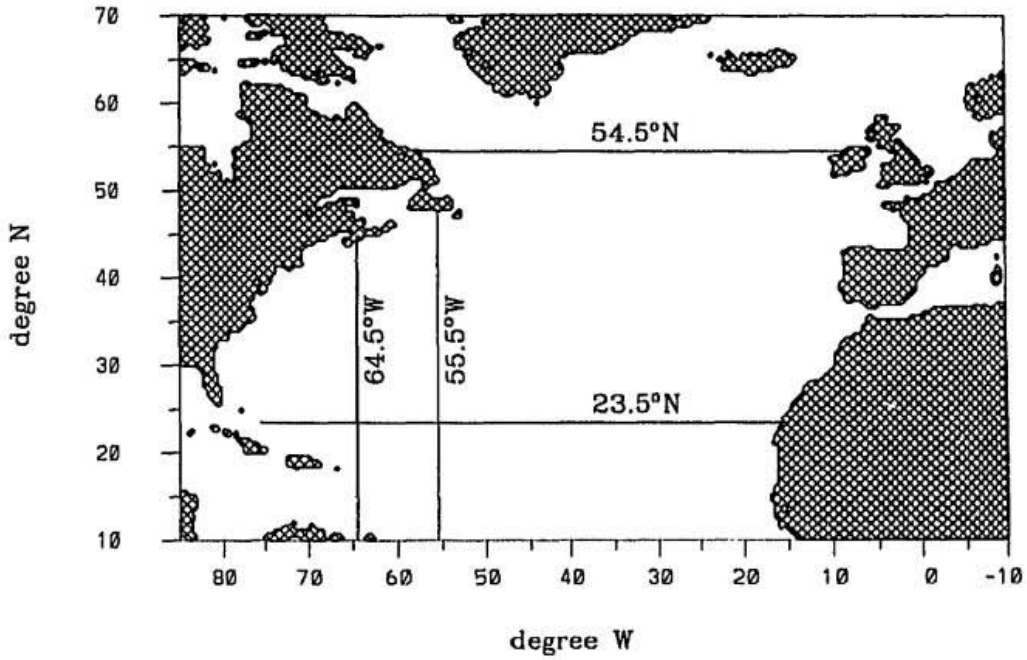

Figure 3.1: *The position of the four sections being studied*

Sv according to other studies using the electromagnetic method). The transport increases north-east to 85 Sv off Cape Hatteras and to 150 Sv by 65°W and then decreases eastward to 37 Sv at 40°W (Knauss, 1969).

Two methods have been used to estimate the absolute Gulf Stream transport for the region 50 – 70°W. In the first, velocity sections were made across the Stream using transport floats — instruments that fall freely through the water and directly measure transport per unit width. The second method combines geostrophic(baroclinic) velocity sections with absolute velocity measured by deep floats or current meters. Both methods have the problem that it is very difficult to determine the limits or edges of the Stream. Velocity sections usually show a

complicated pattern of meanders, multiple crossings of the Stream, eddies, countercurrents and small-scale embedded jets. These features frequently change from section to section, and it is not obvious which of them to include as Gulf Stream transport. Moored current meter measurements under and near the Stream reveal large amplitude time-dependent fluctuations (e.g. Schmitz, 1980). How to suitably combine these strongly fluctuating velocities with the more stable hydrographic and geostrophic features is still unsolved. It is noticed that using the deep float or current meter velocity tends to increase the transport over the geostrophic transport referenced to the sea floor by large amounts. Fuglister(1963) reports an increase from 88Sv relative to zero velocity at the sea floor to 147Sv with float velocities whereas Robinson et al. (1974) report transport of 77Sv referenced to the sea floor and an absolute transport of 226Sv.

We now show results obtained using our model along $55^{o}W$. We begin with this section so that we can compare our results with those of Richardson(1985). We took a section along $55^{o}W$ and between $8-45^{o}N$ and applied the diagnostic model to study the transport and velocity. Three sets of density data - namely, 1950s, 1970s and climatological annual mean data, all from Levitus, have been used to first diagnose the velocity and subsequently, calculate the volume transport through the section.

Figure 3.2a,b shows the model-calculated velocity field through the section (positive being eastward) referenced to 1500m, and to the bottom, respectively.

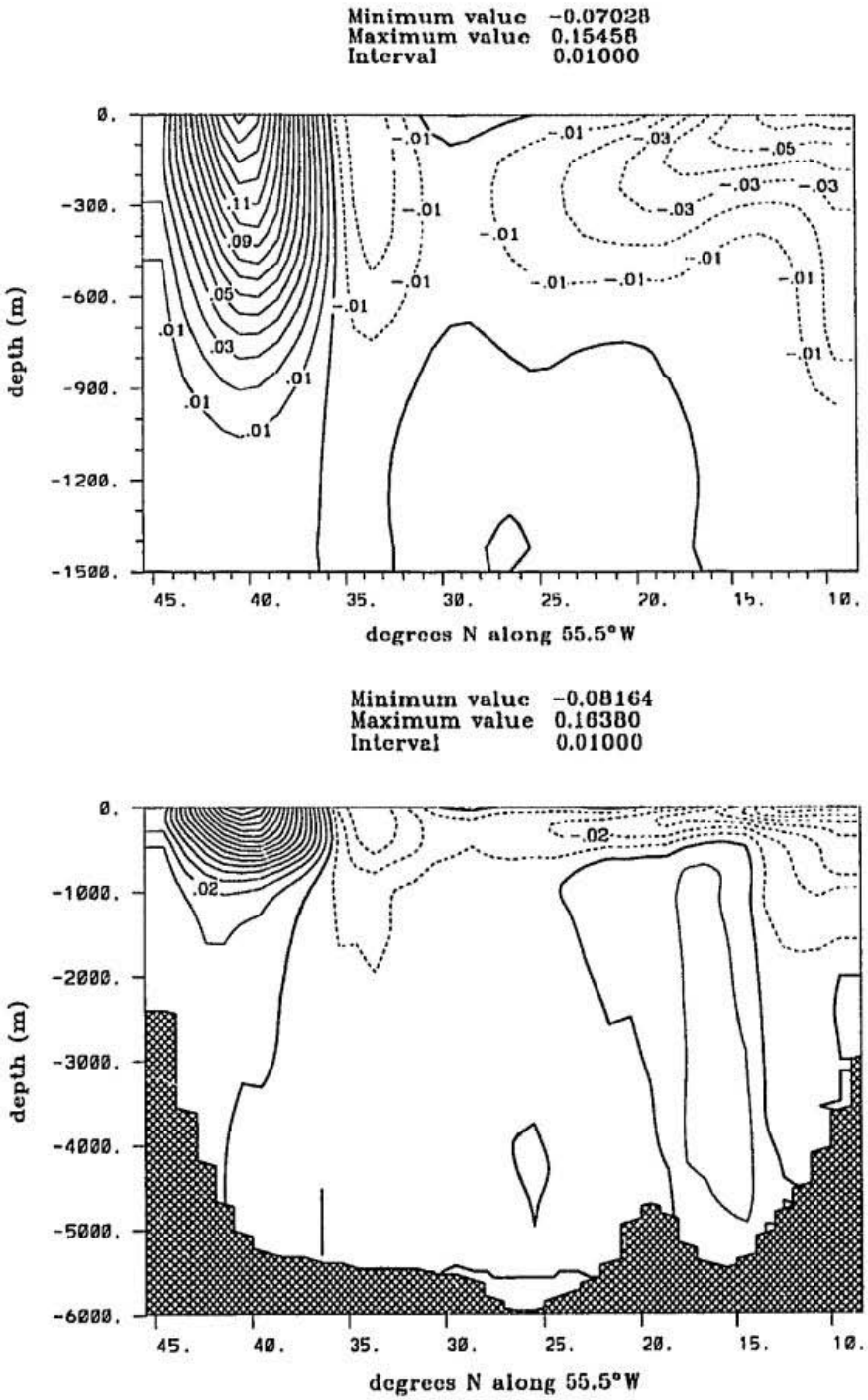

Figure 3.2: *Eastward velocity field using climatological annual mean data (a) the upper panel, referenced to 1500 m (b) the lower panel, referenced to the bottom. The contour interval is* 0.01 ms^{-1}, *with dashed contours indicating westward velocity and solid contours eastward. The minimum and maximum values are given in* ms^{-1}.

The density field is the annual mean from Levitus (1982), and so should be representative of the climatological mean state. In figure 3.2a, the calculation is performed using 20 equally spaced z levels at a horizontal resolution of 1^{o}. In figure 3.2b, the calculation is performed using 80 equally spaced z levels at a horizontal resolution of 1^{o}. In all the calculations, there is no bottom velocity(according to eqn (2.16)). Therefore, the velocity field shown is actually velocity referenced to 1500m and the ocean bottom respectively. From the figures, we can clearly identify the Gulf Stream to be the eastward flow centered near 40°N, extending from 36°N to 44°N, approximately 900 km wide. It has a maximum surface velocity of 17 cms^{-1} referenced to the bottom, centered near 40°N. The Gulf Stream is bounded by the southern countercurrent between 31°N and 36°N which flows westward.

Comparing these figures with the contoured zonal velocity section along $55^{o}W$ in Richardson's paper(his figure 6b) reveal good agreement in the main features. His figure (reproduced here as fig. 3.3) is the velocity from drifters, floats, and current meters with the wind drift velocity removed. Note that his velocity is the absolute velocity and not the velocity referenced to the bottom. There are some similarities between the directly measured velocity(Fig. 3.3) and the model-calculated velocity(Fig. 3.2a,b). The upper level Gulf Stream is similar - both are centered near 40°N and have approximately the same width. In fig. 3.3, the maximum surface velocity referenced to the bottom is about 20 cms^{-1}, which is

agreeable to 17 cms^{-1} in Fig. 3.2a,b. Both show that the Stream is bounded on the south by a countercurrent.

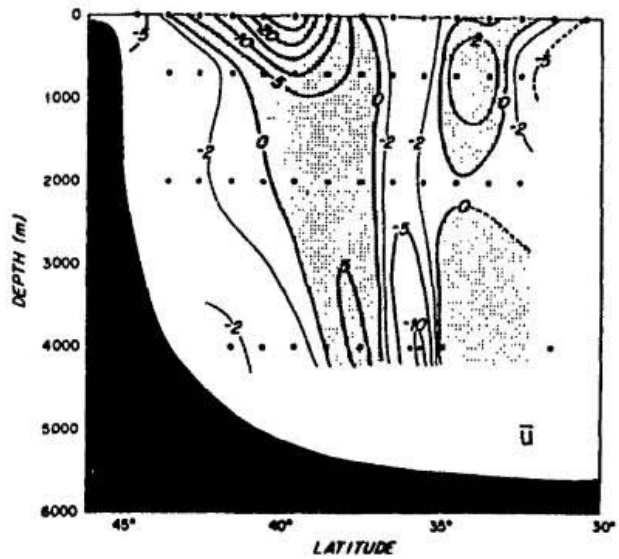

Figure 3.3: *A reproduction of Figure 6b from Richardson, 1985. Contoured zonal velocity section (cm s^{-1}) along 55° W and through the Gulf Stream from drifters, floats, and current meters, with the wind drift velocity removed. Eastward velocity is shaded. Dots indicate centers of boxes used in calculating velocity except at 4000 m, where they show current meter locations.*

Fig. 3.3 shows the subsurface Gulf Stream is bounded on the north by a westward flowing countercurrent with a width of 300 km. Because this countercurrent is bottom intensified, it disappears in Fig. 3.2b which only shows velocity referenced to the bottom, not absolute velocity. In general, the model-calculated velocity(Fig. 3.2a,b) and the directly measured velocity(Fig. 3.3) agree well in showing the size, shape and velocity of the Gulf Stream.

We further investigate the transport calculated from the model along this 55°W section. Fig. 3.4 shows the transport referenced to 1500m and to the

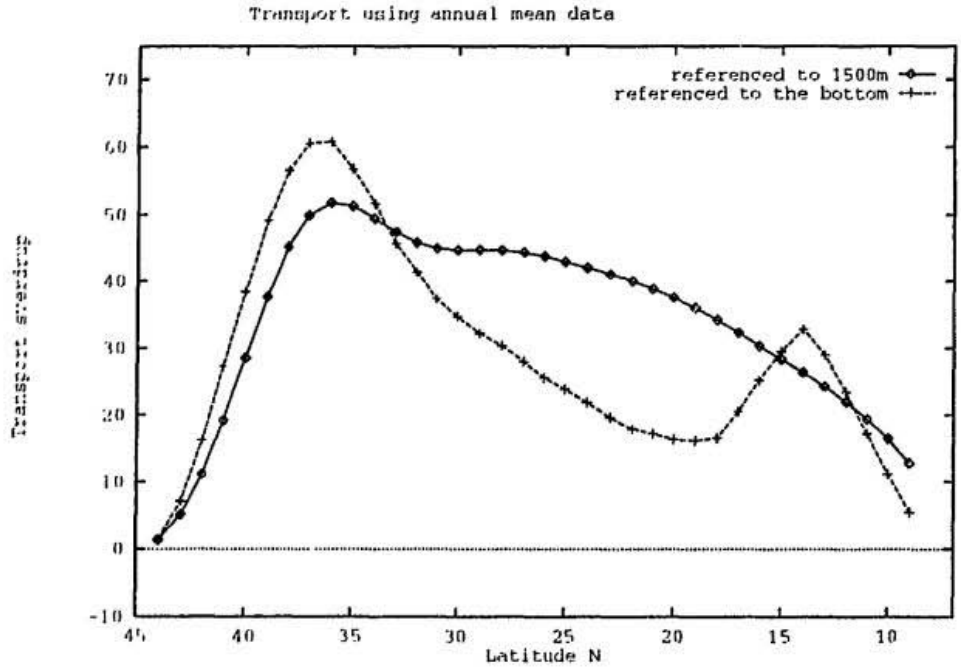

Figure 3.4: *Volume transport using annual mean data*

bottom, respectively, both being obtained from the velocity field shown in fig. 3.2a,b. The eastward Gulf Stream transport referenced to the bottom and the northern boundary is about 60 Sv and the total transport budget across $55°W$ north of $35°N$ is about 50 Sv. Richardson estimated the volume transport of the Gulf Stream by integrating latitudinally and vertically the velocity data obtained from drifters, floats, and current meters. He claimed in his paper that the estimate of the volume transport of the Gulf Stream is 93 Sv, approximately 37 percent of which, or 34 Sv, is independent of depth - the barotropic part. It is this barotropic component that has been impossible to estimate with hydrographic data alone. The depth dependent part of volume transport, i.e. 59 Sv, is very

close to the transport referenced to the bottom calculated from the model.

Similar calculations have also been performed using data from 1970-1974 and 1955-1959 to study the variability between the two pentads. Fig. 3.5, 3.6 and 3.7 show the velocity fields referenced to 1500m and to the bottom which are calculated from the model using 1970-1974 data, 1955-1959 data and the difference between the two, respectively. When viewing these figures, it should be remembered that the model calculates the velocity field referenced to the bottom and that the figures do not, therefore, show the absolute velocity field through the section, but rather its vertical structure. The Gulf Stream is also clearly evident in both cases with a maximum surface velocity of $0.18ms^{-1}$ in 1955-59 and $0.14ms^{-1}$ in 1970-74. This shows a weaker Gulf Stream in the early 1970s compare to the late 1950s, with a maximum surface velocity drop of about 4 cms^{-1}. The velocity in 1970-1974 decreases over the whole depth range in the Gulf Stream region, especially in deep water where a considerable decrease occurs. There is also evidence of a westward countercurrent near $35^{o}N$ in the late 1950's that is a much weaker feature in the later pentad. The difference field (Fig. 3.7) shows a banded structure, with the vertical shear tending to be of the same sign throughout the water column and with changes in the density field in the deep water, below 1500 m, making a significant contribution. As noted by Levitus(1989c), density changes below 1500 m may not be reliable because of insufficient data. Given this note of caution, the Gulf Stream nonetheless appears

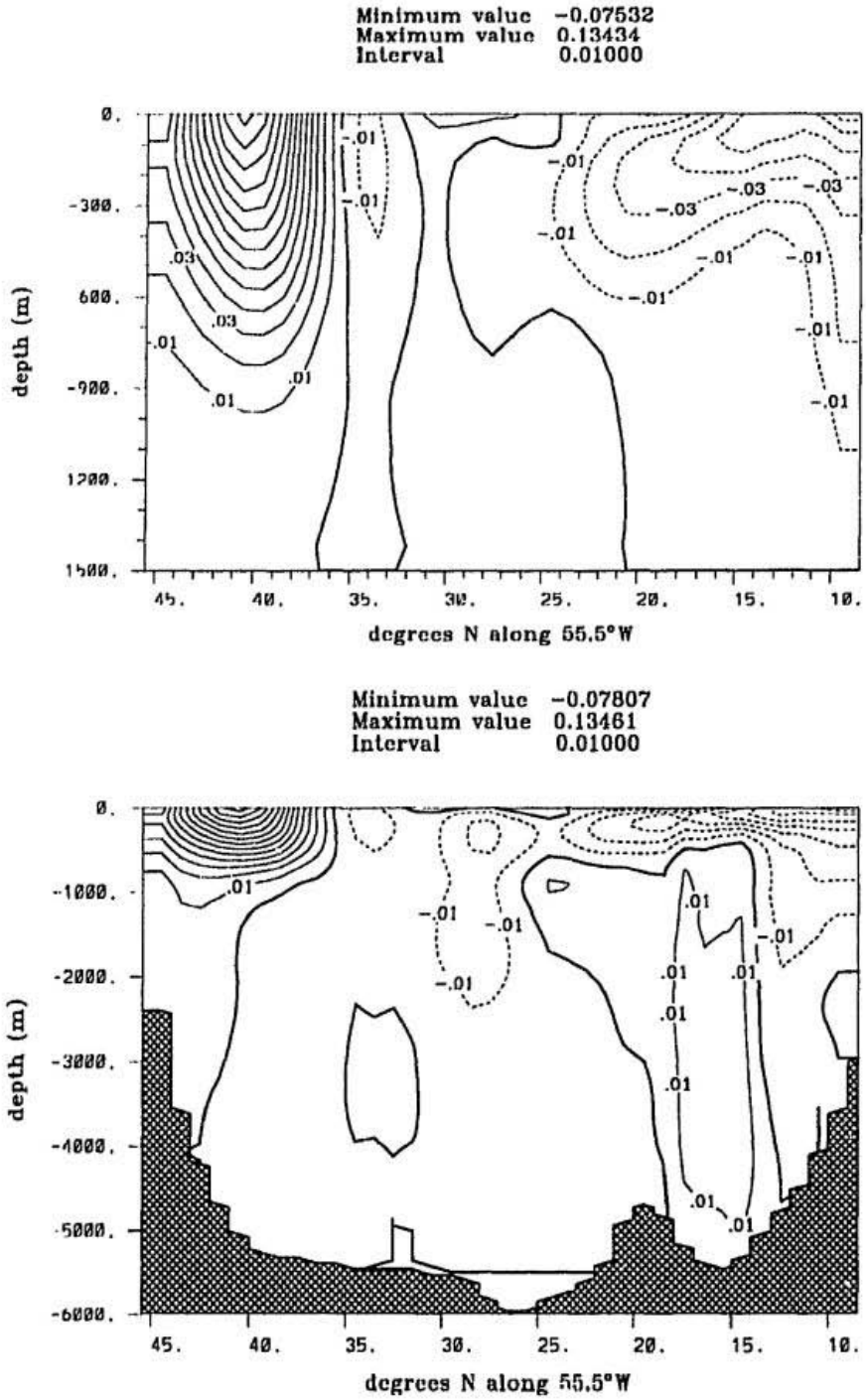

Figure 3.5: *Eastward velocity field using 1970-1974 data. (a) the upper panel, referenced to 1500 m (b) the lower panel, referenced to the bottom. The contour interval is* 0.01 ms^{-1}, *with dashed contours indicating westward velocity and solid contours eastward. The minimum and maximum values are given in* ms^{-1}.

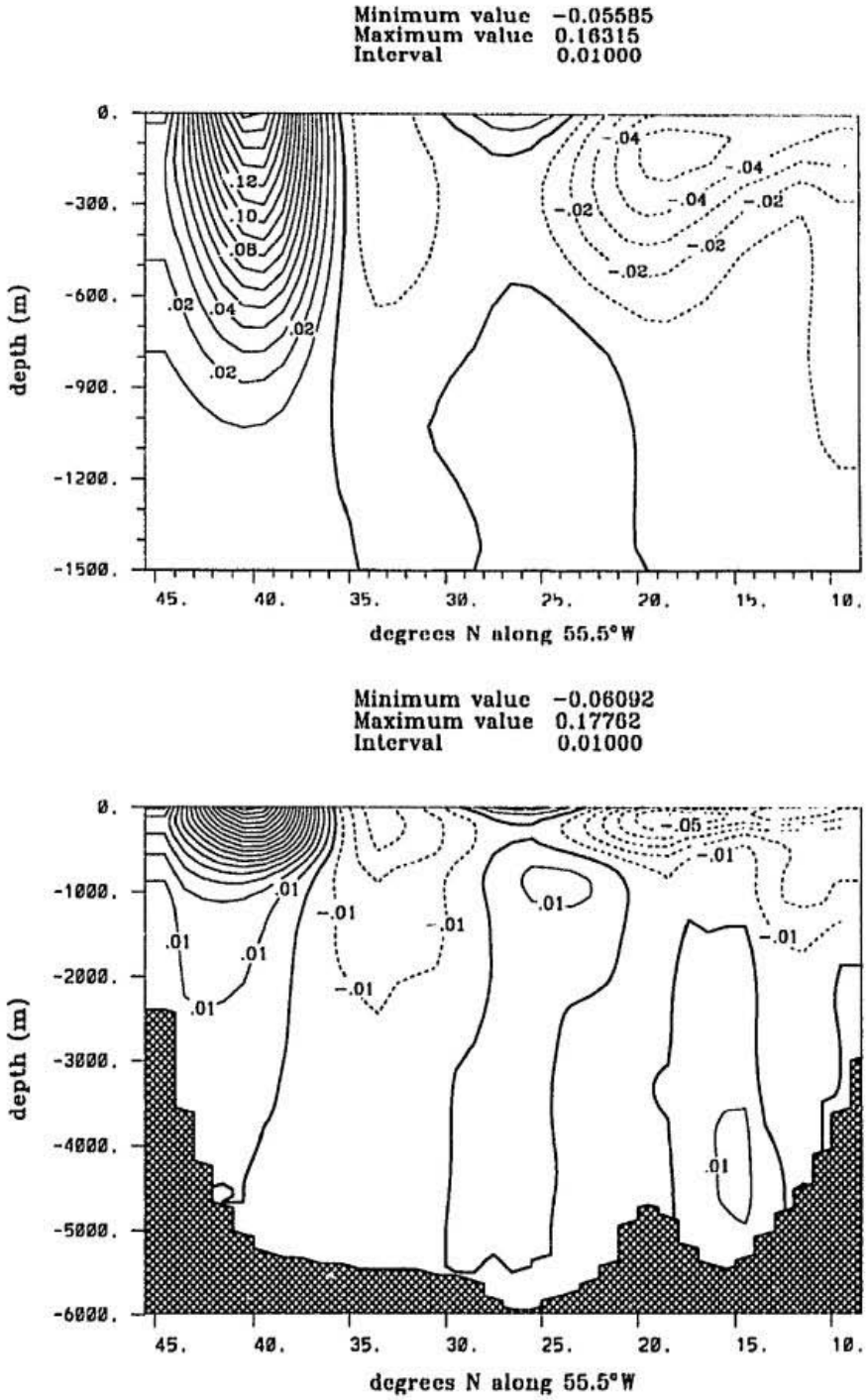

Figure 3.6: *Eastward velocity field using 1955-1959 data. (a) the upper panel, referenced to 1500 m (b) the lower panel, referenced to the bottom. The contour interval is* 0.01 ms^{-1}, *with dashed contours indicating westward velocity and solid contours eastward. The minimum and maximum values are given in* ms^{-1}.

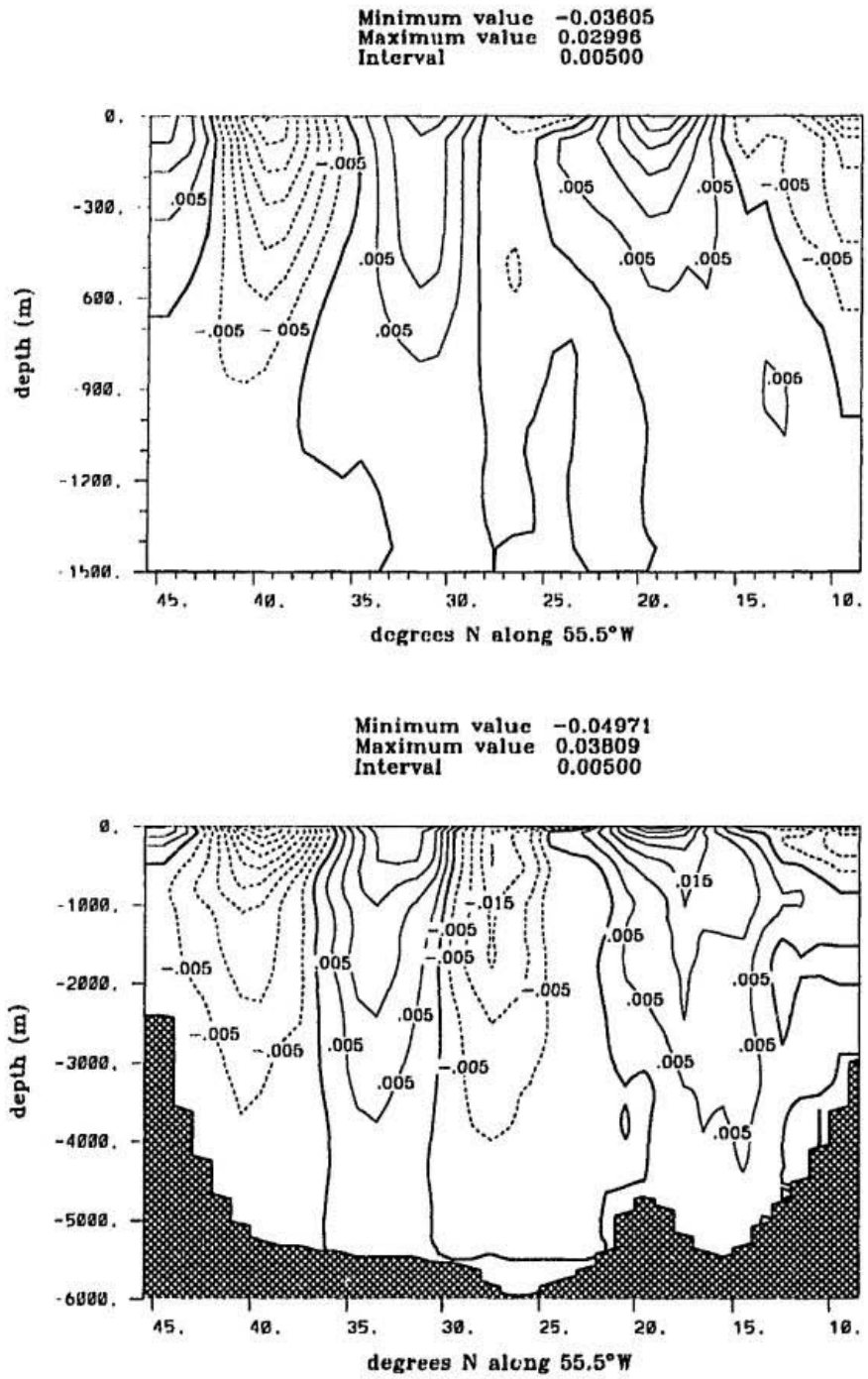

Figure 3.7: *Eastward velocity field of 1970-1974 minus 1955-1959 result. (a) the upper panel, referenced to 1500 m (b) the lower panel, referenced to the bottom. The contour interval is* 0.005 ms^{-1}, *with dashed contours indicating westward velocity and solid contours eastward. The minimum and maximum values are given in* ms^{-1}.

as a shallower feature in 1970-74 than 1955-59. This means that the vertical shear in the deep water is reduced in the later pentad, as would be consistent with a weakened deep western boundary undercurrent and/or northern recirculation gyre (Hogg et al, 1986). The latter can be seen in fig. 3.3 (this is the westward flow near 4000 m depth and $40^{o}N$).

Fig. 3.8a,b, 3.9a show the volume transport in 1970-1974, 1955-1959 and 1970-74 minus 1955-59, respectively, all being calculated from the velocity field. The differences of velocity field results in a big drop of volume transport referenced to the bottom, from the 1970-1974 pentad to the 1955-1959 pentad, of up to 30 Sv to the southern end of the Gulf Stream. However, fig. 3.7 also shows a decrease of velocity in the southern countercurrent during 1970-1974, which implies a weaker countercurrent. Hence, the weaker eastward Gulf Stream in 1970-1974 is somewhat compensated by a weaker westward countercurrent, with result that the total transport budget referenced to the bottom north of 30°N only drops about 5 Sv (see fig. 3.9, upper panel). Comparisons between the difference field referenced to 1500m to that referenced to bottom show that in the former, the eastward transport of the Gulf Stream drops only 7 Sv in 1970s, whereas it drops 30 Sv in the later. This arises because of the significant difference of velocity between the two pentads in the deep ocean (as can be seen in Fig. 3.7b).

Superimposing an externally specified absolute transport through the section to our results allows us to investigate the volume transport associated with the

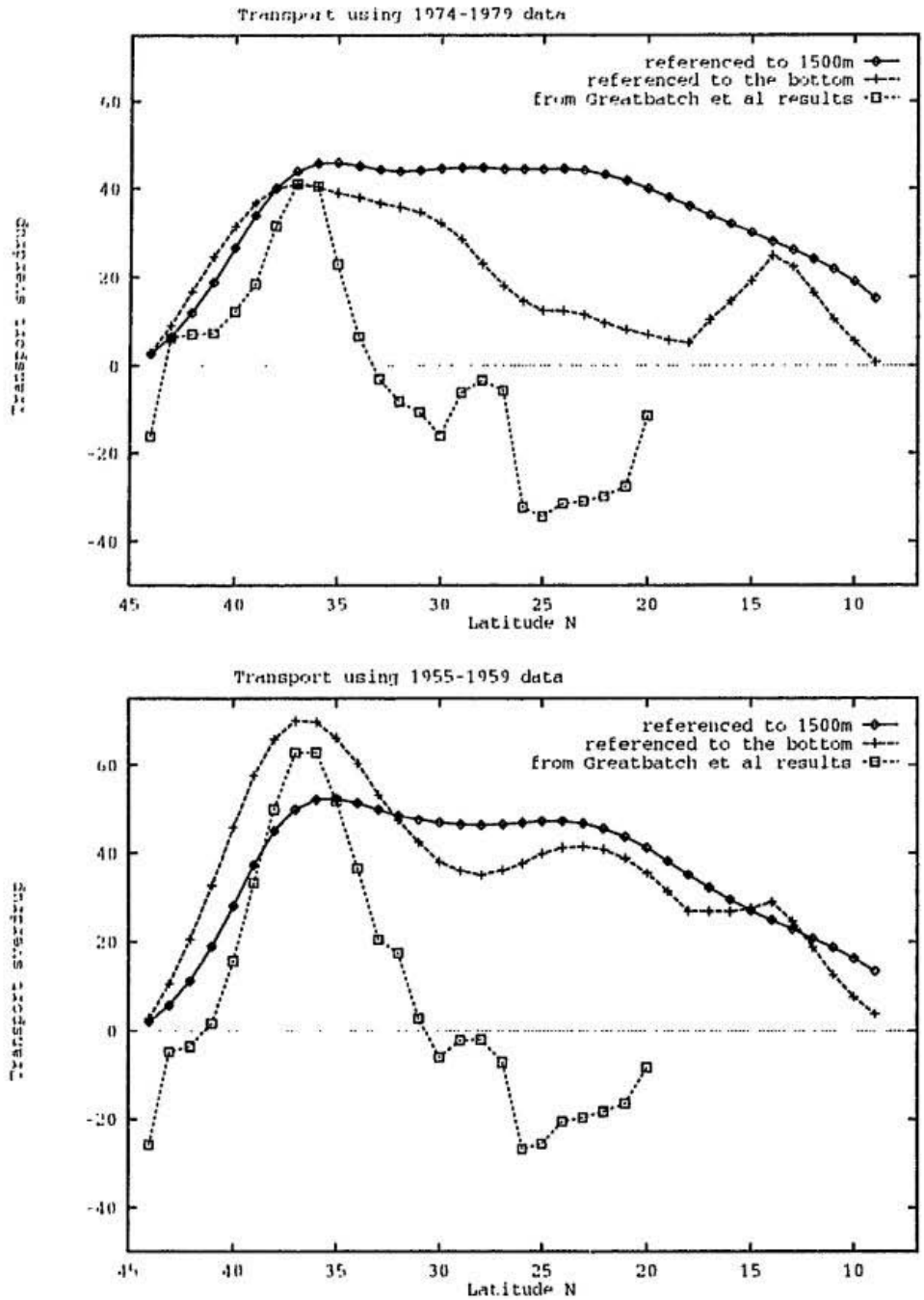

Figure 3.8: *Volume transport using (a) the upper panel, 1970-1974 and (b) the lower panel, 1955-1959 data*

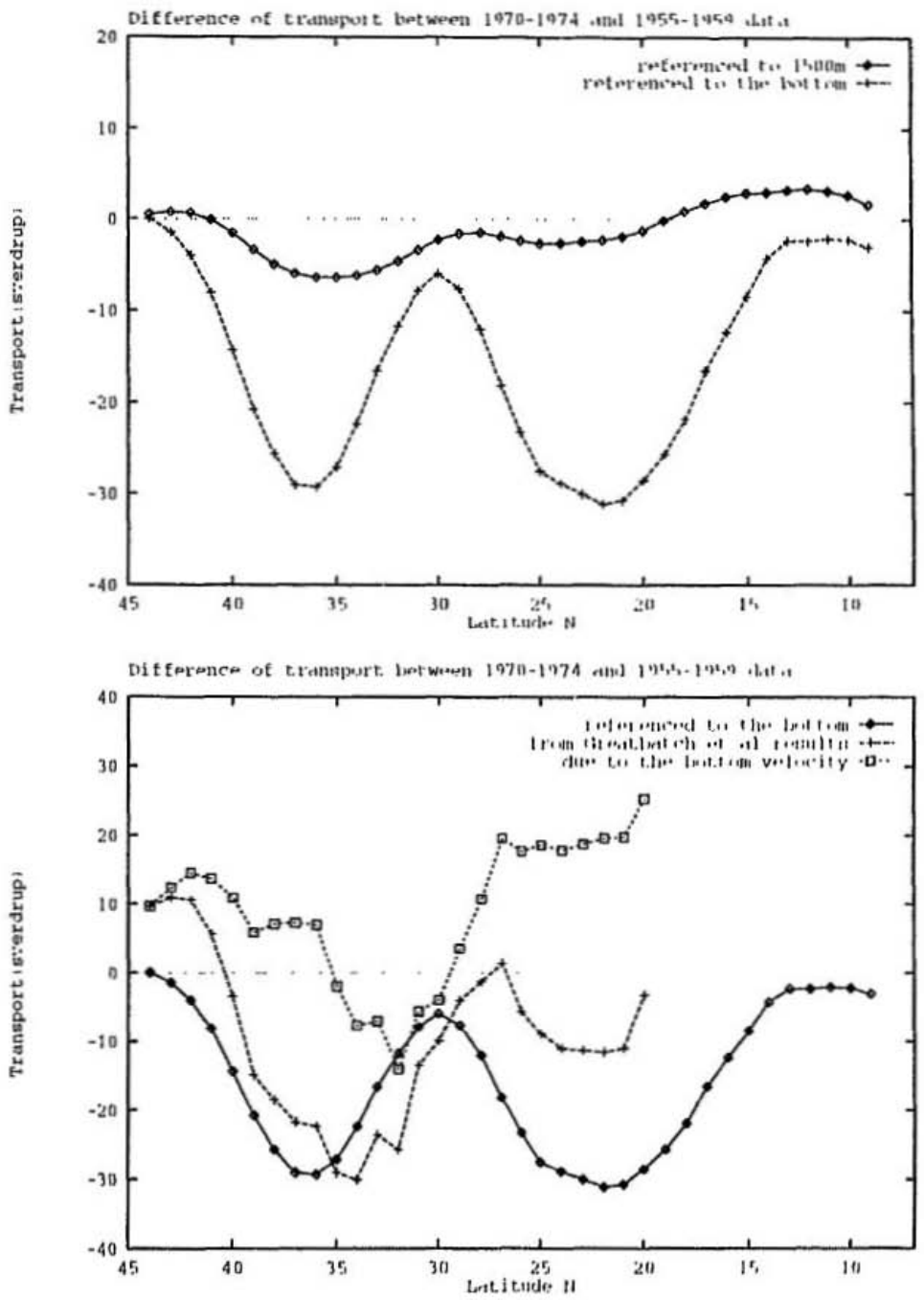

Figure 3.9: *Volume transport using 1970-1974 minus 1955-1959 data*

non-zero bottom velocity. Fig. 3.8a,b plots the absolute transport diagnosed by Greatbatch et al.(1991) for the $55°W$ section and compares it to the transport calculated referenced to the bottom. Fig 3.9b(lower panel) plots the change in these transports 1970-74 minus 1955-59 and also the difference between these curves. The change in surface Ekman transport is such a small part of this difference that it can almost entirely be attributed to changes in bottom velocity. Clearly, changes in bottom velocity play an important part in Greatbatch et al.'s results. North of about $42°N$, bottom velocities are required to become more eastward and between 42 and $40°N$, more westward. This is consistent with a weakening of the northern recirculation in the slope region to the north of the Gulf Stream. (In the calculation of Mellor et al.(1982) this is a very barotropic feature, as can be seen from Mellor et al.'s Figs.14 and 15.) Greatbatch et al. also calculated the transport change implied by the density changes above 1500 m only (see their Fig.12b). This calculation gives a total eastward transport change across the Gulf Stream of about $20Sv$ through $55°W$, roughly three times the eastward transport change calculated referenced to 1500 m shown in fig. 3.9a. This is interesting because it shows that even if the density changed only at depths above 1500m, significant changes in the velocity field below 1500m can still occur. It is easy to understand how this can be by referring to equation (19) in Greatbatch et al. (or, equivalently, equation (6) in Holland(1973)) i.e.

$$\beta V = \frac{1}{\rho_0}\left(\hat{\underline{k}} \cdot curl(\underline{\tau}^s) + \hat{\underline{k}} \cdot curl(p_b \nabla H)\right) \qquad (3.1)$$

where $\hat{\underline{k}}$ is a unit vector in the vertical upwards direction, $\underline{\tau}^s$ is the surface wind stress, $\beta = \frac{1}{a}\frac{df}{d\phi}$ (the northward gradient of the Coriolis parameter) and p_b is the bottom pressure. This says that the southward transport across a line of latitude is due to the curl of the surface wind stress and the bottom pressure torque (the first and second terms on the right hand side, respectively; bottom stress has been neglected). As noted by Greatbatch et al. the difference in the wind stress curl between the two pentads makes only a very small contribution in eqn.(3.1), from which it follows that the change in transport must be associated with changes in the bottom pressure torque and, therefore, bottom velocities (Holland, 1973). This is true no matter where in the water column the density changes responsible for the transport change occur, as long as the corresponding change in the north-south transport cannot be accounted for by the wind stress curl term in (3.1).

The study of the dynamic height difference field, which also represents the change in steric sea level, reveals significant difference between two pentads. The steric sea level difference field (fig. 3.10) for the 0 to 1500m depth interval exhibits steric sea level during 1970s increase as large as 8 dyn cm in the Gulf Stream region but decrease in the central portion of the subtropical gyre region, up to about 7 dyn cm along $55°W$ section. This calculation is the same as the steric sea level calculated by Levitus(1990) (see fig. 1.3) directly from the density field with an assumption of a depth of no motion at 1500m and agrees with his results, the

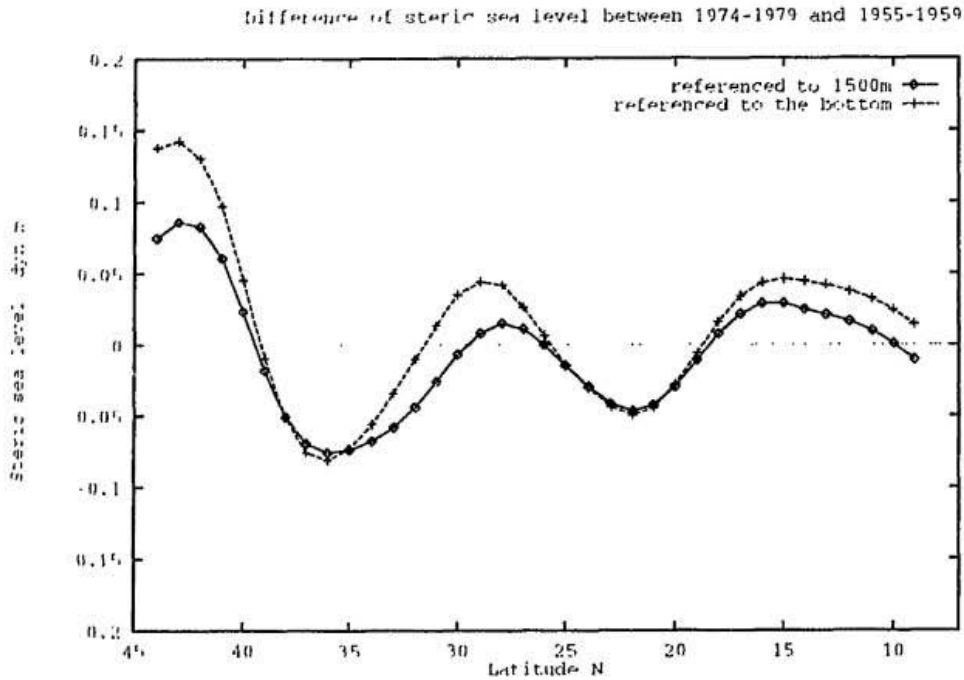

Figure 3.10: *Steric sea level differences for 1970-1974 minus 1955-1959 results*

only difference being that our model now allows the calculation to be extended into water shallower than the assumed level of no motion (this is in essentially the same way as described by Csanady(1979) as discussed in chapter one). The steric sea level difference field for the 0 to the bottom depth interval is calculated referenced to the deepest depth on the section, assuming that the bottom pressure at that depth was the same in both pentads. The effect of referencing relative to the deepest depth rather than 1500m is to increase the magnitude of the signal but does not change its general character. Fig. 3.10 also reveals that, referenced to the deepest depth on the section, steric sea level during 1970s increase more in the Gulf Stream region, up to 15 dyn cm.

One final point to note is that the transport of the Gulf Stream referenced to the bottom through this section is about $57Sv$ when calculated using the annual mean density data of Levitus(1982), $65Sv$ using density data from 1955-59 and only about $40Sv$ using density data from 1970-74. All except the 1970's value agree well with Richardson's(1985) estimate of $59Sv$ referenced to the bottom (this includes the Ekman transport which should be added to our calculations but in fact amounts to only about $1Sv$). Worthington(1977) noted a dramatic increase from 1974-75 to 1977 in the transport calculated for the Gulf Stream from section data using 2000m as a level of no motion.

We continue our study by taking a section along $65°W$ and between $19.5 - 43.5°N$. Of particular interest is the interpentadal steric sea level difference field, especially those for Halifax and Bermuda, which lie on the section.

Figure 3.11a,b shows the velocity field across this $65°W$ section referenced to 1500m and to the bottom, respectively, with positive being eastward and negative being westward. The annual mean density data from Levitus (1982) is used to represent the climatological mean state. In figure 3.11a, the case referenced to 1500m, 20 equally spaced $z-$levels in the vertical and a resolution of 1° in the horizontal are used to calculate the velocity. In figure 3.11b, the case referenced to the bottom, 80 equally spaced $z-$levels in the vertical and a resolution of 1° in the horizontal are used. Once again, according to equation (2.16), bottom velocity is zero. It follows that the velocity field is that referenced to 1500m

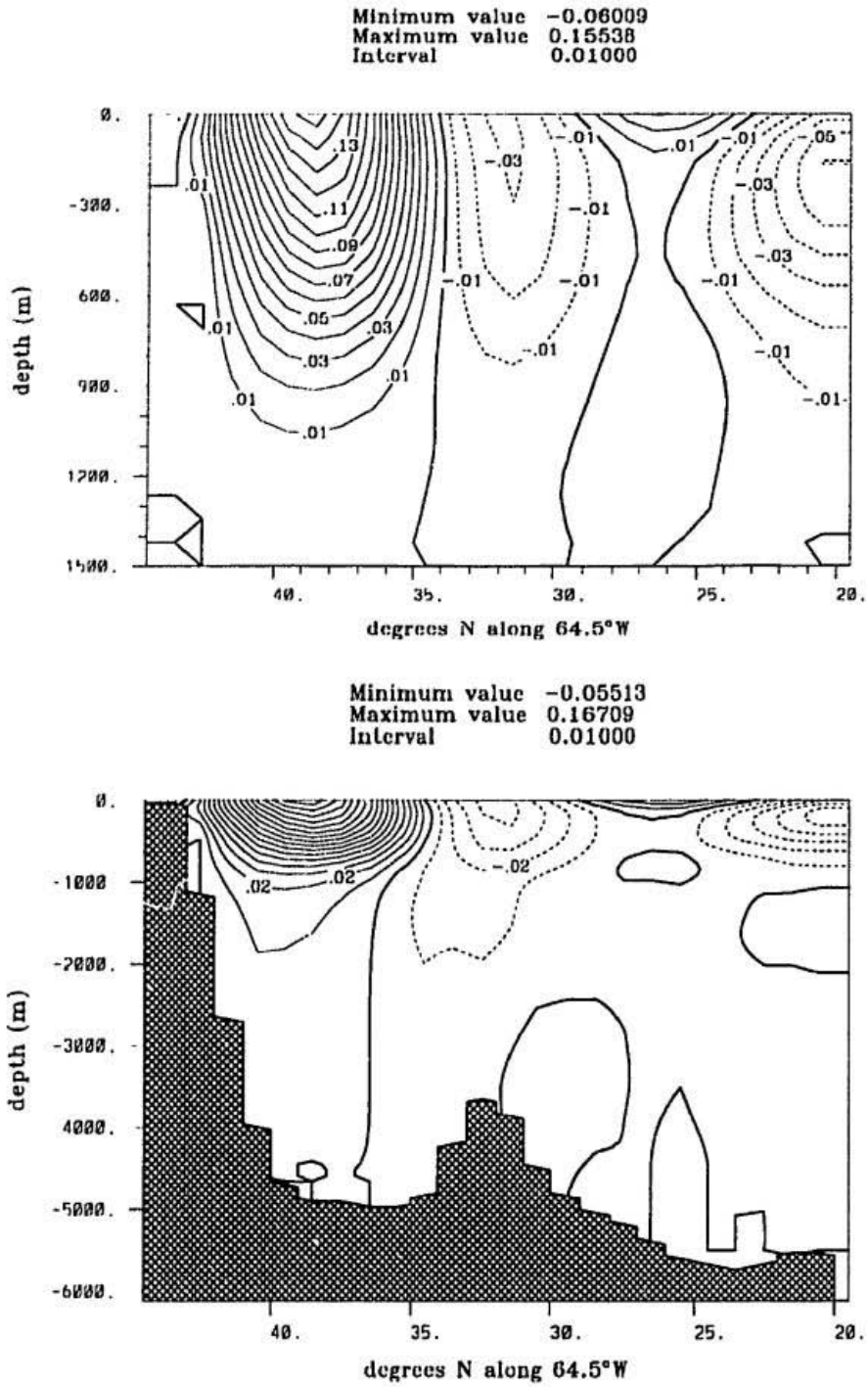

Figure 3.11: *Eastward velocity field using annual mean data. (a) the upper panel, referenced to 1500 m (b) the lower panel, referenced to the bottom. The contour interval is* 0.01 ms^{-1}, *with dashed contours indicating westward velocity and solid contours eastward. The minimum and maximum values are given in* ms^{-1}.

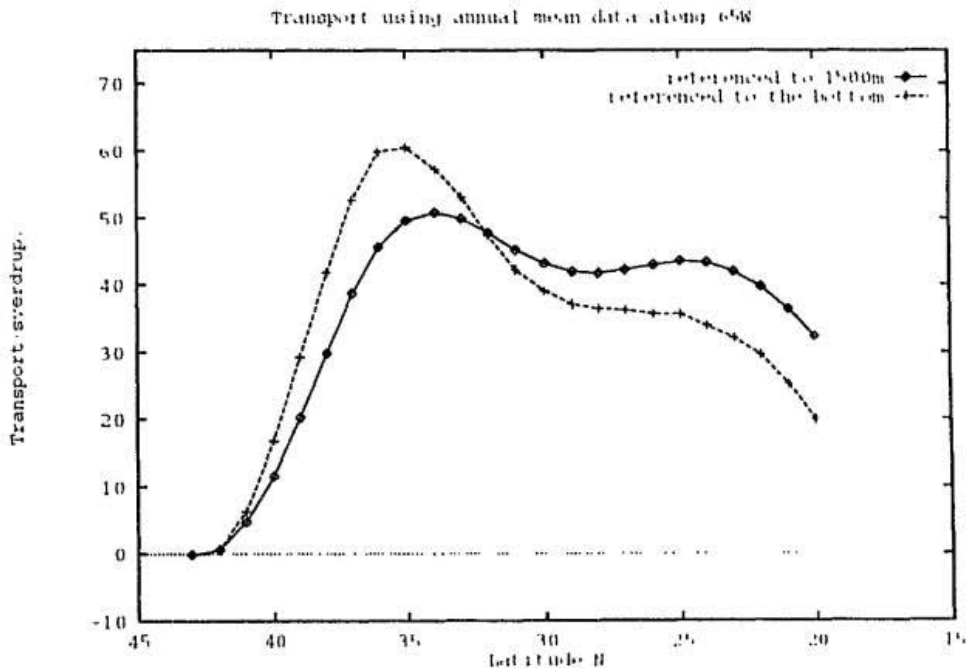

Figure 3.12: *Volume transport using annual mean data*

and the bottom respectively. The figures show basically similar features to those found along $55°W$. The Gulf Stream can also be clearly identified by the strong eastward flow. However, compare to $55°W$ section, the position of this flow moves a bit south, centering near 38.5°N and extending from 35°N to 42°N, with approximately the same width as that of $55°W$ section. The maximum surface velocity occurs near 38.5°N and has a magnitude of about 17 cms^{-1} referenced to the bottom. In the south, the Gulf Stream is also bounded by the southern countercurrent which flows westward.

Figure 3.12 shows the transport calculated from the model along this $65°W$ section, referenced to 1500m and to the bottom respectively. The Gulf Stream

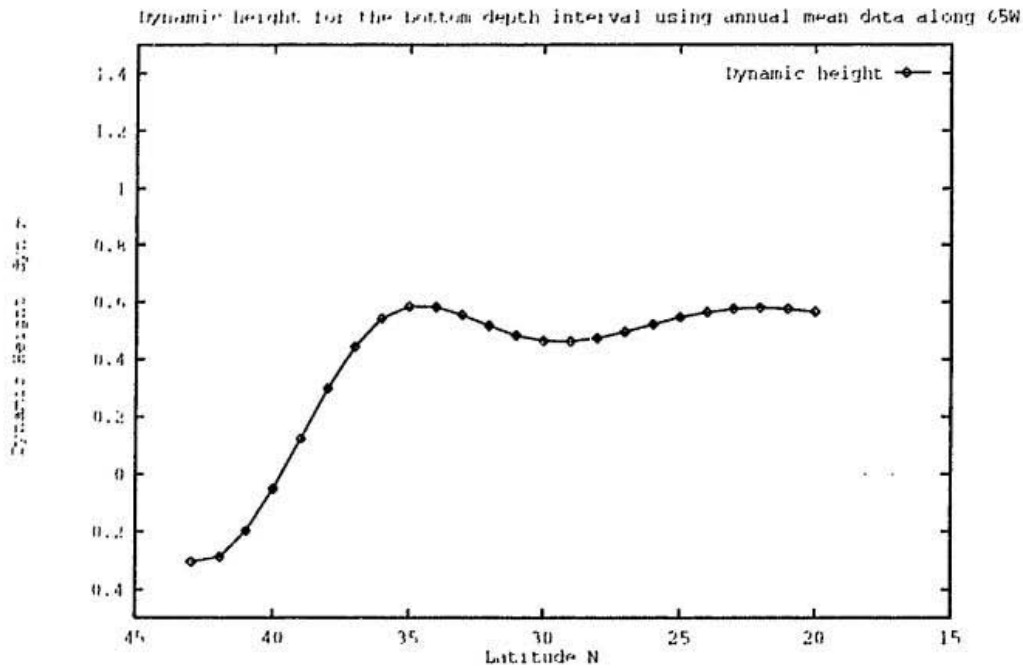

Figure 3.13: *Dynamic height for the bottom to surface depth interval using annual mean data*

transport referenced to the bottom is about 60 Sv, which is about the same as that along $55°W$ section and also agrees well with the depth dependent part of volume transport estimated by Richardson.

Figure 3.13 shows the dynamic height field calculated from the model along $65°W$ section, assuming a level of no motion at the deepest depth. The reference density is 1040 $kg\ m^{-3}$ in a constant density water column. We can see that the sea level at the northern end of the Gulf Stream is about 90 dyn cm lower than that at the southern end of the Gulf Stream. This is due to the strong eastward current.

We move on to investigate the interpentadal variability between the two peri-

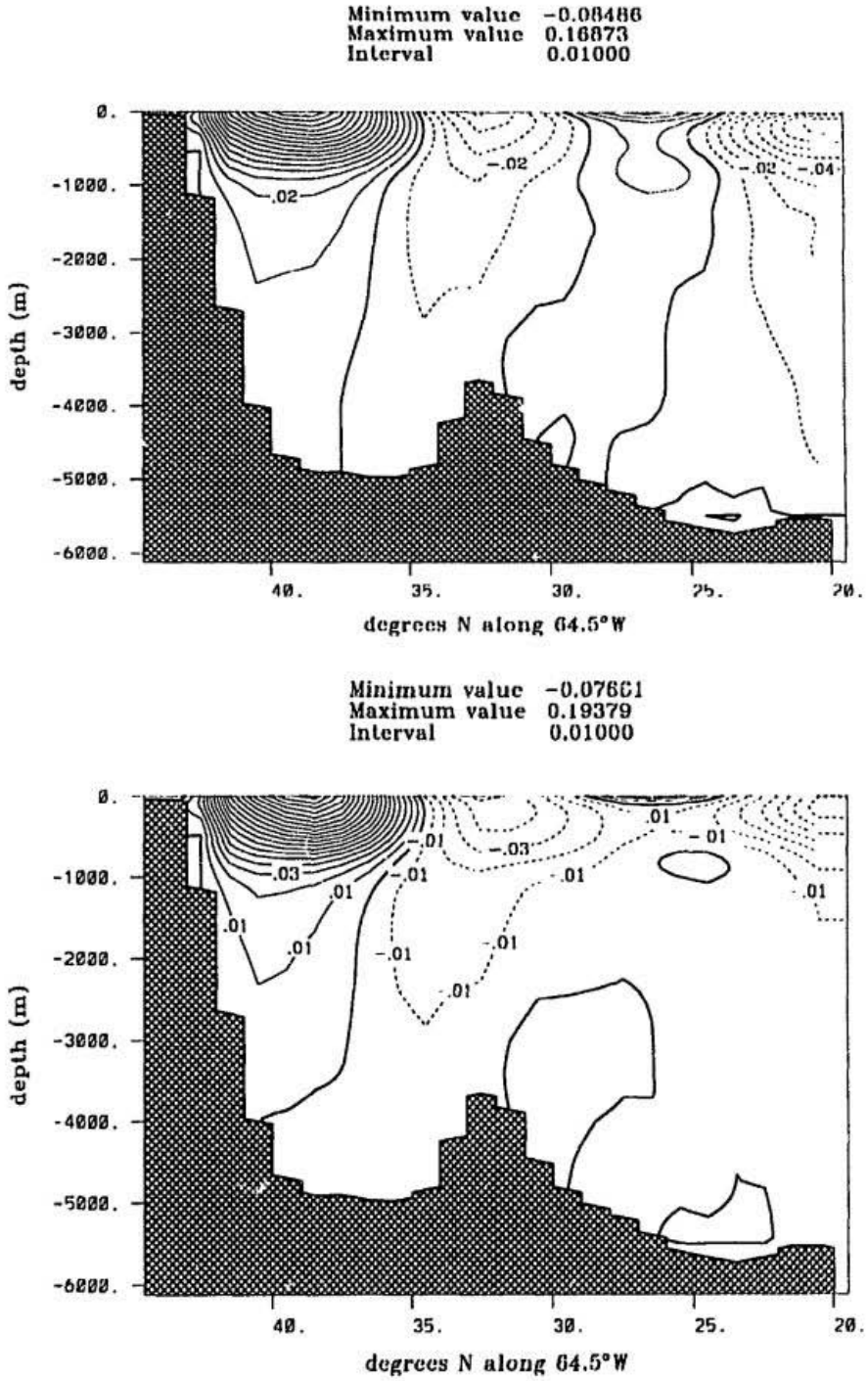

Figure 3.14: *Eastward velocity field referenced to the bottom using (a) the upper panel, 1970-1974 and (b) the lower panel, 1955-1959 data. The contour interval is* 0.01 ms^{-1}, *with dashed contours indicating westward velocity and solid contours eastward. The minimum and maximum values are given in* ms^{-1}.

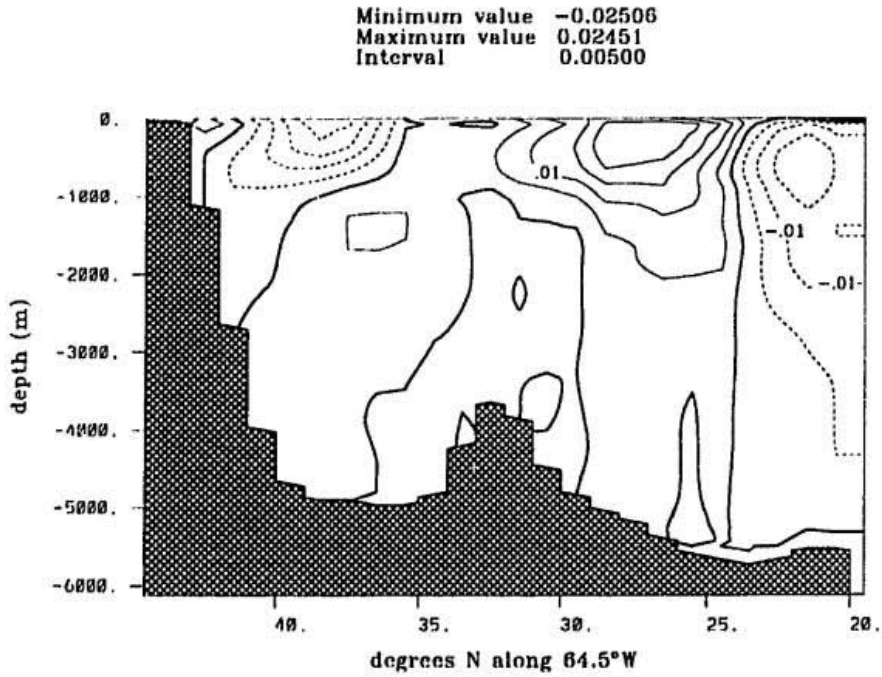

Figure 3.15: *Eastward velocity field referenced to the bottom, using 1970-1974 minus 1955-1959 result. The contour interval is* 0.005 ms^{-1}, *with dashed contours indicating westward velocity and solid contours eastward. The minimum and maximum values are given in* ms^{-1}.

ods by using 1970-1974 and 1955-1959 pentad data. The velocity field calculated from the model using 1970-1974 data, 1955-1959 data and the difference between the two are shown in figures 3.14a,b and fig. 3.15, respectively. The Gulf Stream is again weaker in the early 1970s compare to the late 1950s, with a maximum surface velocity drop of about 2.5 cms^{-1}, rather smaller than that along $55°W$ section. The velocity in the 1970s decreases in the Gulf Stream region, but increases in the deep water underneath the Gulf Stream, especially under the southern part of the Gulf Stream region. This results in little changes in volume transport(decrease by 3 Sv, fig. 3.16) in the Gulf Stream region referenced to the

bottom. This small difference is also compensated by the difference due to the southern countercurrent so that the bottom-referenced volume transport budget north of 30°N almost remains the same between the two pentads.

Figure 3.17 shows the dynamic height difference field for the 0 to 1500m depth interval and for the 0 to the bottom depth interval, respectively. In the former case, the steric sea level during the early 1970s increases by as much as 2.5 dyn cm at the northern side of the Gulf Stream but decreases in the central portion of the subtropical gyre region, with a peak magnitude of 7 dyn cm in the southern end of the Gulf Stream. All these features can be confirmed by comparison with Levitus's(1990) calculation(see Fig. 1.4). The dynamic height difference field for the surface to the bottom depth interval, shows similar steric sea level changes to that for the 0 to 1500m depth interval, except for the difference south of 30°N.

It is worth noting that, from figure 3.17, the steric sea level for the early 1970s increases about 2 dyn cm right up to the coast of Nova Scotia, but decreases about 6 dyn cm at Bermuda(32°N). Figure 3.18 shows annual mean anomaly sea level records from Halifax and Bermuda, using the observed sea level data from tide gauges. Both time series exhibit statistically significant temporal variability. Averaging the yearly mean sea level anomalies for each pentad, we note that at Halifax the 1955-1959 and 1970-1974 period exhibited average anomalies of 0.2 cm and 2.0 cm, respectively. This results in a 1.8 cm increase of sea level in the early 1970s compared to the late 1950s. This increase agrees quite well with figure

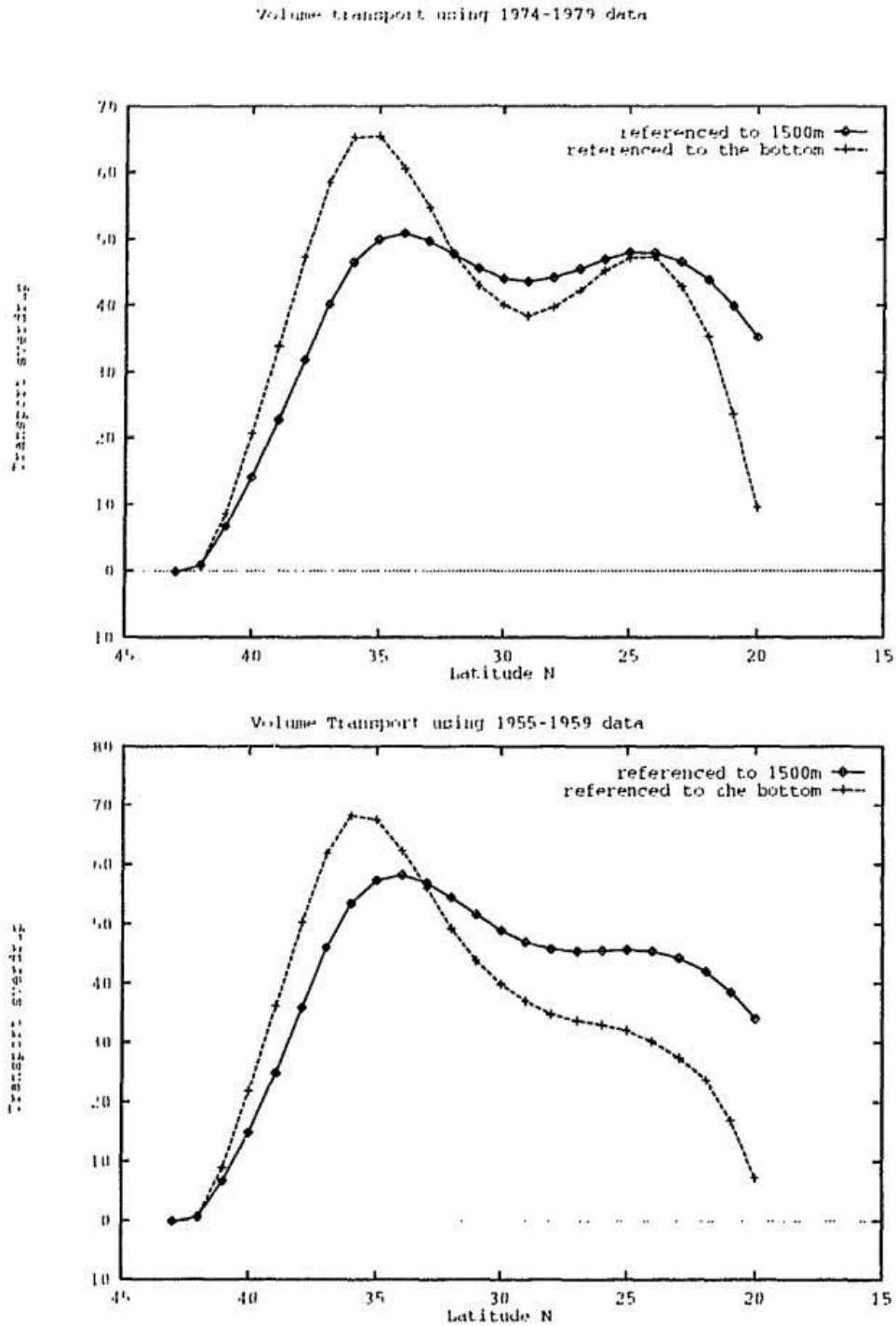

Figure 3.16: *Volume transport using (a) the upper panel, 1970-1974 and (b) the lower panel, 1955-1959 data*

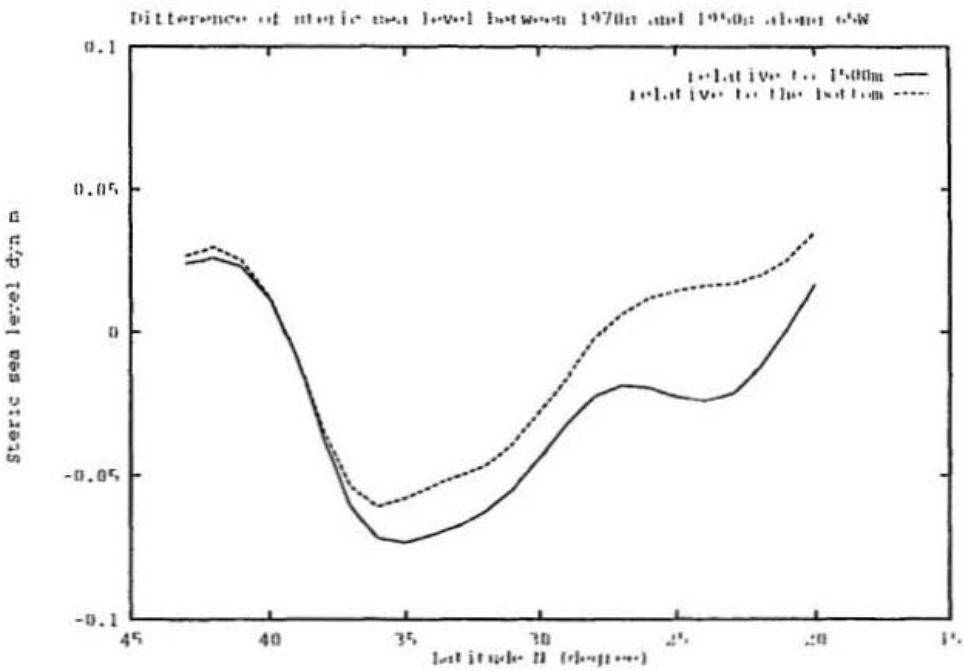

Figure 3.17: *Steric sea level differences using 1970-1974 minus 1955-1959 results*

3.17, which shows an increase of about 2 dyn cm to the coast of Nova Scotia. Roemmich(1985) found a 10 cm decrease in both sea level and steric sea level from the 1955-1959 pentad to 1970 at Bermuda. His results then indicate a sharp increase in both quantities until about 1974, when both quantities attained their 1955-1959 maxima. When averaging over the 1970-1974 period, the decrease in sea level from the 1955-1959 pentad to 1970-1974 pentad is in good agreement with the steric sea level changes revealed in figure 3.17.

The above studies along two sections, 55°W and 65°W, show similar features of the Gulf Stream in its shape and size. The estimates of the velocity and volume transport referenced to the bottom are also supported by previous works of various oceanographers. The investigation of the significant changes between two pentads, 1955-1959 and 1970-1974, are also attempted and some interesting results have been presented. Next, we continue our journey to study two sections along two lines of latitude, 24°N and 54°N.

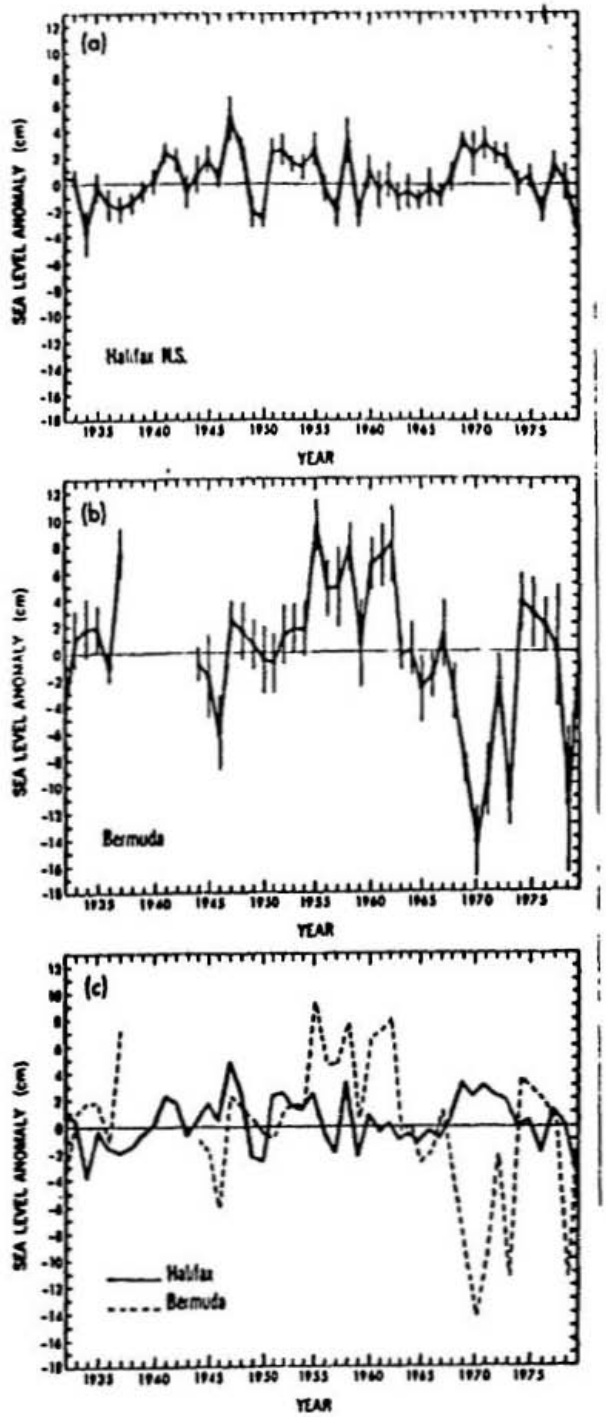

Figure 3.18: *Annual mean anomaly sea level (in centimeters) for (a) the upper panel, Halifax and (b) the middle panel, Bermuda, (c) the lower panel, Halifax and Bermuda, using the observed sea level data from tide gauges, according to Levitus, 1990*

3.2 Section through 54°N and 24°N latitude

A lot of effort has been spent on the understanding of the general circulation of the North Atlantic. Although the general pattern of the general circulation of the North Atlantic, the subtropical and subpolar gyres, has been agreed upon, the quantitative details of the subtropical and subpolar gyres, such as the velocity structure and poleward volume transport and heat transport, still remain poorly understood. In particular, the poleward heat transport by ocean currents has been given widespead attention by oceanographers during the last decade. For annual mean conditions, the Sun heats the Earth unevenly, with the greatest insolation occurring at the tropics and the least at the poles. This gives rise to a global meridional heat flux from the tropics to the polar region in order to balance the ocean-atmosphere system. Undoubtedly, the ocean plays an important role in contributing to this heat transport, for otherwise the planet we live on would have a much harsher climate everywhere. However, it was not until 1970s when several important papers (VonderHaar and Oort, 1973; Oort and VonderHaar, 1976; Bunker, 1976) convincingly suggested that the ocean heat transport might be comparable in magnitude to the atmospheric heat transport. In this section we will show some results along 54°N and 24°N latitude.

We now start by showing results obtained using our model along 54°N. The section is taken along 54°N latitude and between 55°W to 10°W, crossing the whole North Atlantic. The same three sets of density data as before, i.e. Levitus

(1982; 1989a,b,c) have been used to diagnose the velocity field and then calculate the poleward volume and heat transport.

Fig. 3.19a,b show the model-calculated velocity field through the section (positive being northward) referenced to 1500m and the bottom, respectively. The density field is the annual mean from Levitus (1982), and so should be representative of the climatological mean state. In figure 3.19a, the calculation is performed using 20 equally spaced z-levels at a horizontal resolution of 1°. In figure 3.19b, the calculation is performed using 80 equally spaced z-levels at a horizontal resolution of 1°. As before, there is no bottom velocity(according to eqn (2.14)). Therefore, the velocity field shown is actually velocity referenced to 1500m and the bottom, respectively. The figures show northward flow across the eastern part of the section which can be identified as the north-eastward North Atlantic Current. The wide current is from $47°W$ to the west coast of Europe in the upper 250m and from $35°W$ to the west coast of Europe in deep water. It has a maximum surface velocity of 4 cms^{-1} referenced to the bottom and the velocity decreases with depth, getting very weak in deep water. On the western side of the North Atlantic, there is a southward flow along the continental shelf and upper slope with a maximum surface velocity of 4 cms^{-1} referenced to the bottom. This southward flow can be identified as the Labrador Current.

Comparing these figures with the maps of the horizontal geostrophic circulation at two levels (100m and 1000m) by Olbers et. al.(1985)(fig. 3.20), we can

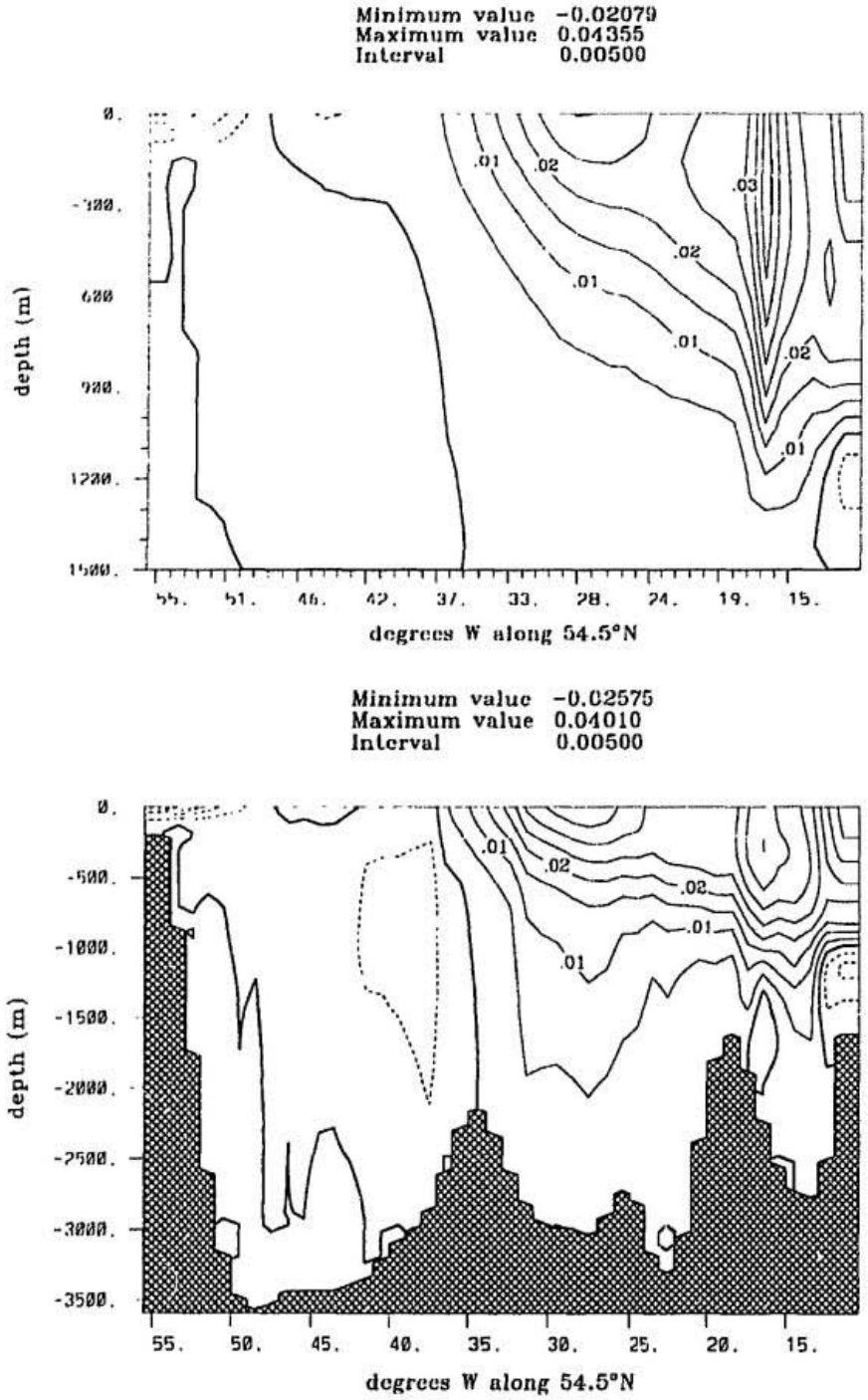

Figure 3.19: *Northward velocity field using annual mean data. (a) the upper panel, referenced to 1500 m (b) the lower panel, referenced to the bottom. The contour interval is* 0.01 ms^{-1}, *with dashed contours indicating southward velocity and solid contours northward. The minimum and maximum values are given in* ms^{-1}.

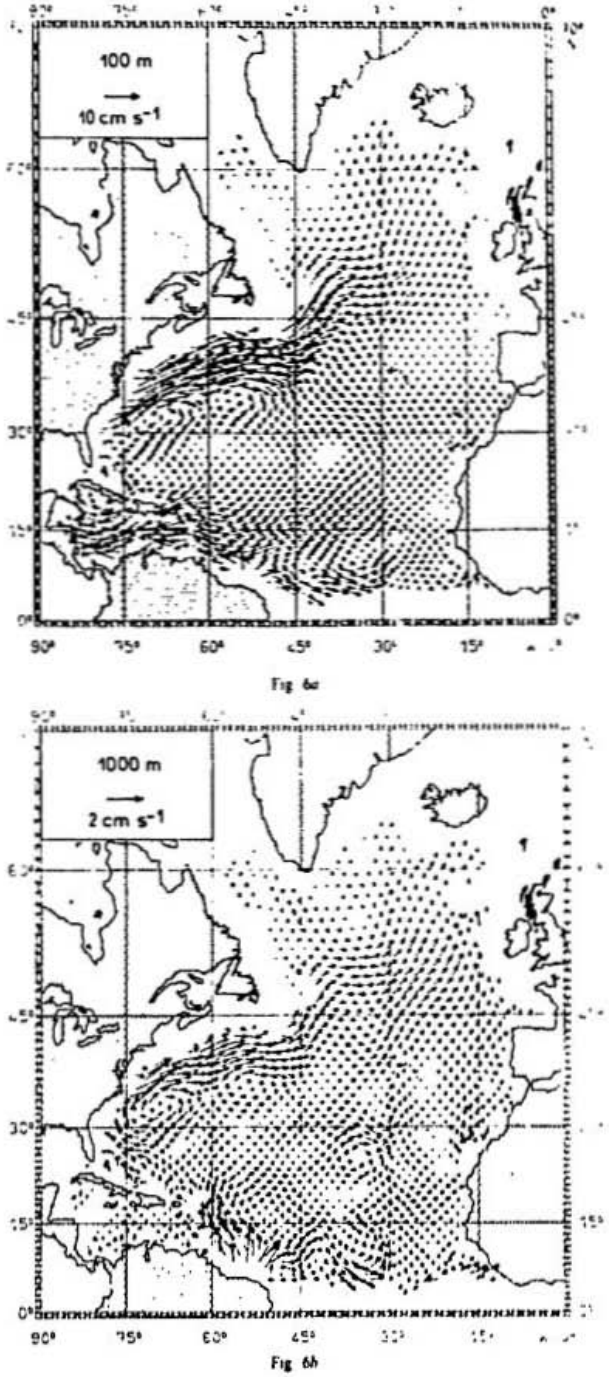

Figure 3.20: *Maps of horizontal geostrophic circulation referenced to 2000 m at (a) the upper panel, 100 m depth and (b) the lower panel, 1000 m depth, according to Olbers et. al.(1985), fig. 6*

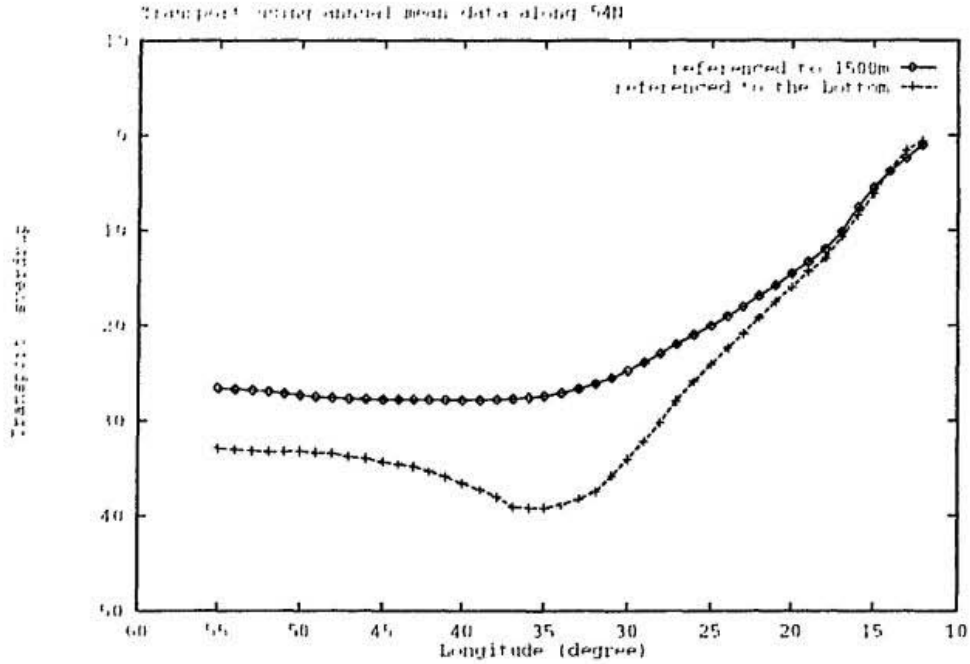

Figure 3.21: *Volume transport using annual mean data*

find good agreements in main features. They also used Levitus' (1982) climatological hydrographic data. Their figures were obtained by the classic calculation of the geostrophic velocity using the thermal wind relations. The horizontal velocities are referenced to 2000m, where a level of no motion is assumed. The profile across 54°N agrees quite well with that calculated from our model, both qualitatively and quantitatively. Both show the broad North Atlantic Current in the east part of the ocean with return southward flow in the west.

We further investigate the transport calculated from the model along this 54°N section (integrating westward from the eastern boundary). Fig 3.21 shows the transport referenced to 1500m and to the bottom respectively. The transport

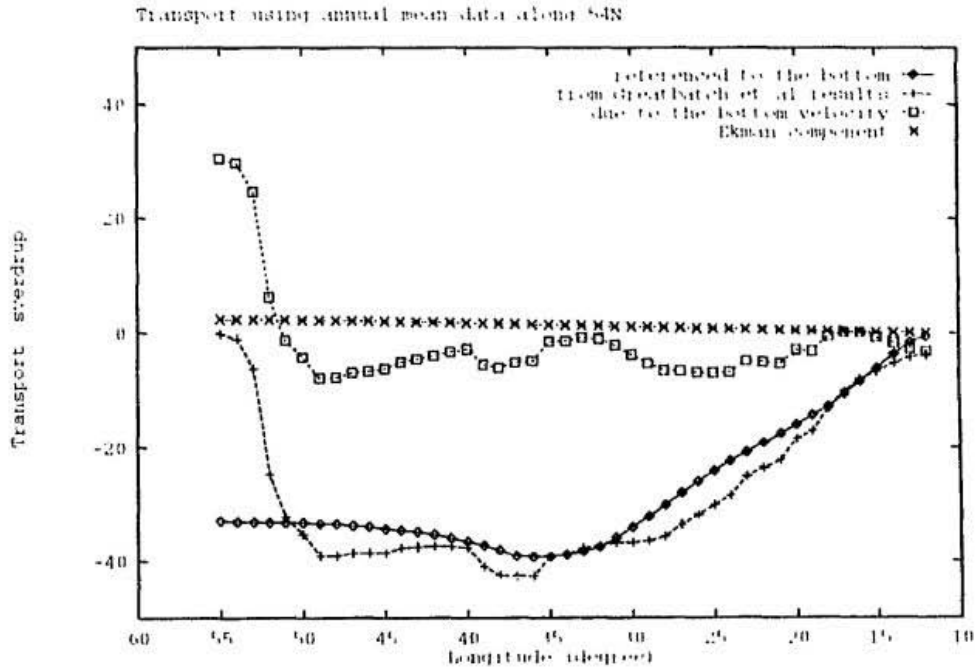

Figure 3.22: *Volume transport using annual mean data*

of the North Atlantic Current referenced to 1500m is about 25 Sv and the one referenced to the bottom is about 40 Sv. The return southward flow in the west is very weak with only about 5 Sv. This indicates that the southward return flow, particularly the Labrador Current, may have a strong barotropic part which can allow the total budget of volume transport be equal to zero, which is required by the conservation of mass. The mass budget is summed in Table 3.1 (see page 82).

We also attempted to investigate the bottom velocity by imposing an externally specified absolute transport through the section on our results. The externally specified absolute transport is obtained from the results of Greatbatch

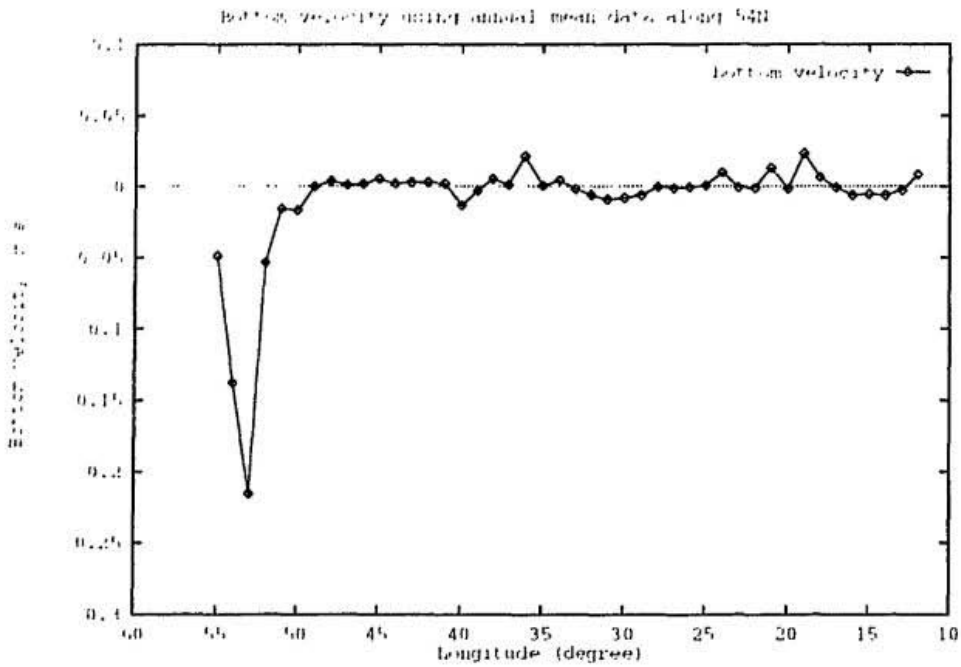

Figure 3.23: *Bottom velocity in annual mean case*

et al.(1991), being plotted in fig. 3.22. Their results show an essentially similar transport of the North Atlantic Current to that from our model, but exhibit a large amount of transport in the west continental shelf and slope region. The difference field (with Ekman transport also being removed) is also plotted in fig. 3.22, which represents the transport due to the bottom velocity. It clearly indicates a strong barotropic southward flow in the west continental shelf and slope region, with a maximum velocity of 20 cms^{-1} (fig. 3.23). This is what Lazier and Wright(1992) call the "deep Labrador Current", as distinct from the shelf break jet traditionally called the Labrador Current (Lazier and Wright present evidence from current meter data for the existence of the"deep" current).

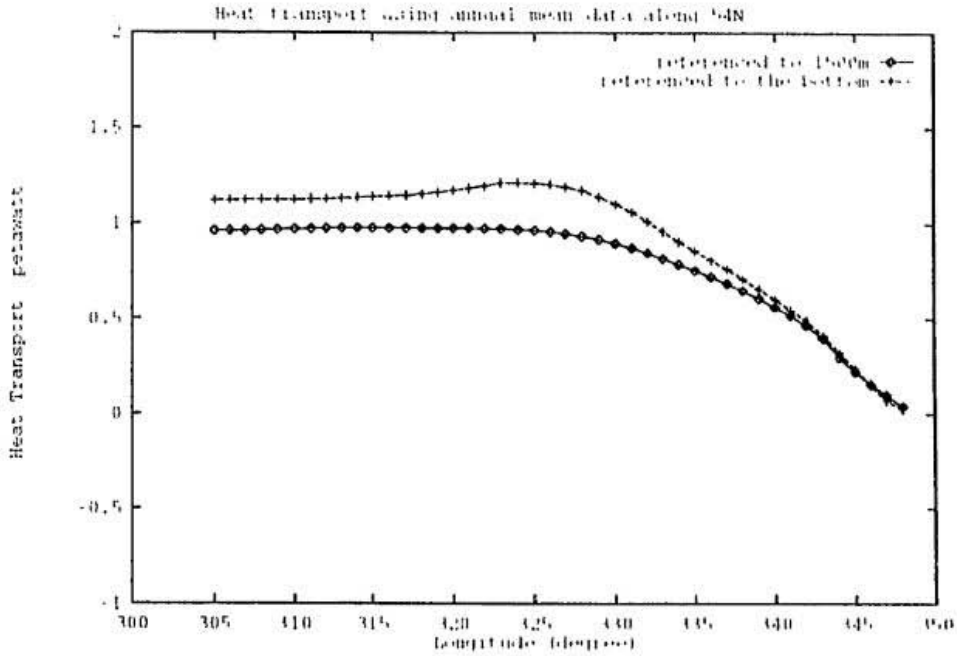

Figure 3.24: *Heat transport using annual mean data*

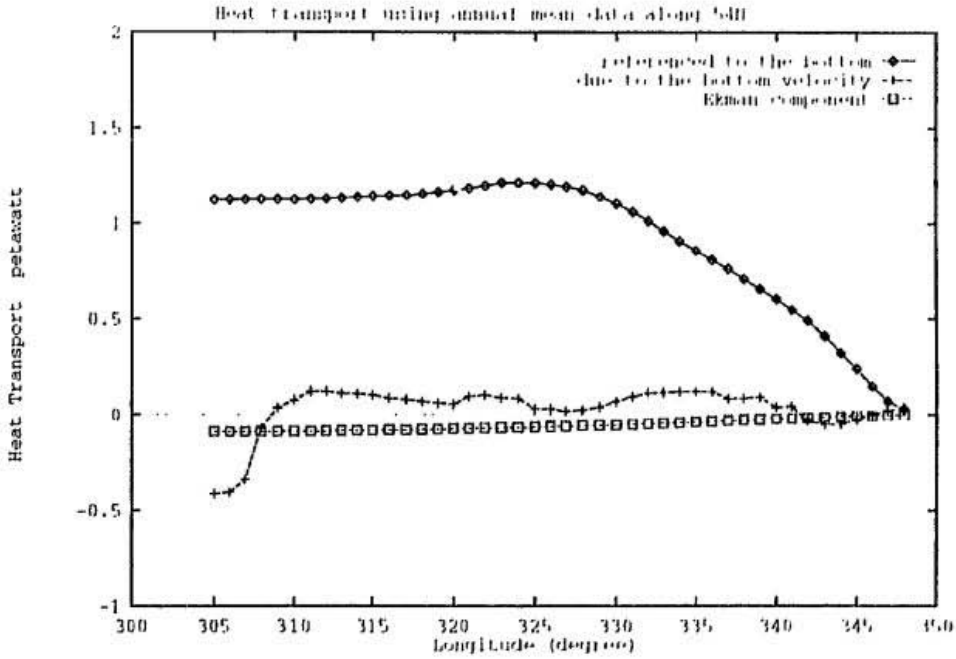

Figure 3.25: *Heat transport using annual mean data*

Fig 3.24 exhibits the heat transport referenced to 1500m (defined using equation(2.44) but with v_T substituted by the velocity referenced to 1500m and set to zero below 1500m) and to the bottom respectively (defined as before in eqn (2.44)). The heat transport of the North Atlantic Current referenced to 1500m is about 1.0 petawatts and that referenced to the bottom is about 1.1 petawatts. Again, the weak southward return flow referenced to the bottom contributes little because it has a strong barotropic part which can not be obtained from the model. Having the volume transport due to the bottom velocity as shown in fig. 3.22, we can calculate the heat transport due to the bottom velocity (fig. 3.25)(defined by eqn. (2.45). We can see that most of the heat transport due to the bottom velocity is in the continental shelf and slope region at the western end of the section, with an amount of about -0.4 petawatts(negative means southward). Fig. 3.25 also shows the Ekman heat transport of about -0.09 petawatts, indicating a prevailing eastward component of the wind. The sum of these three heat transport components, i.e., the Ekman heat transport, the heat transport referenced to the bottom, and the heat transport due to the bottom velocity, gives the total heat budget of poleward heat transport of about 0.6 petawatts carried by ocean currents towards the pole. This result agrees with previous estimates based of surface heat balance calculations (Hastenrath, 1980; Bunker, 1976). This net northward heat t ansport is mainly due to the relatively warm water carried by the North Atlantic Current to the north, whereas on the west side, the relatively

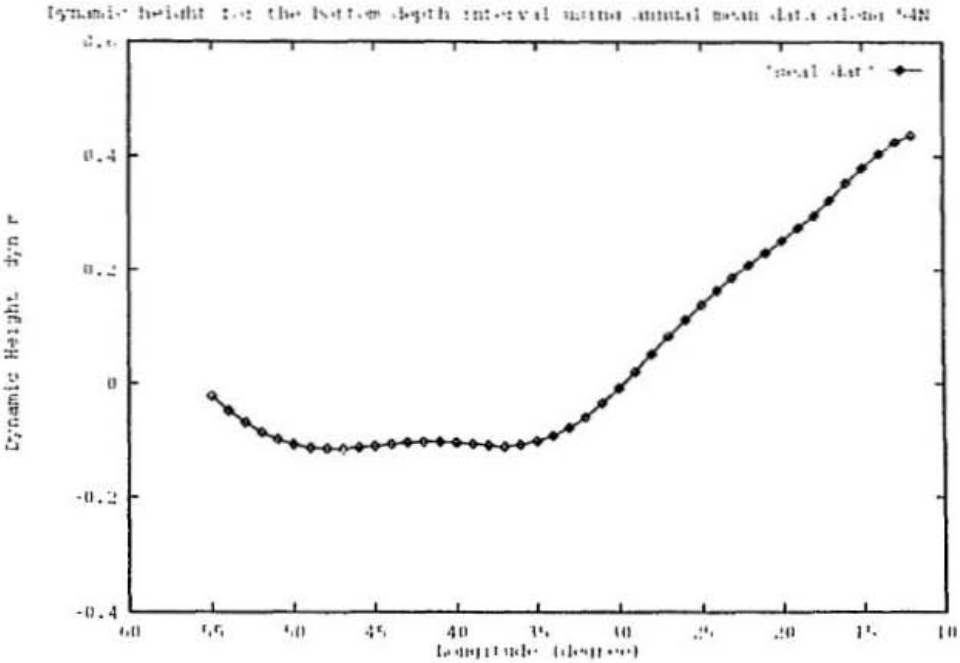

Figure 3.26: *Dynamic height for the bottom depth interval using annual mean data*

cold water carried in the Labrador Sea to the south. That is why that although the volume transport is nearly zero across the section by conservation of mass, there is net poleward heat transport.

Fig. 3.26 exhibits the dynamic height field for the surface to the bottom interval. The reference density is 1035.7 $kg\ m^{-3}$ in a contant density water column. The plot clearly shows that in the east part of the section, the dynamic height increases eastward, representing the North Atlantic Current flowing northward as the flow of the subpolar gyre system. In the western end, the dynamic height increases westward, indicating a southern flow.

Similar calculations have also been performed using 1970-1974 data and 1955-

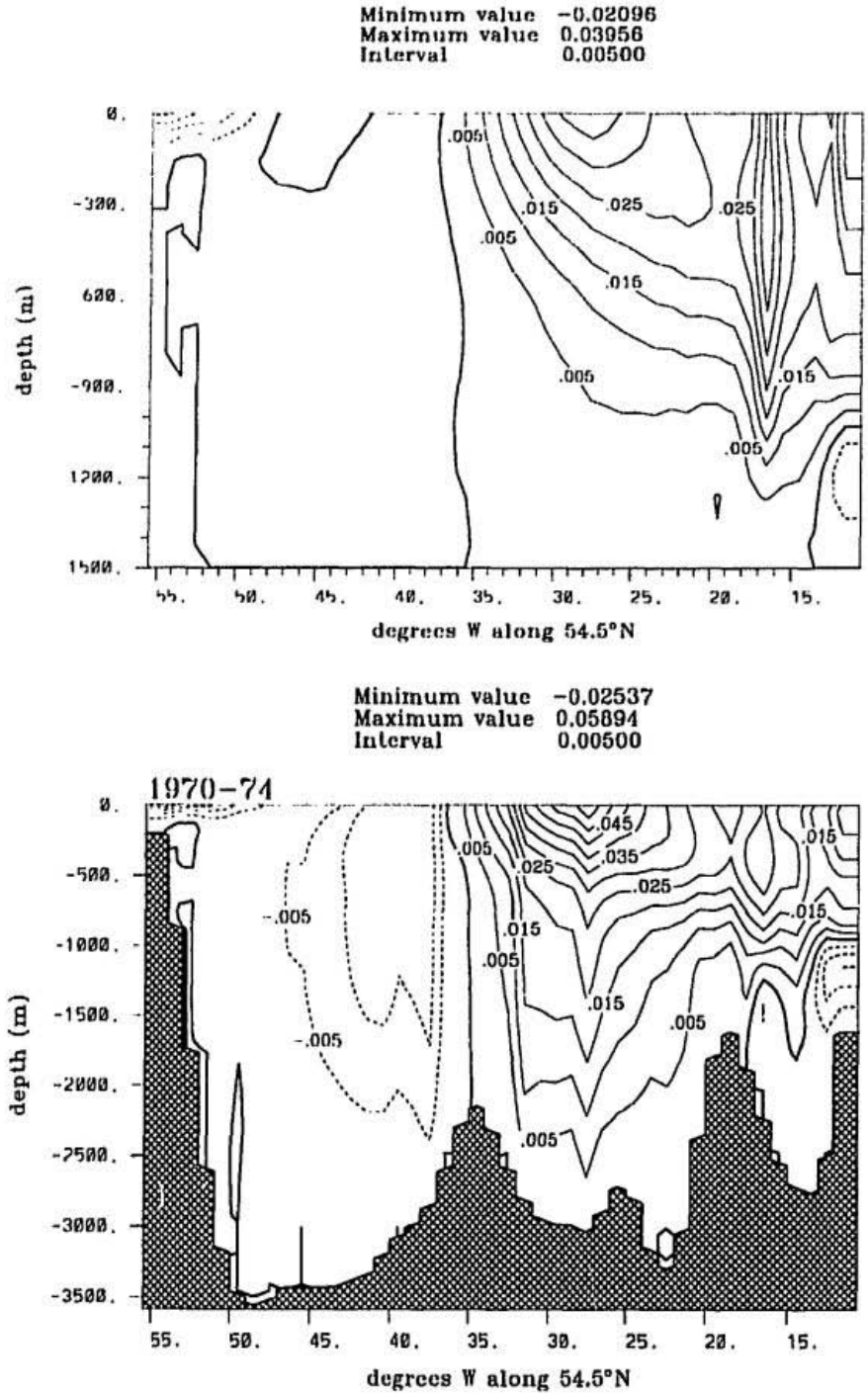

Figure 3.27: *Velocity field using 1970-1974 data. (a) the upper panel, referenced to 1500 m (b) the lower panel, referenced to the bottom. The contour interval is* 0.005 ms^{-1}, *with dashed contours indicating southward velocity and solid contours northward. The minimum and maximum values are given in* ms^{-1}.

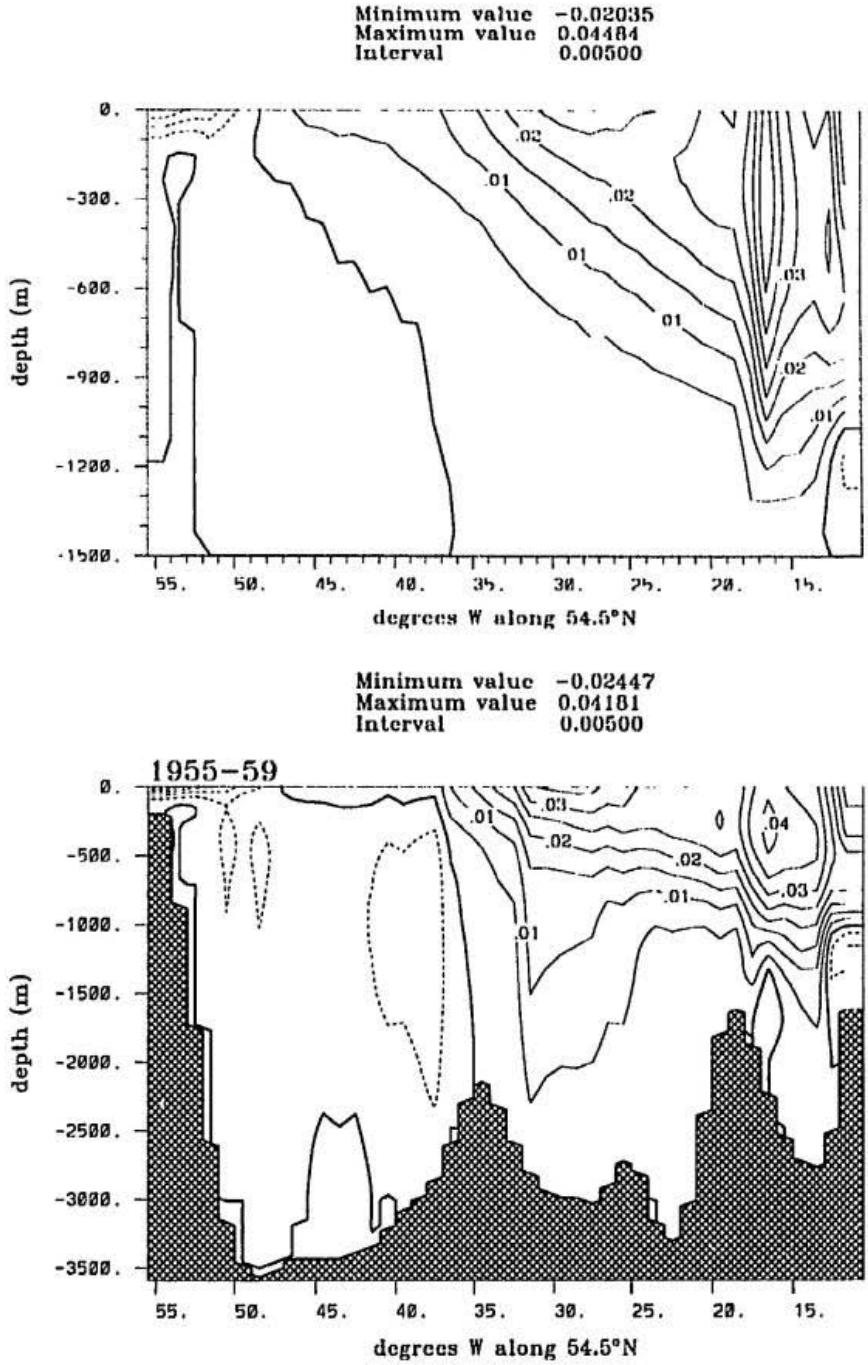

Figure 3.28: *Velocity field using 1955-1959 data. (a) the upper panel, referenced to 1500 m (b) the lower panel, referenced to the bottom. The contour interval is* 0.005 ms^{-1}, *with dashed contours indicating southward velocity and solid contours northward. The minimum and maximum values are given in* ms^{-1}.

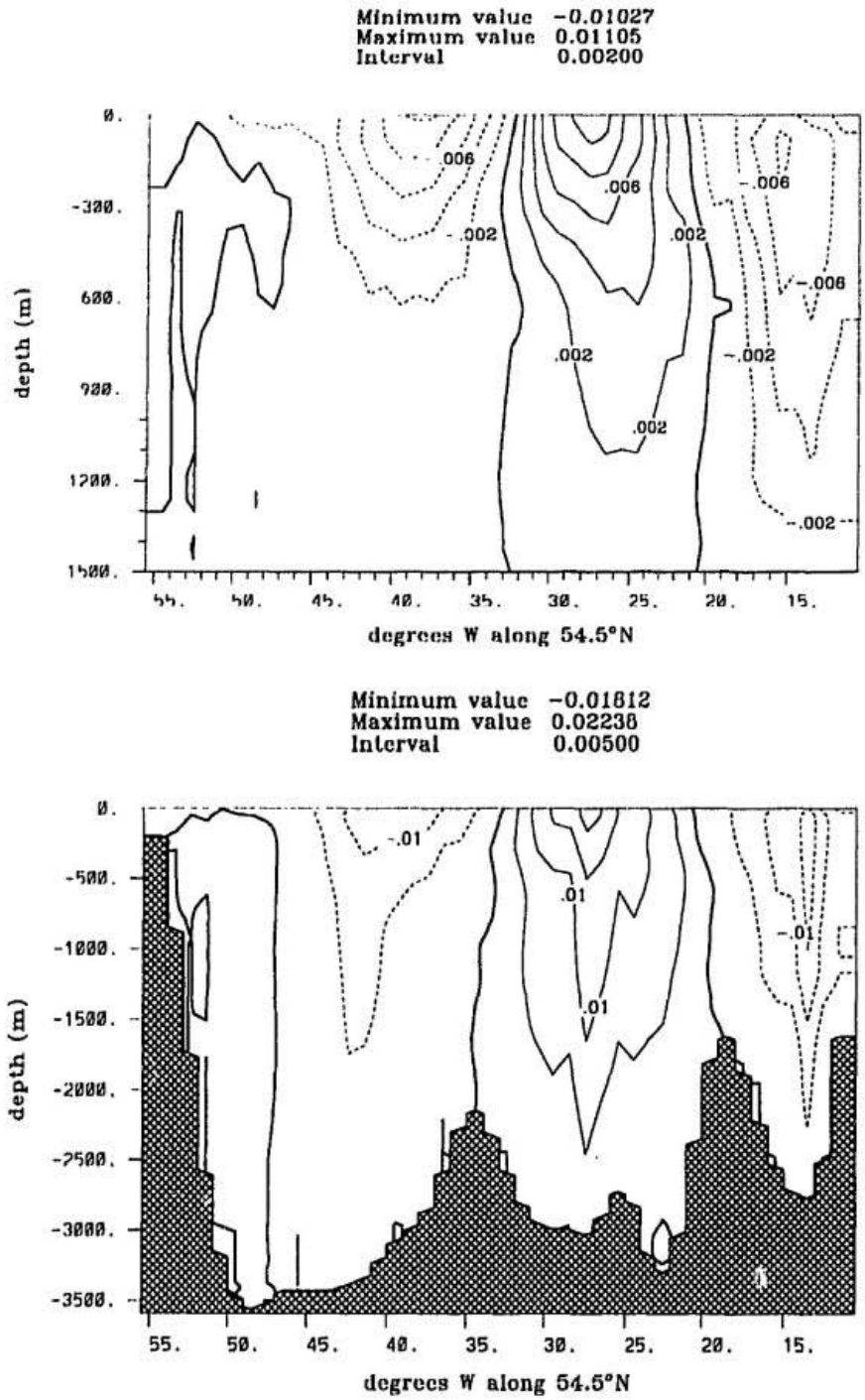

Figure 3.29: *Velocity field difference 1970-1974 minus 1955-1959. (a) the upper panel, referenced to 1500 m (b) the lower panel, referenced to the bottom. The contour interval is* 0.005 ms^{-1}, *with dashed contours indicating southward velocity and solid contours northward. The minimum and maximum values are given in* ms^{-1}.

1959 data to study the interpentadal variability between the two periods. Fig. 3.27a,b, 3.28a,b and 3.29a,b show the velocity field calculated from the model using 1970-1974 data, 1955-1959 data and the difference between the two, respectively, with (a) the upper panel, being that referenced to 1500 m and (b) the lower panel, referenced to the bottom. During 1955-1959 and 1970-1974, the flow pattern is basically the same as that of annual mean case, i.e., with the northward North Atlantic Current on the east side and with a southward return flow on the west side of the ocean. However, fig. 3.29 suggests that, comparing 1970-1974 to 1955-1959, the North Atlantic Current became weaker in its east part but stronger in its west part, both by a maximum magnitude of about 2 cms^{-1}. This is consistent with the northwestward shift of this part of the subpolar gyre noted by Greatbatch et al.(1991). The return southward flow also appears to be a more pronounced feature in the 1970-74 pentad. As along $55^{o}W$, the difference field (fig. 3.29) shows significant shear both below and above 1500m depth with the shear being of basically the same sign throughout the water column.

The differences in velocity field between 1970-1974 and 1955-1959 give rise to the differences in volume transport, heat transport, steric sea level, to mention a few. Fig. 3.30, 3.31 and 3.32 exhibit the volume transport during 1970-1974, 1955-1959, and the difference between the two, respectively. Comparing to 1955-1959, the transport referenced to the bottom of the North Atlantic Current increases about 8 Sv in 1970-1974, but this increase is compensated by the stronger

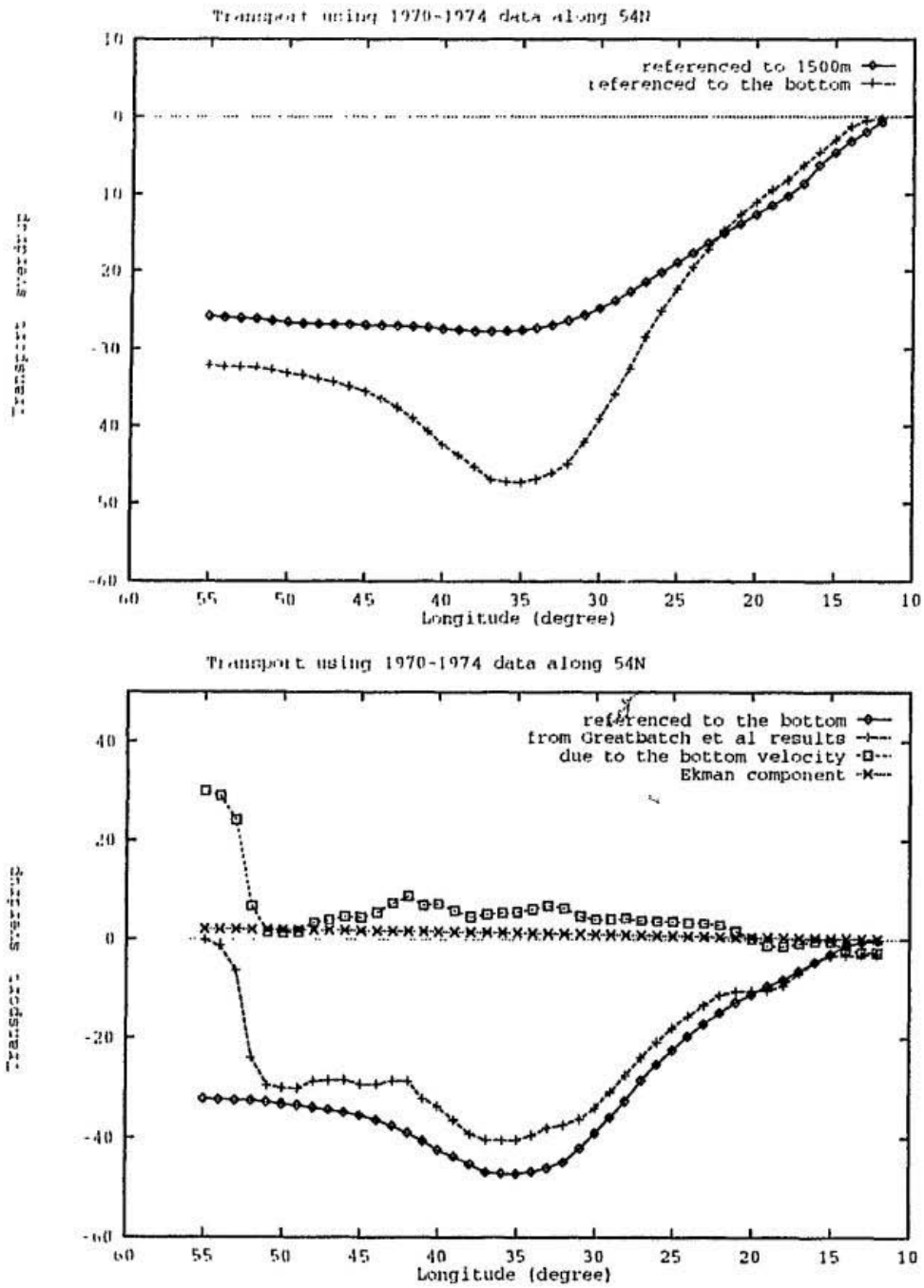

Figure 3.30: *Volume transport using 1970-1974 data*

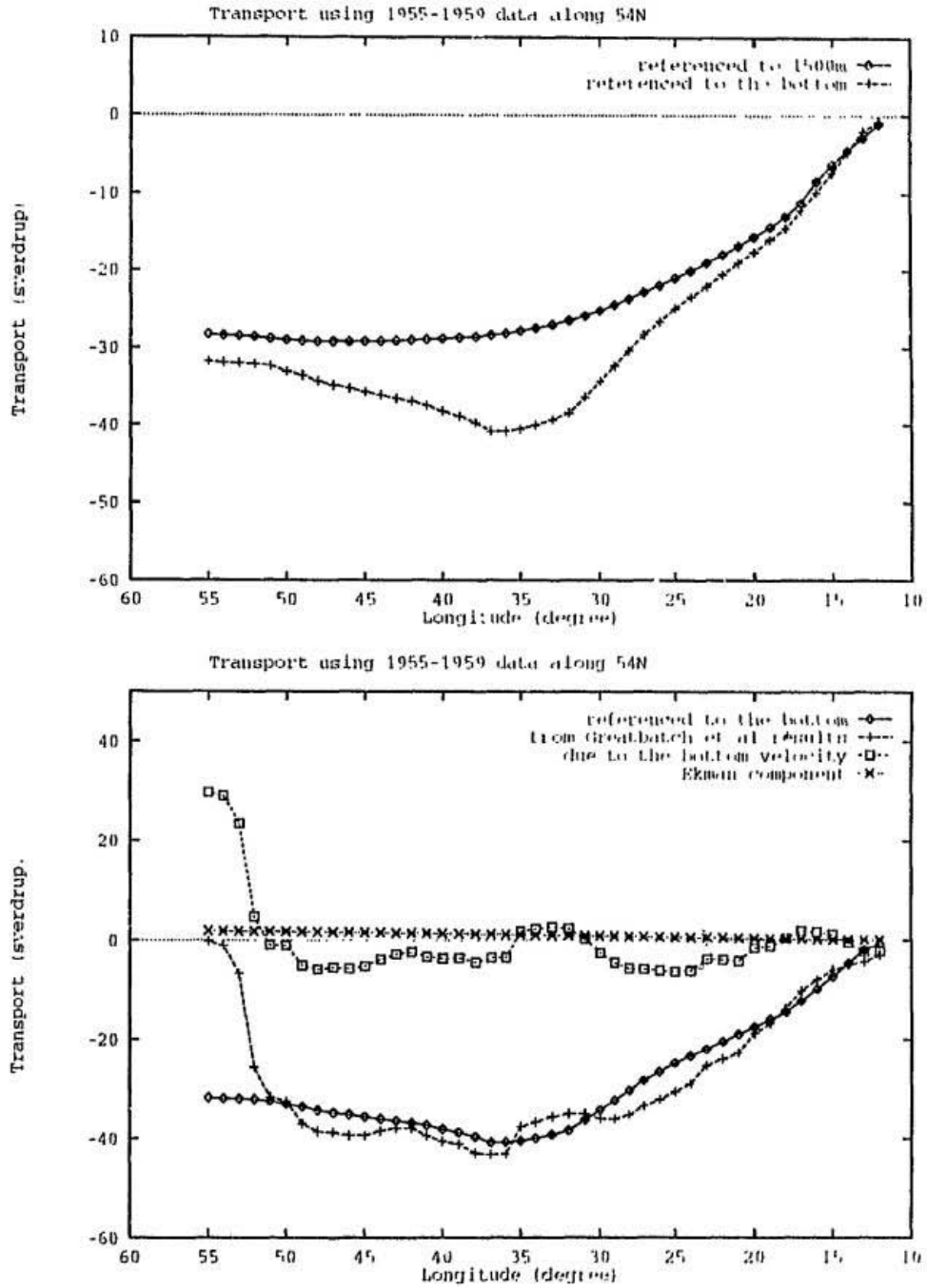

Figure 3.31: *Volume transport using 1955-1959 data*

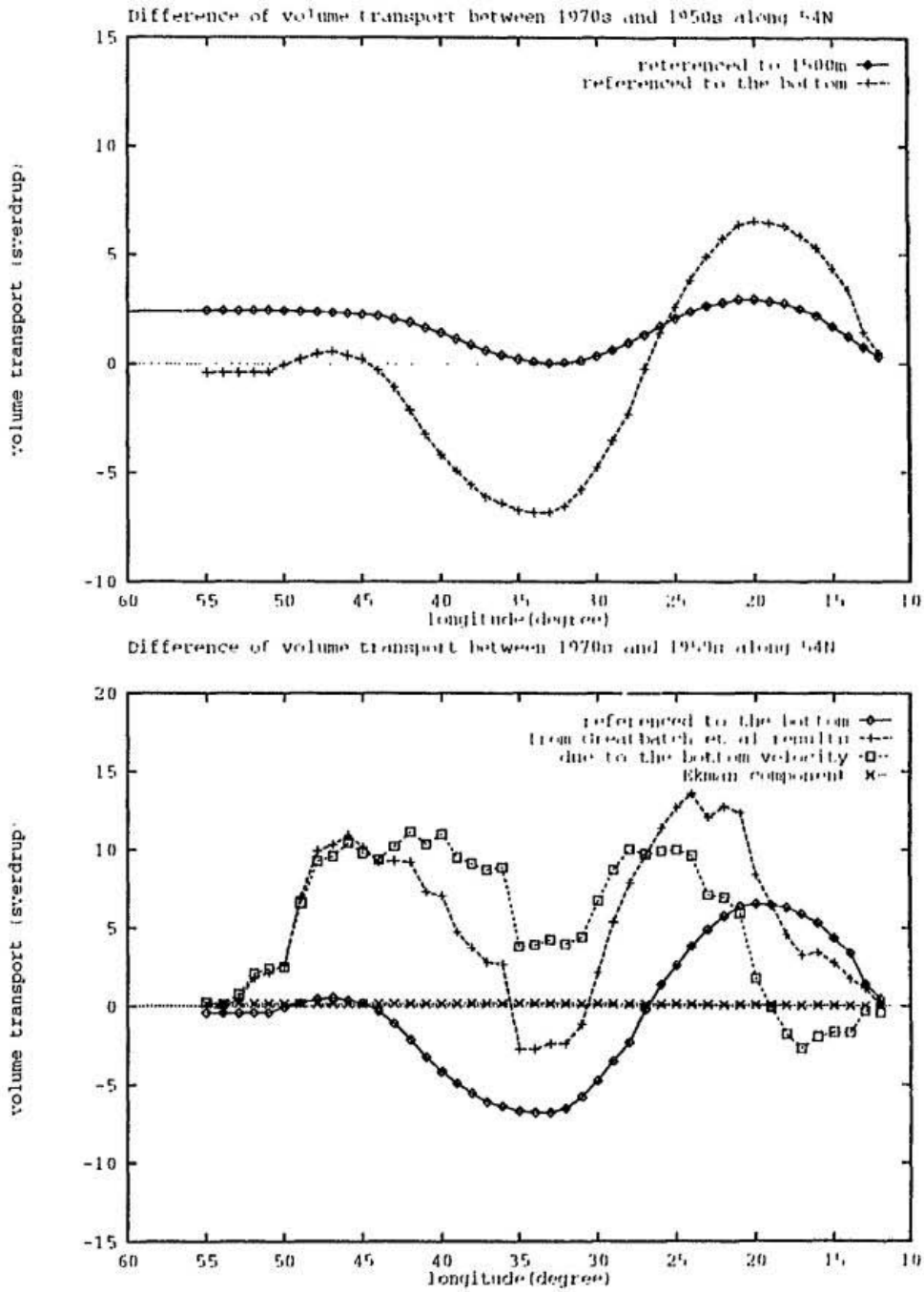

Figure 3.32: *Volume transport difference 1970-1974 minus 1955-1959*

return southward flow in 1970-1974, leaving the total differences in volume transport referenced to the bottom across the section almost zero. Figure 3.32 also indicate that a large part of the transport change referenced to the bottom occurs due to changes in velocity at or below 1500m (the transport is integrated westwards from the eastern boundary). By contrast, the volume transport in 1970s and 1950s themselves indicate that a large part of the bottom referenced transport in each pentad occurs referenced to 1500m, this being especially so in 1955-59 when the transport referenced to 1500m varies between about two-thirds and three quarters of the total referenced to the bottom.

Again, we impose the externally specified absolute transport through the section to our results. Fig. 3.30, 3.31 and 3.32 also show the plots of volume transport calculated by Greatbatch et al.(1991) for 1955-59, 1970-74 and the difference field 1970's minus 1950's. Also shown is the transport due to the bottom velocities obtained by subtracting the transport referenced to the bottom and the wind-driven Ekman transport (which totals about $2Sv$ in each pentad when integrated across the basin) from that calculated by Greatbatch et al.(1991). It is interesting that in the 1950's almost all the transport takes place referenced to the bottom. This is also true of the climatological annual mean case (fig. 3.22). In the 1970-74 pentad, the northward transport referenced to the bottom generally exceeds that diagnosed by Greatbatch et al., indicating the need for southward bottom velocities in some latitude ranges (e.g. near $20°W$). It is also

of interest that in each pentad (and also the climatological annual mean case as discussed before), mass balance can only be achieved by having a barotropic southward flow west of $50°W$ in the slope region off the coast of Labrador in what Lazier and Wright(1992) call the "deep Labrador Current". One worrying aspect of this is that there is no evidence of vertical shear associated with a deep western boundary undercurrent in the transport calculated referenced to the bottom, indicating that this is a very weak feature in the Levitus(1982,1989a,b,c) data sets (probably because of the smoothing associated with the objective analysis). The possible error due to this missing deep western boundary undercurrent (DWBU) will be discussed later. Looking at the difference field (Fig. 3.32), it is clear that the transport associated with the change in the bottom velocity is an important contributor to the total change in transport between the pentads. The tendency for bottom velocities to be more southward in the eastern part of the section is indicated by the upward trend as one moves to the west in the bottom transport curve in Fig. 3.32. The mass balance in each pentad is summarised in Table 3.1.

Fig. 3.33, 3.34 and 3.35 show the heat transport referenced to the bottom (as defined in eqn (2.44)) during 1970-1974, 1955-1959, and the difference between the two, respectively. The heat transport referenced to the bottom carried by the North Atlantic Current (from the coast of Europe to about $35°W$) is the same during two pentads period, indicating the water in 1955-1959 is, on average, warmer than that in 1970-1974, given the fact that the volume transport in

54.5°N	Climatology	1955-59	1970-74
relative to 1500 m	26.7	28.3	25.8
relative to bottom	33.0	31.8	32.2
transport due to bottom velocity	-30.6 (-31.2)	-29.9	-30.2
surface Ekman transport	-2.4 (-1.8)	-1.9	-2.0

54.5°N	Climatology	1955-59	1970-74
HT_{1500}	0.94	1.03	0.89
HT_T	1.09	1.16	1.05
HT_B	-0.43 (-0.43)	-0.38	-0.49
HT_{EK}	-0.09 (-0.07)	-0.08	-0.07
TOTAL	0.58 (0.59)	0.69	0.49

Table 3.1: *Volume transport (in Sverdrups) and Heat transport (in petawatts) through 54°N. Positive represents northward and negative, southward. In the climatology case, figures in brackets are calculated using da Silva and Levitus' wind stress.*

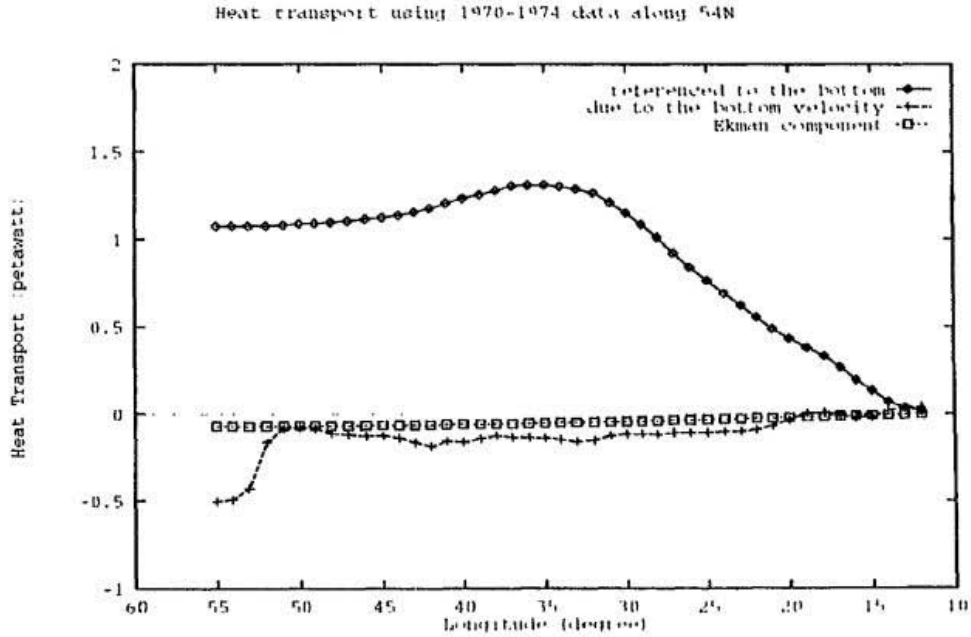

Figure 3.33: *Heat transport using 1970-1974 data*

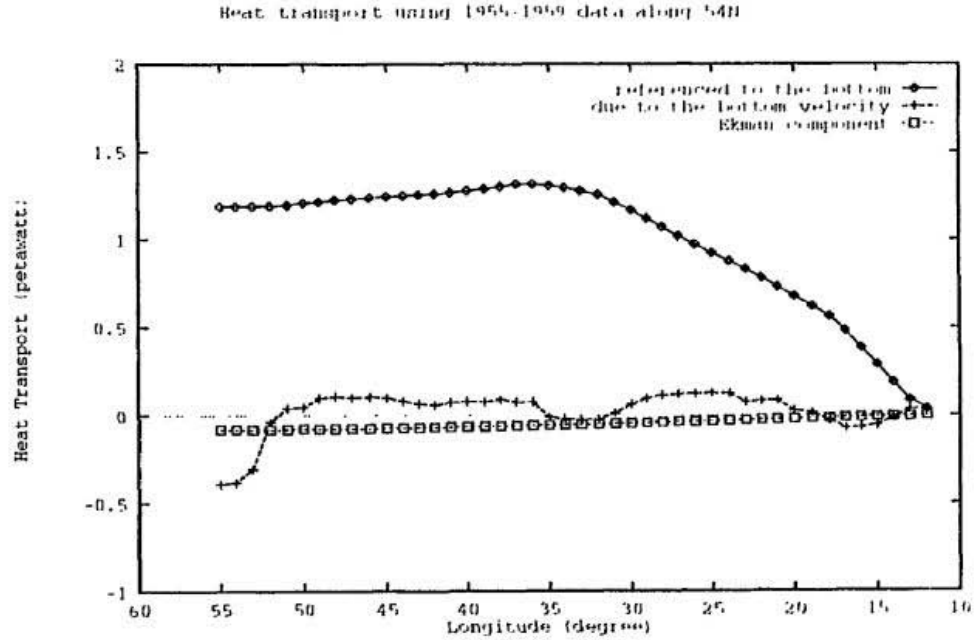

Figure 3.34: *Heat transport using 1955-1959 data*

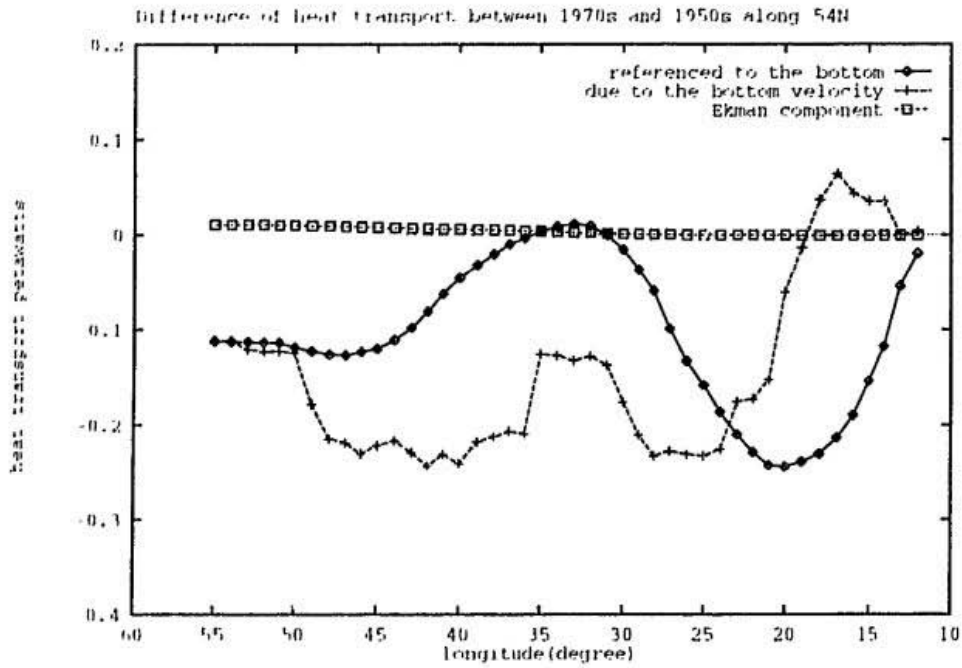

Figure 3.35: *Heat transport difference 1970-1974 minus 1955-1959*

1955-1959 is about 20 percent less that that in 1970-1974. The stronger return southward flow in 1970-1974 gives rise to a drop of the heat transport referenced to the bottom, a magnitude of about 0.12 petawatts. Having the bottom velocity (obtained as above) and the potential temperature field, we can calculate the heat transport associated with this bottom velocity (see eqn. (2.45)), which is also shown in Fig. 3.33, 3.34 and 3.35. The heat transport due to the bottom velocity in 1970-1974 is about 0.12 petawatts less (i.e. more southward) than that in 1955-1959. (see fig. 3.33, 3.34 and 3.35, and also in Table 3.1.) Combining the difference of the heat transport referenced to the bottom, 0.12 petawatts southward, the Ekman component, 0.01 petawatts northward and the difference

due to the bottom velocity, 0.12 southward, the total heat budget in 1970-1974 drops about 0.2 petawatts, as being summed up in Table 3.1.

The Table 3.1 also includes the heat transport decomposition in the annual mean case. It indicates a climatological annual mean northward heat transport of 0.6 PW as noted previously. The values calculated for 1955-59 and 1970-74 are $0.7PW$ and $0.5PW$, respectively. It is not clear whether these values are significantly different from each other. It is difficult to estimate the error in the calculations at this latitude. The biggest source is likely to be in the representation of the DWBU, which as we saw when discussing Fig. 3.22, appears as a barotropic flow in the continental slope region off Labrador. One way to assess this error is to assume that all the transport associated with this flow where at a potential temperature representative of this flow. If we take this to be $1.5°C$, then since the vertically average potential temperature in this part of the section is $2.5°C$, it follows that this contribution to the northward heat transport in equation (2.46) will be increased, leading to a revised estimate for the annual mean northward heat transport of $0.8PW$ - i.e. an increase of $0.2PW$. It should be noted, however, that it is unlikely all the $30Sv$ required to satisfy mass balance through this section takes place in the DWUC, so that the $0.2PW$ represents an upper bound on the magnitude of this error. It should also be noted that this estimate of error does not include the effect of eddies. It is clear from the table that the difference between the pentads occurs partly because of the change in the

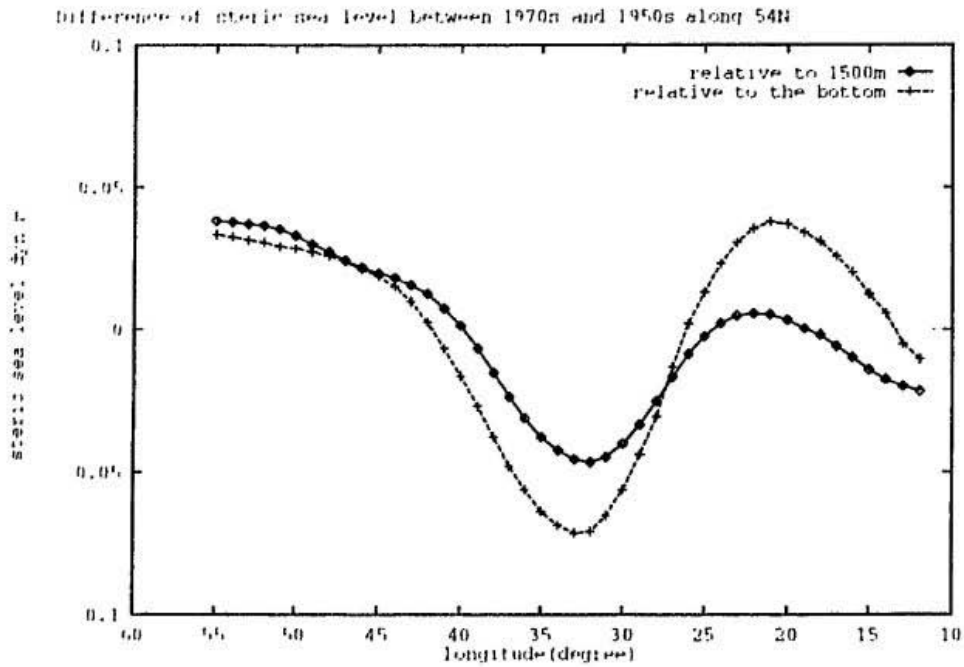

Figure 3.36: *Steric sea level changes 1970-1974 minus 1955-1959*

heat transport due to the transport referenced to the bottom and partly because of the change in the heat transport associated with the bottom velocities.

The study of the dynamic height difference field, which also represents the change in steric sea level, reveals differences between two pentads. The steric sea level difference field for the 0 to 1500m depth interval (fig 3.36) shows that the steric sea level during 1970s increase by as much as 4 dyn cm in the west continental shelf and slope region, and decrease by as much as 5 dyn cm in the western side of the North Atlantic Current compared to the 1950s. The increase is because of the stronger southward return flow (referenced to the bottom) in the west part of the section during 1970-1974 whereas the decrease pattern is

due to the stronger northward North Atlantic Current on its west part. Levitus's calculation (see fig. 1.4) of the dynamic height difference field calculated directly from the density with an assumption of a depth of no motion at 1500m agrees very well with our results.

We now turn to the section that crosses the subtropical gyre at 24°N and between 75.5−17.5°W, i.e., from the Bahama Islands to the west coast of Africa. Of particular interest is the total poleward heat transport across the North Atlantic, which includes not only the heat transport from the section we are studying, but also that from Florida Current. The latter part is taken from other author's results.

Figure 3.37a,b show the velocity field across this 24°N section referenced to 1500m and the bottom, respectively, diagnosed from the model, with positive being northward and negative being southward. Both figures represent the climatological mean state and are calculated using Levitus (1982) annual mean density data. They show that this section is dominated by southward flow, stronger in the upper 1000m of the water column, with a maximum value of 3 cms^{-1} near surface and weaker towards the bottom. The upper layer southward flow is the flow which Leetmaa et al.(1977) and, later, Roemmich and Wunsch(1985), associate with the wind-driven gyre. On the west end of the section, there exists a northward flow concentrated down to about 1000m, with a magnitude of up to 2.5 cms^{-1}. This can be identified as the northward Antilles Current.

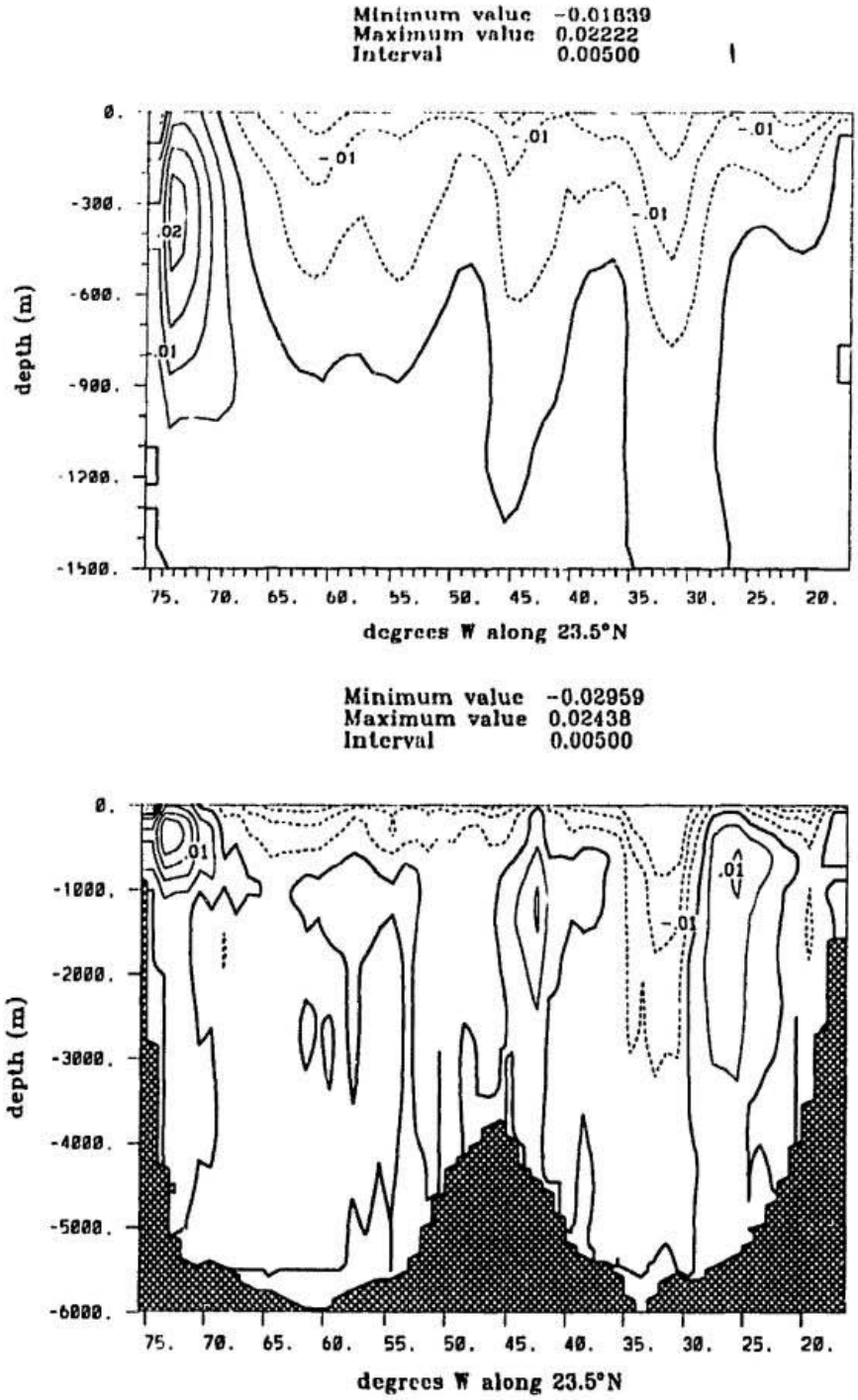

Figure 3.37: *Northward velocity field using annual mean data. (a) the upper panel, referenced to 1500 m (b) the lower panel, referenced to the bottom. The contour interval is* 0.005 ms^{-1}, *with dashed contours indicating southward velocity and solid contours northward. The minimum and maximum values are given in* ms^{-1}.

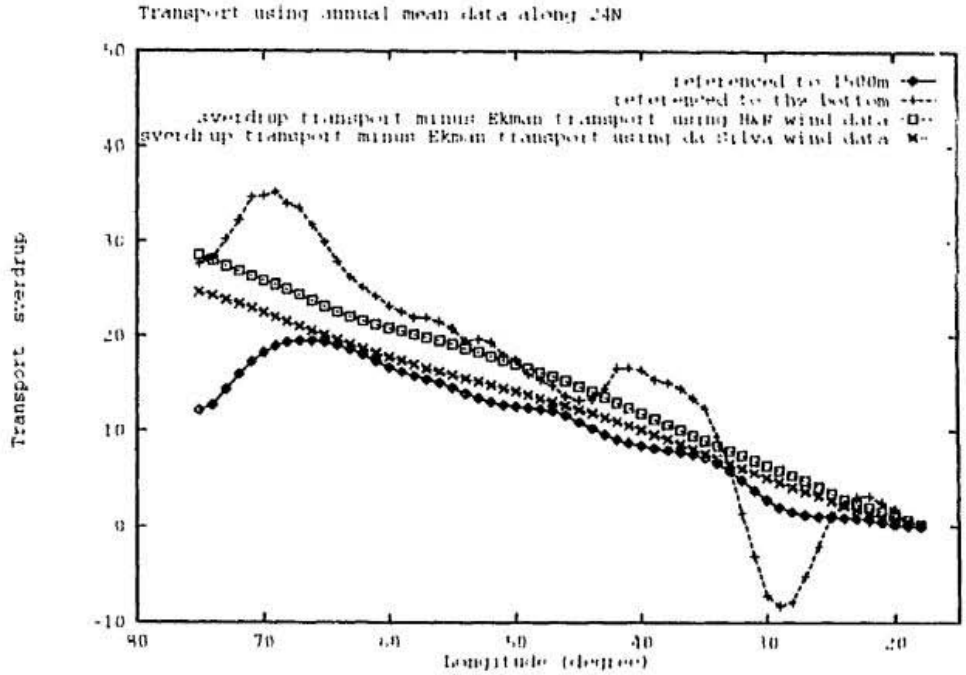

Figure 3.38: *Volume transport using annual mean data*

Figure 3.38 exhibits the volume transport referenced to 1500m (considering only the water column above 1500 m) and to the bottom, respectively, which is calculated from the model along this 24°N section. It shows that the transport referenced to 1500m increases steadily to a value of $20Sv$ near $65°W$, after which it drops again by about $8Sv$ in association with the Antilles Current. Also plotted in Fig. 3.38 is the geostrophic transport associated with the wind-driven gyre assuming a linear vorticity balance (i.e. the difference between the flat-bottomed Sverdrup transport and the Ekman transport) as given by the climatological annual mean wind stress of Hellerman and Rosenstein (1983) and da Silva and Levitus. The similarity between these curves and the transport referenced to

1500m (in particular, their common slopes) is the same result as found by Leetmaa et al.(1977) using the Bunker(1976) wind stress field. However, as pointed out by Roemmich and Wunsch(1985), there is also a thermohaline component to the circulation through the section. Indeed, the total bottom-referenced transport through the section (including the Antilles Current) is $28Sv$ to the south. This is balanced by $6Sv$ of northward Ekman transport and the $30Sv$ northward flow in the Florida Current, implying that an additional $8Sv$ must flow southward through the section in association with non-zero bottom velocities.

Similar to what we did for the 54°N section, we attempted to estimate the transport due to the bottom velocity by imposing an externally specified absolute transport through the section on our results. The attempt to impose the absolute transport diagnosed by Greatbatch et al(1991) did not give satisfactory results because their total transport through the section from the west coast of Africa to Bahama is only about 16 Sv southward. This, in turn, requires the same amount of water flow northward through Florida Strait by conservation of volume. This amount (16 Sv) obtained by Greatbatch et al. is far less than the measured transport of about 30 Sv through the Florida Straits (Niller and Richardson, 1973; Larsen, 1992), possibly because of the big error of Greatbatch et al.'s model in low latitude where the Coriolis parameter f is small. Instead of using Greatbatch et al.'s results for this 24°N section, we assume that the total southward transport through the section must be balanced by the north-

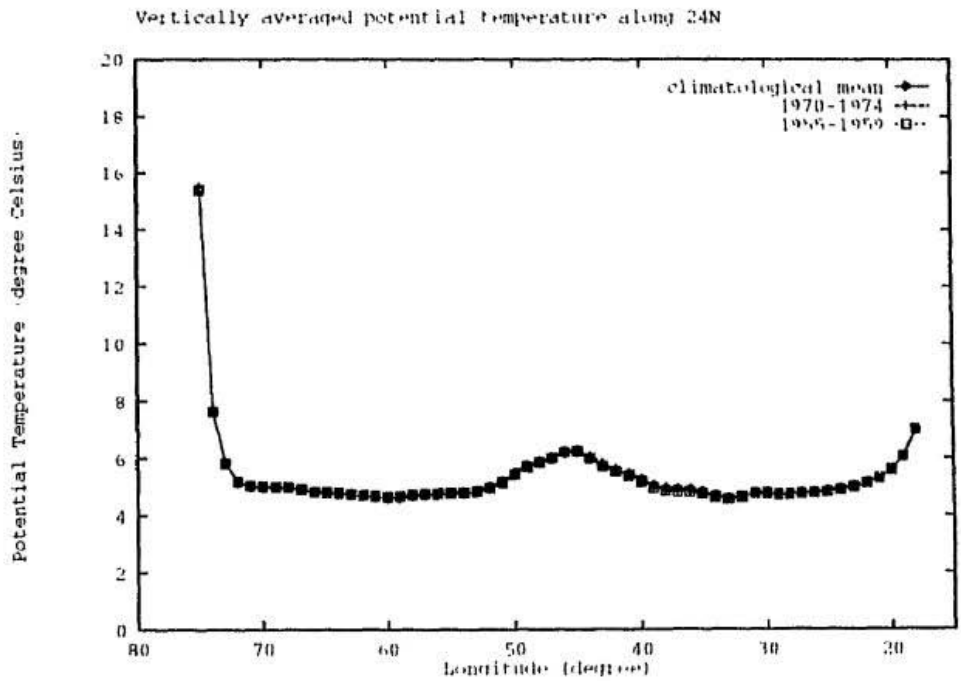

Figure 3.39: *Vertically averaged potential temperature along 24°N*

ward flow through the Florida Straits. We take the northward flow through the Florida Straits to be the $29.5Sv$ annual mean transport between Miami and Bimini as found by Niiler and Richardson(1973) rather than the $32.2Sv$ annual mean transport given by Larsen(1992) for the transport east of Jupiter Inlet further north (Larsen attributes this difference to flow through the Northwest Providence Channel).

When calculating the heat transport, we adopted an approach very similar to that used by previous authors (Hall and Bryden,1982; Roemmich and Wunsch, 1985; Molinari et al.,1990). By conserving the mass through the section, we require some $8Sv$ of southward transport associated with non-zero bottom veloc-

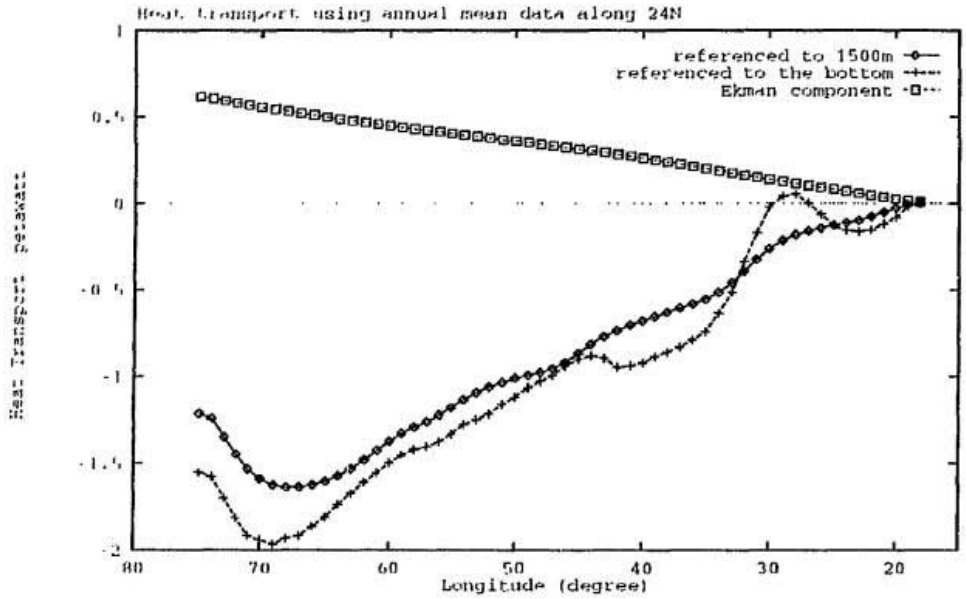

Figure 3.40: *Heat transport using annual mean data*

ities through the section in the case of the climatological annual mean transport. Fig. 3.39 shows the vertically averaged potential temperature along $24°N$, which illustrates that, except for the Mid-Atlantic Ridge region and the coast regions, the vertically averaged potential temperature is nearly uniform throughout the section. By making use of the fact that the vertically averaged potential temperature on the section is almost uniform from east to west (see Hall and Bryden, 1982, Fig.3 and Levitus, 1987, Fig.1), we do not need to know how this transport is distributed across the section. This makes evaluation of the bottom velocity part of the heat transport in equation (2.45) a straightforward matter.

The heat transport referenced to the bottom shown in figure 3.40 exhibits a

magnitude of about 1.5 petawatts (southward) carried by the southward ocean transport across the full width of this section, excluding the Florida Straits. The Ekman heat transport is shown in figure 3.22, which is about 0.6 petawatts northward when using wind stress of Hellerman and Rosenstein (1983), and is about 0.5 petawatts northward when using wind stress of da Silva and Levitus. The northward Ekman heat transport is a direct result of the prevailing easterly trade wind. Combining the Ekman part and the part referenced to the bottom gives rise to a southward heat transport of 1.6 petawatts. As mentioned before the part associated with non-zero bottom velocity can be easily calculated by making use of the fact that the vertically averaged potential temperature on the section is almost uniform. If we can estimate the heat transport through the Florida Straits, the total poleward heat transport across the ocean can thus be obtained.

We estimate the heat transport through the Florida Straits by using Larsen's (1992) results. He estimated the heat flux into the North Atlantic to be,

$$Q(t) = \rho C_p[\theta_{FC}(t) - \theta_{NA}(t)]T(t) \tag{3.1}$$

where $\theta_{FC}(t)$ is the flow temperature of the northward moving Florida Current, $\theta_{NA}(t)$ is the flow temperature of the southward moving North Atlantic east of the Florida Straits, and $T(t)$ is the transport of the Florida Current. Here the flow temperature is the velocity weighted potential temperature. He assumed that

$\theta_{NA}(t)$ has the constant value $9.43°C$ and $\theta_{FC}(t)$ has the constant value $19.10°C$, the latter being based on the measurements taken in the Florida Current. Based on 4170 daily mean values, he obtained the heat flux into the North Atlantic to be 1.27 petawatts, with transport of the Florida Current $T(t)$ being 32.2 Sv. Doing a simple calculation, we can derive the heat transport of the Florida Current alone to be $\rho C_p \theta_{FC}(t) T(t)$ - 2.31 petawatts northward. In this calculation, we assume the volume transport of the Florida Current to be 29.5 Sv rather than 32.2 Sv used by Larsen(1991) but continue to use a flow temperature of $19.10°C$. 29.5 Sv is the value more appropriate at this latitude ($24°N$). Considering every component of heat transport across $24°N$, we obtained a total poleward heat transport of about 1.2 petawatts, in excellent agreement with the previous estimates of $1.2PW$ by each of Hall and Bryden(1982), Roemmich and Wunsch(1985) and Molinari et al.(1990) for $25°N$, $24°N$ and $26.5°N$, respectively. When the wind stress field of da Silva and Levitus is used instead of Hellerman and Rosenstein(1983), the climatological annual mean value gives a similar result. This is summarised in Table 3.2 (page 98).

Similar calculations have also been performed using 1970-1974 data and 1955-1959 data to study the interpentadal variability between the two periods. Fig. 3.41a,b, 3.42a,b and 3.43a,b show the velocity field calculated from the model using 1970-1974 data, 1955-1959 data and the difference between the two, respectively, with (a) the upper panel, being that referenced to 1500 m and (b)

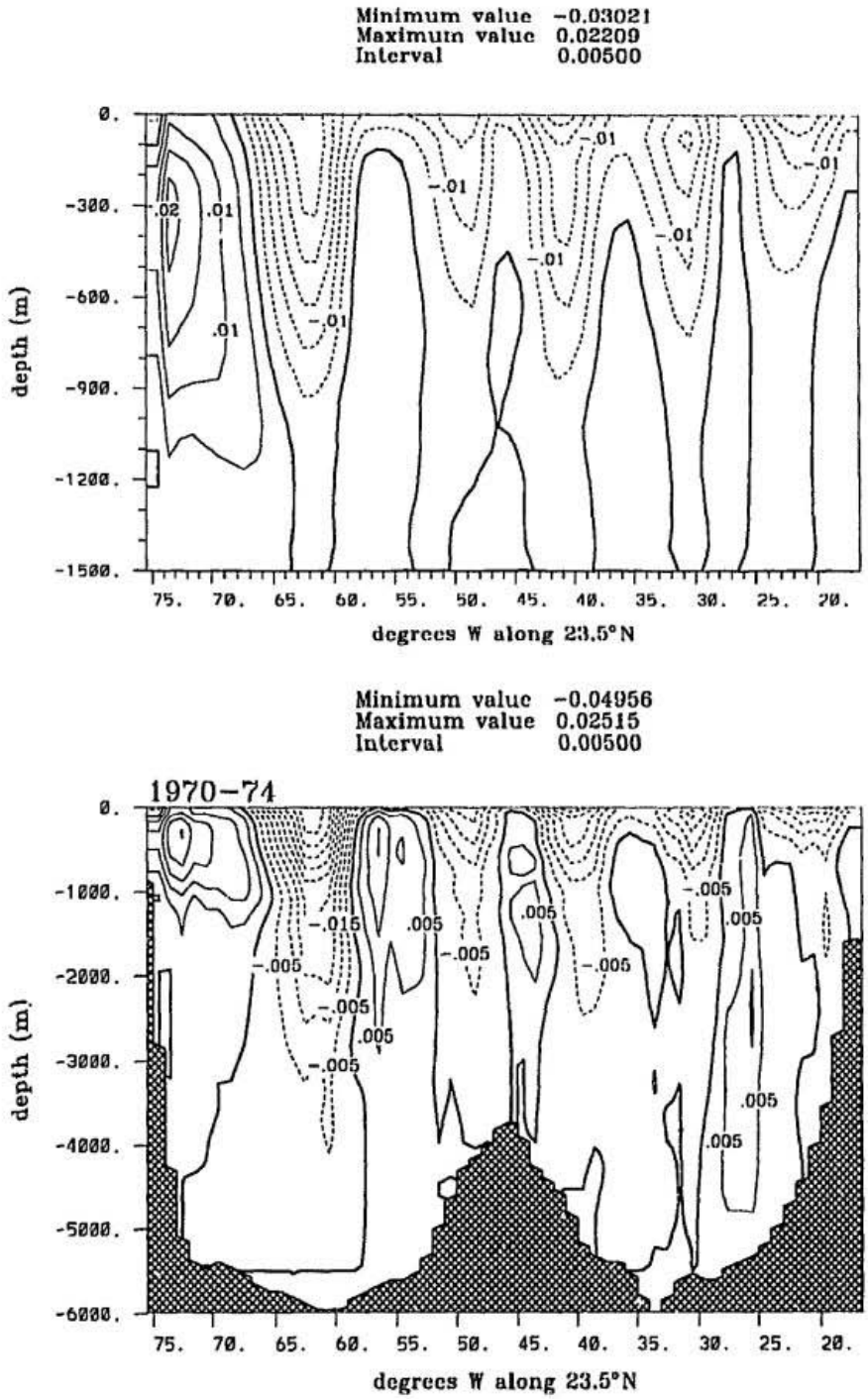

Figure 3.41: *Velocity field using 1970-1974 data. (a) the upper panel, referenced to 1500 m (b) the lower panel, referenced to the bottom. The contour interval is* 0.005 ms^{-1}, *with dashed contours indicating southward velocity and solid contours northward. The minimum and maximum values are given in* ms^{-1}.

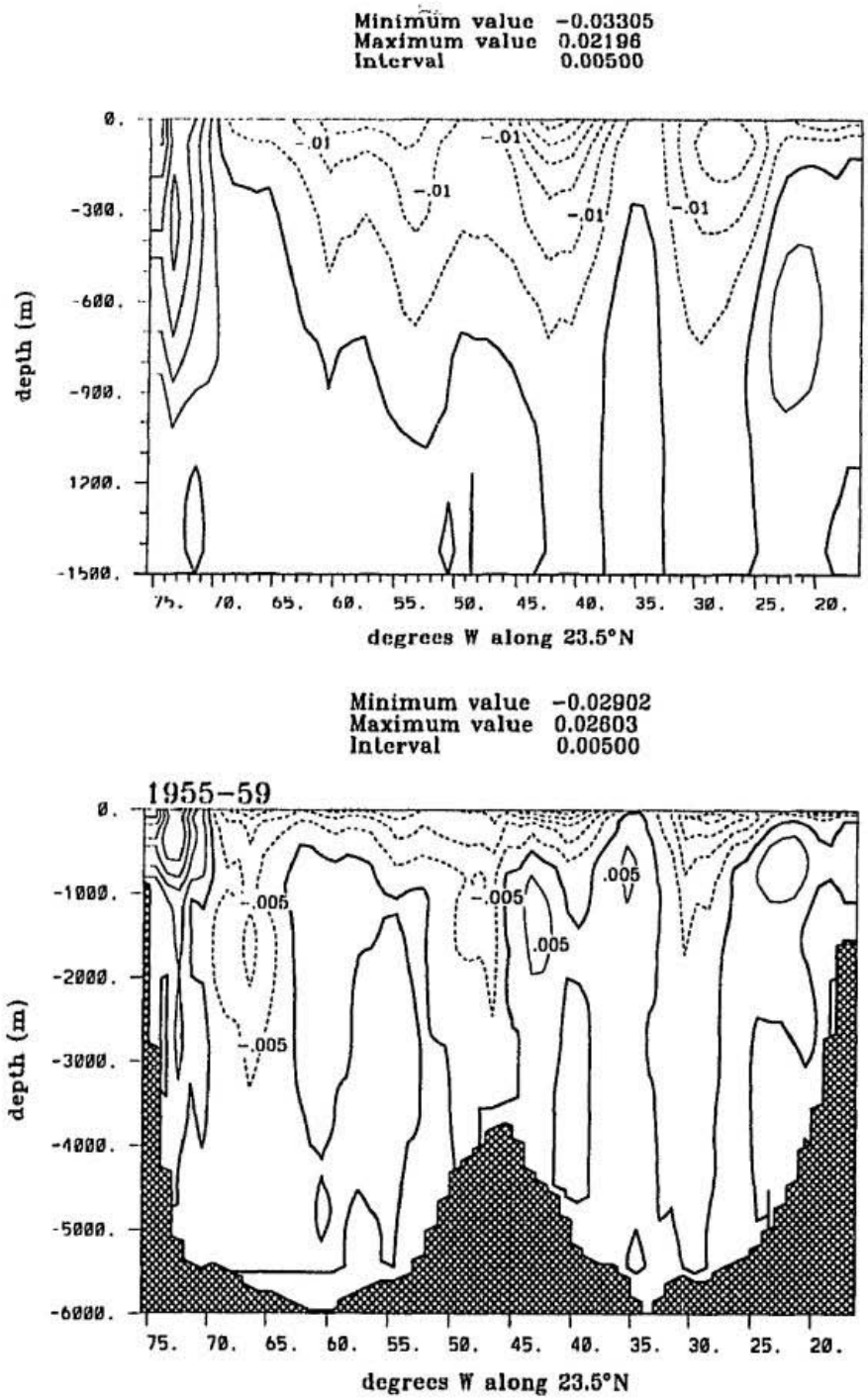

Figure 3.42: *Velocity field using 1955-1959 data. (a) the upper panel, referenced to 1500 m (b) the lower panel, referenced to the bottom. The contour interval is* 0.005 ms^{-1}, *with dashed contours indicating southward velocity and solid contours northward. The minimum and maximum values are given in* ms^{-1}.

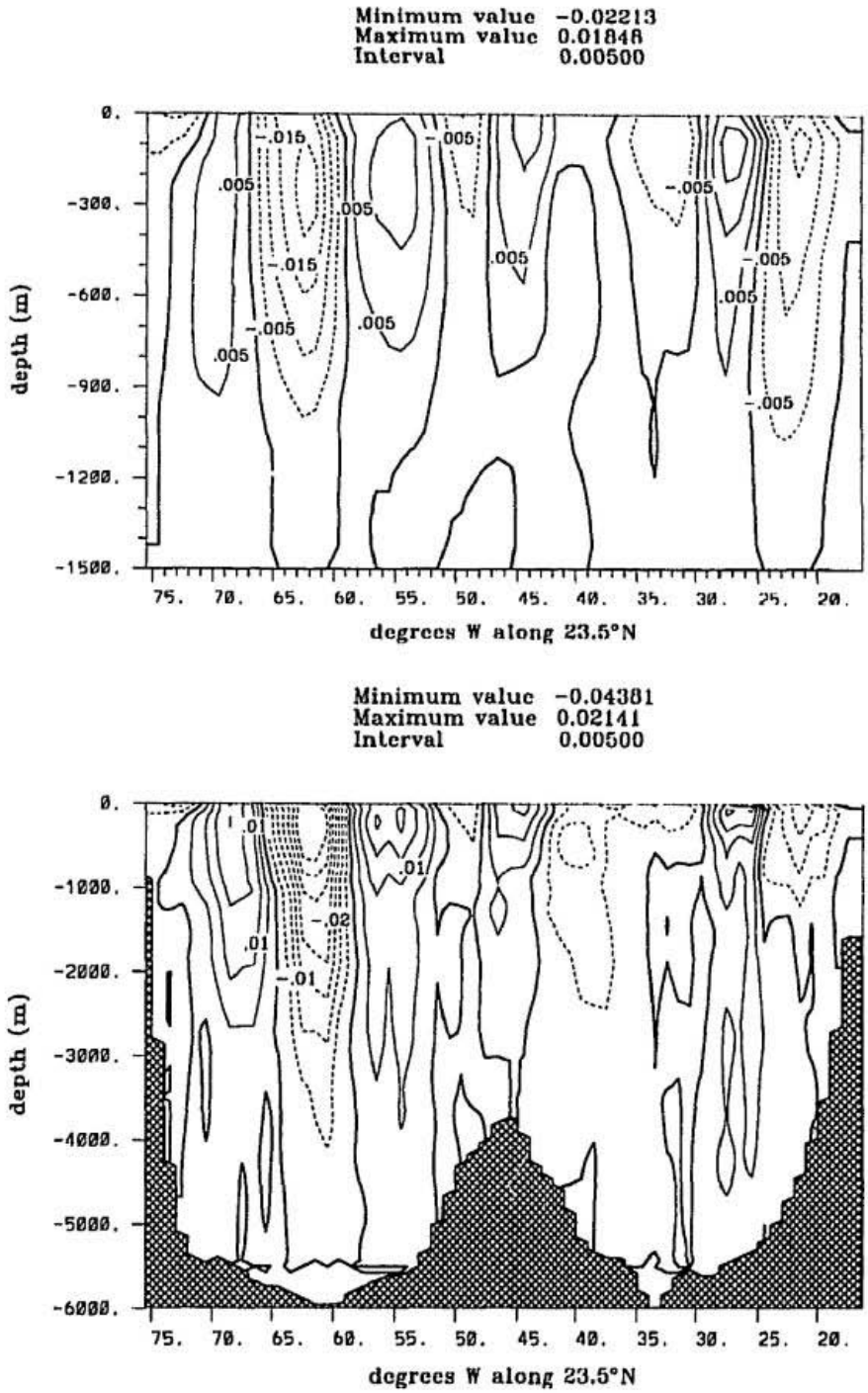

Figure 3.43: *Velocity field difference 1970-1974 minus 1955-1959. (a) the upper panel, referenced to 1500 m (b) the lower panel, referenced to the bottom. The contour interval is* 0.005 ms^{-1}, *with dashed contours indicating southward velocity and solid contours northward. The minimum and maximum values are given in* ms^{-1}.

23.5°N	Climatology	1955-59	1970-74
relative to 1500 m	-12.2	-13.3	-17.3
relative to the bottom	-27.7	-28.2	-31.7
transport due to bottom velocity	-7.8 (-6.8)	-6.1	-3.4
surface Ekman transport	6.0 (5.0)	4.8	5.6
Florida Straits	29.5	29.5	29.5

23.5°N	Climatology	1955-59	1970-74
HT_{1500}	-1.18	-1.29	-1.52
HT_T	-1.51	-1.63	-1.95
HT_B	-0.17 (-0.15)	-0.14	-0.08
HT_{EK}	0.60 (0.50)	0.50	0.55
Florida Straits	2.31	2.31	2.31
TOTAL	1.23 (1.16)	1.04	0.84

Table 3.2: *Volume transport (in Sverdrups) and Heat transport (in petawatts) through 24°N. Positive represents northward and negative, southward. In the climatology case, figures in brackets are calculated using da Silva and Levitus' wind stress.*

the lower panel, referenced to the bottom. West of $50°W$, we see large oscillations in the 1970-74 pentad, with strong southward flow extending down to the bottom being partially balanced by return flows on either side. It is known that this is an area of strongly variable flow, with variations on space scales of hundreds of kilometers (Roemmich and Wunsch, 1985; Schmitz et al. 1992) and on a characteristic time scale of 100 days (Lee et al., 1990). Variability in this region is also a feature of the Kiel version of the WOCE Community Model, as discussed by Böning et al.(1991). Interestingly, this variability does not appear in our annual mean case here. One reason for this may be the smoothing inherent in the Levitus(1982) data set, another the "composite" nature of the data set. This raises a question as to whether the large oscillations in the 1970-74 case are real and, in particular, if they may be the result of inadequate sampling. One further point to note is that all three cases, climatological annual mean, 1955-59 and 1970-74, show an increase in the southward transport below 1500 m starting at about $60°W$ in association with what may be the manifestation of the Deep Western Boundary Undercurrent (DWBU) in the model. It should be noted, however, that this is farther east and is associated with somewhat weaker vertical shear than the DWBU identified by Rosenfeld et al. (1989) and Leaman and Harris(1990) just east of the Bahamas at $26.5°N$.

Figures 3.44, 3.45 and 3.46 exhibit the volume transport during 1970-1974, 1955-1959, and the difference between the two, respectively. The figures show

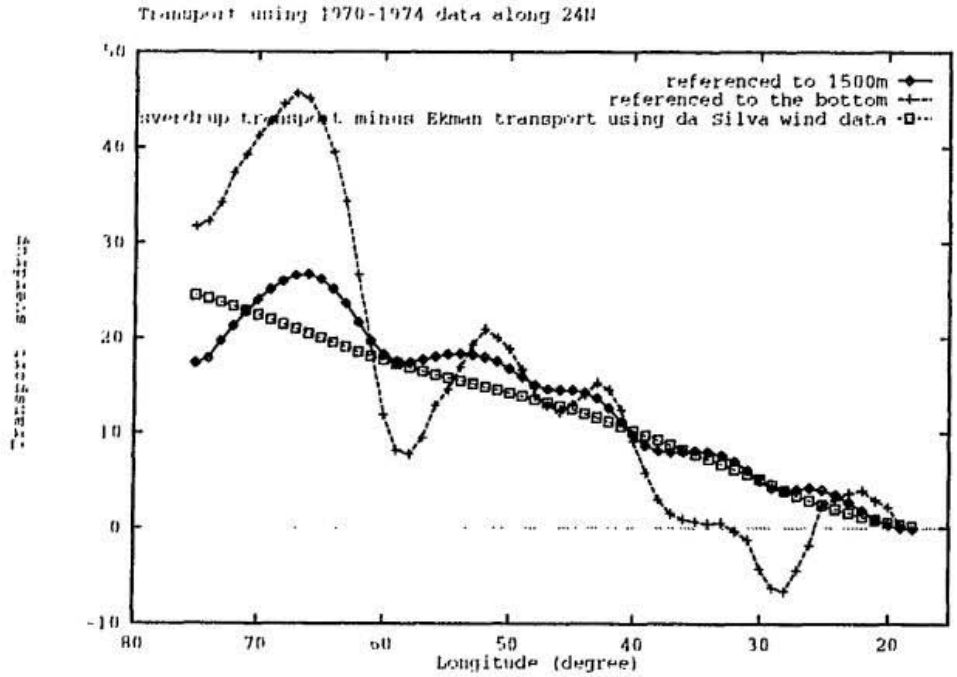

Figure 3.44: *Volume transport using 1970-1974 data*

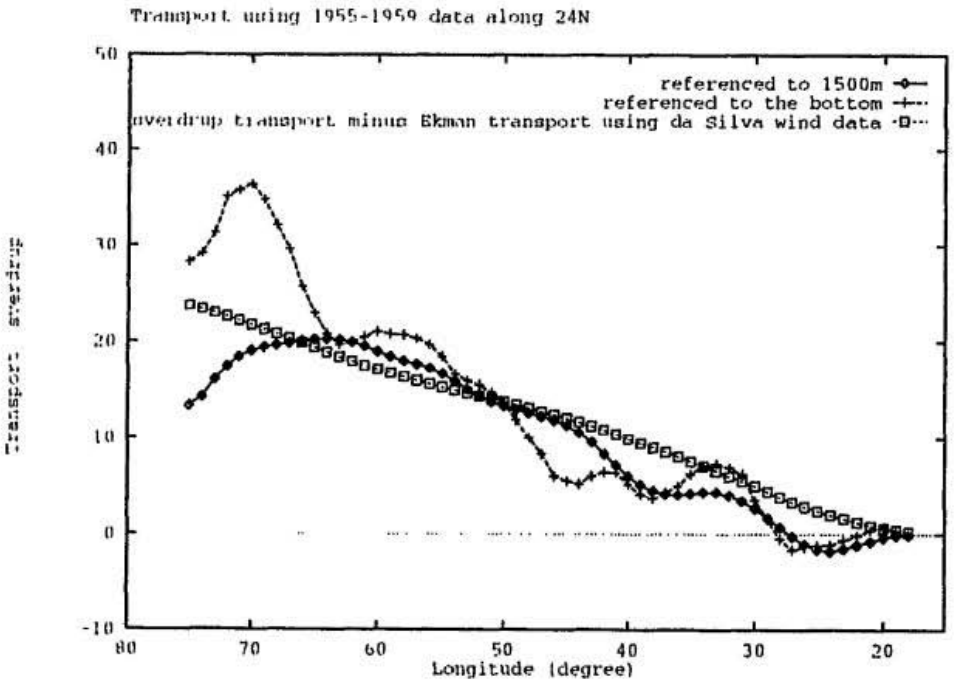

Figure 3.45: *Volume transport using 1955-1959 data*

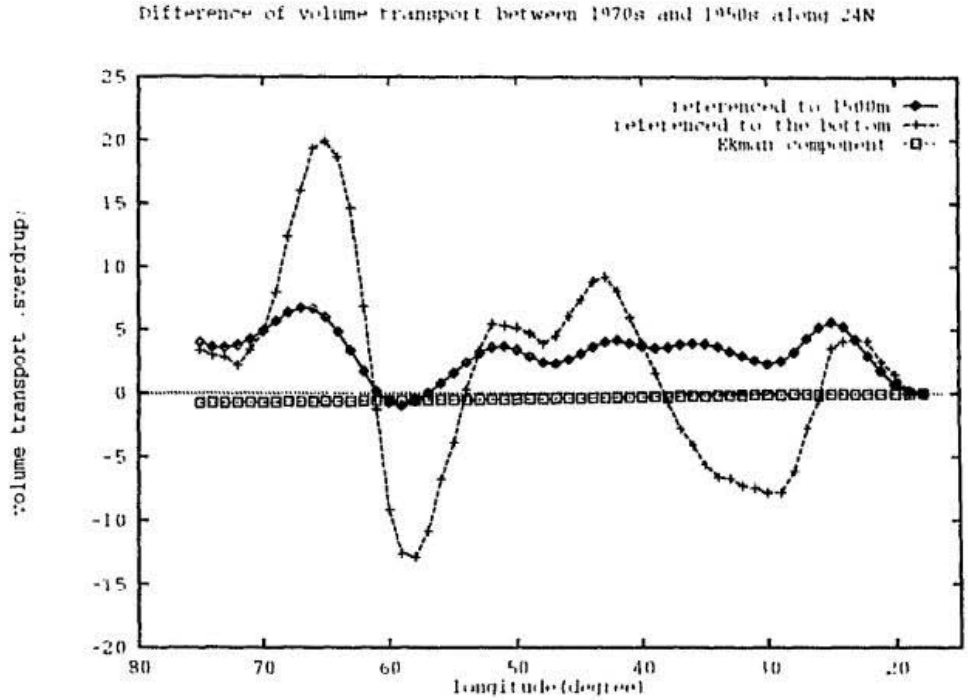

Figure 3.46: *Volume transport difference 1970-1974 minus 1955-1959*

that in the pentads 1955-59 (Fig. 3.45), most of the bottom-referenced transport was confined above 1500m and in 1970-74 (Fig. 3.44) there is a tendency for the flow at and below 1500m to be northward in the region to the east of 60°W. This strongly suggests that in 1970-74, the southward transport below 1500m was considerably reduced in comparison with the climatological annual mean and also in comparison with 1955-59. The mass balance for each of the pentads 1955-59 and 1970-74 is also presented in Table 3.2 (results in the climatological case differ slightly if the climatological annual mean wind stress of da Silva and Levitus is used, as indicated by the figures in brackets. For the two pentads, da Silva and Levitus wind stress data is used). As in the annual mean case, we take the

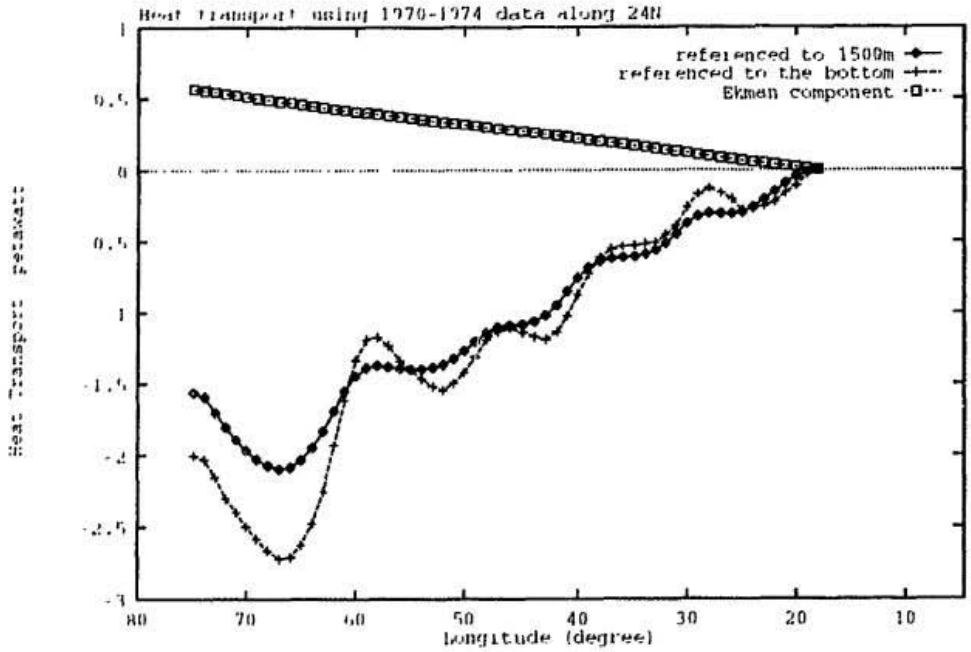

Figure 3.47: *Heat transport using 1970-1974 data*

northward flow through the Florida Straits to be the $29.5Sv$, assuming that the transport of the Florida Current is the same in both pentads and equal to the climatological annual mean transport. This is a major assumption that may not be true. However, we know of no authoritive transport data for the Florida Straits for the pentad 1955-59. Rather, we appeal to Larsen(1992), who noted that cable-derived transport data for the periods 1969-74 and 1981-90 (including 1970-1974) shows no long-term trend. Using $29.5Sv$ as the northward flow through the Florida Straits in both pentads, we see that the bottom transport required to achieve mass balance is only $3Sv$ in 1970-74 compared to $6Sv$ in 1955-59.

Adopting the same approach as used in annual mean case, the heat transport

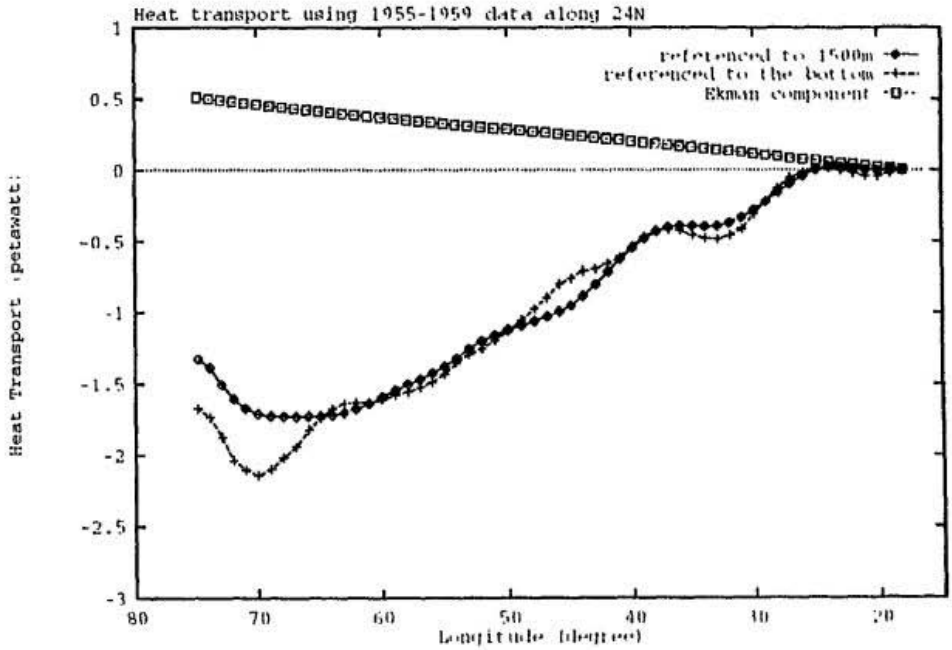

Figure 3.48: *Heat transport using 1955-1959 data*

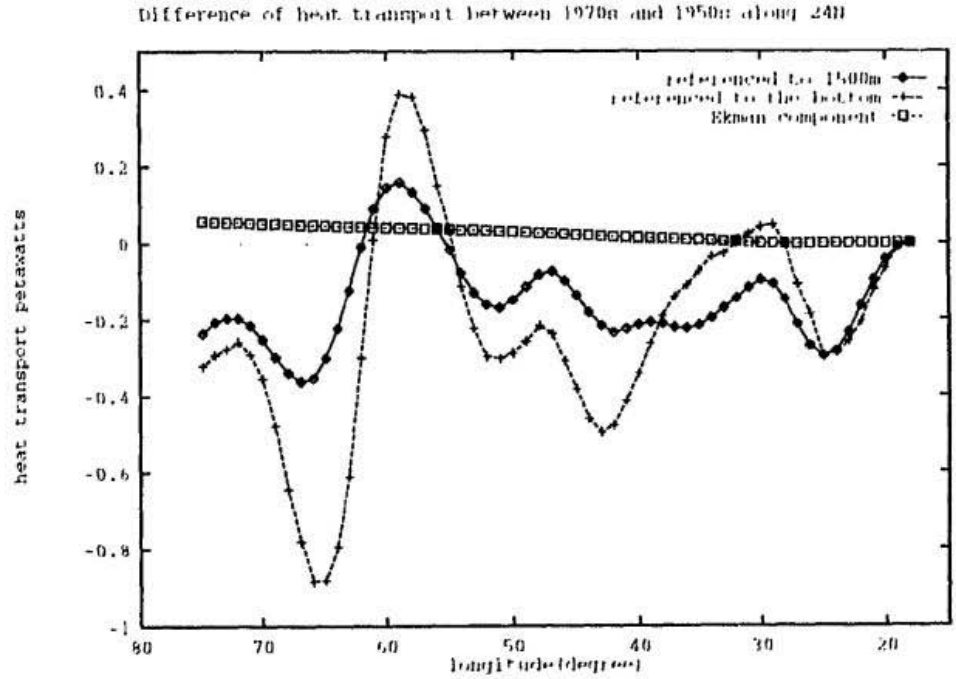

Figure 3.49: *Heat transport difference 1970-1974 minus 1955-1959*

can be calculated in both pentads. For both pentads, we use the same "flow" temperature for the Florida Current as that of the climatological mean. Fig. 3.47, 3.48 and 3.49 show the heat transport during 1970-1974, 1955-1959, and the difference between the two, respectively. Table 3.2 sums up the heat transport. For the 1970-74 pentad we obtain the total poleward heat transport of $0.8PW$ and for the 1955-59 pentad, $1.0PW$, indicating a reduction of $0.2PW$ between the pentads. It is interesting to note that the heat transport in both pentads is smaller compared to that of the climatological annual mean. Tabie 3.2 indicates that the reason for the lower total heat transport in the pentads compared to the climatological annual mean is the greater southward transport associated with HT_T, i.e. the heat transport referenced to the bottom, in each pentad. Comparing 1970-74 with 1955-59, we see that the effect of increased southward HT_T is partially compensated by slightly increased northward Ekman and bottom heat transport, HT_{EK} and HT_B, in 1970-74 compared to 1955-59.

Chapter 4

Summary and Conclusions

In this thesis, the velocity structure of the North Atlantic is evaluated through four sections, two across a line of longitude - 55°W and 65°W, two across a line of latitude - 24°N and 54°N. In order to accomplish this task, we have developed a two-dimensional, vertical-section model to diagnose the velocity structure. Our objective is to understand the velocity structure associated with the circulations (both wind-driven and thermohaline) in the North Atlantic and the interpentadal changes between the 1970-1974 and 1955-1959 pentads. Further, we also calculated the volume transport, poleward heat transport and sea level to investigate the changes between 1970-1974 and 1955-1959.

This density-stratified model is a generalization of the standard geostrophic velocity computation which calculates the velocity field from density input. The model includes the vertical mixing of momentum and parameterises the bottom

stress in terms of bottom velocity in order to show that in a two-dimensional, vertical-section model, it is natural to reference velocities to the bottom as discussed in Chapter 2. By making use of independent estimates of the absolute transport and estimates of the Ekman transport from wind stress data, information can be obtained on the transport due to non-zero bottom velocities. This enables us to analyse the volume transport, heat transport and sea level across the sections.

The results along $55.5^{o}W$ show that referenced to the bottom, the eastward transport of the calculated Gulf Stream was some $30Sv$ less in 1970-74 than in 1955-59, in general agreement with the results of Greatbatch et al.(1991). However, the maximum transport reduction referenced to the bottom is shifted from that obtained by Greatbatch et al.(1991), indicating the importance of changes in bottom velocity in the latter calculations. This is shown to be the case even if the density is assumed to be the same in each pentad below 1500m.

The results along $64.5^{o}W$ show that the calculated transport of the Gulf Stream also underwent dramatic changes between 1970-74 and 1955-59 pentads. It is also suggested that the steric sea level during 1970-74 increases by about 2 dyn cm right up to the coast of Nova Scotia, but decreases about 6 dyn cm at Bermuda, compared to 1955-1959.

The calculations of poleward heat transport across $54.5^{o}N$ and $23.5^{o}N$ for each of the climatological annual mean, 1955-59 and 1970-74 cases are also attempted.

As discussed in the introduction, a change in the poleward heat transport from the 1955-59 to 1970-74 pentads would be especially interesting because of the important role played by the poleward transport of heat in maintaining the equilibrium of the earth's climate system (see Bryan, 1982 and Weaver and Hughes, 1992). Rintoul and Wunsch(1991) have noted that heat transport calculations carried out using smoothed data (such as Levitus, 1982;1989a,b,c) can be in error due to the inadequate representation of the western boundary currents. Indeed, we have noted that the DWBU (deep western boundary undercurrent) at both $23.5^{o}N$ and $54.5^{o}N$ may not be adequately represented in our data sets. On the other hand, Molinari et al.(1990) made use of Levitus(1982) data in the region east of the Bahamas in order to estimate the annual cycle of heat transport at $26.5^{o}N$. Their annual mean northward heat transport across $26.5^{o}N$ is $1.2PW$ and is the same as found by other investigators at this latitude (Hall and Bryden,1982, and Roemmich and Wunsch, 1985). They also found that including data from Rosenfeld et al.(1989) for the region immediately to the east of the Bahamas, which included a better represention of the DWBU, did not have a significant influence on the calculation. This gives us confidence that our calculations are meaningful.

Calculations of the poleward heat transport through $54.5^{o}N$ indicate values of $0.6PW$, $0.7PW$ and $0.5PW$ for the climatological annual mean case and the pentads 1955-59 and 1970-74, respectively. The climatological value is in agreement

with previous estimates based on surface heat balance calculations (Hastenrath, 1980; Bunker, 1976). However, given that we estimate the error to be $\pm 0.2PW$ it is not clear how significant is the difference between the pentads. However, there is the suggestion, at least, that the poleward heat transport was marginally less in 1970-74 than in 1955-59 and this is attributed to a combination of a deeper (and therefore colder) North Atlantic Current in 1970-74 compared to 1955-59 and a warmer return flow in the Labrador Sea in the later pentad.

Along $23.5°N$, the calculated poleward heat transports are $1.2PW$, $1.0PW$ and $0.8PW$ for the climatological annual mean, 1955-59 and 1970-74, respectively. In the climatological annual mean case, a similar value is obtained if the wind stress field of da Silva and Levitus is used instead of Hellerman and Rosenstein(1983). The climatological value agrees with previous estimates (Hall and Bryden, 1982; Roemmich and Wunsch, 1985; Molinari et al., 1990). Between the 1970-74 and 1955-59 pentads, the model results suggested a reduction of $0.2PW$. It is not clear exactly how significant this difference is. Hall and Bryden(1982) and Molinari et al. (1990) indicate that the error in their calculations is $\pm 0.3PW$. Given the similarity of the methods used, this is probably a good measure of the error in our calculation too. This suggests that the difference of $0.4PW$ between the 1970-74 case and the climatological annual mean may be significant. Our calculation does have the additional assumption, however, that the volume transport and the "flow" temperature of the Florida Current are the

same for each calculation. We have already noted, however, that Larsen(1992)'s data provides support for this assumption in the case of the volume transport. To assess the assumption of a constant"flow" temperature, we note that to achieve an increase in the northward heat transport through the Straits of $0.4PW$ (and thereby cancel out the $0.4PW$ reduction) would require an increase in the flow temperature to $22.4°C$, an increase for which there is no precedent in the available data. We may tentatively conclude that the poleward heat transport through $24°N$ in 1970-1974 appears to be less than the climatological mean value.

We are not aware of previous work that has diagnosed an interannual change in the poleward heat transport of the ocean. Roemmich and Wunsch(1985) compared the International Geophysical Year (1957) section along $24°N$ with a section made in 1981 and could find no difference in the calculated poleward heat transport for the two sections. If the differences in heat transport we have calculated are real, then they are quite exciting. Experiments using idealised basin geometry and surface forcing with the Bryan/Cox Ocean General Circulation Model have already raised the possibility that the thermohaline circulation in the ocean could exhibit decadal-time-scale variability (Weaver and Sarachik, 1991) and such variations would be expected to be associated with changes in the poleward heat transport. Such variations could, in turn, have an effect on the atmosphere and be part of the natural variability of the coupled ocean-atmosphere system, as suggested by Bjerknes (1964).

REFERENCES

Bjerknes, J., 1964: Atlantic Air-Sea Interaction. *Adbv. Geophys.*, 10, 1-82.

———, H. Solberg and T. Bergeron 1933: Physikalische hydrodynamik. *Julius Springer*, Berlin.

Böning, C.W., R. Döscher and R.G. Budich, 1991: Seasonal transport variation in the western subtropical North Atlantic: Experiments with an eddy-resolving model. *J.Phys.Oceanogr.*, 21(9), 1271-1289.

Bryan, K., 1962: Measurements of meridional heat transport by ocean currents. J. Geophys. Res., 67(9), 3403-3414.

———, 1969: A numerical method for the study of the circulation of the world ocean. *J. Comput. Phys.*, 4, 347-376.

———, 1982: Poleward heat transport by the ocean: Observations and Models. *Ann. Rev. Earth Planet Sci.* 10: 15-38.

———, 1986: Poleward buoyancy transport in the ocean and mesoscale eddies. *J.Phys.Oceanogr.*, 16, 927-933.

Bryden, H.L., 1973: New polynomials for thermal expansion, adiabatic temperature gradient and potential temperature gradient of sea water. *Deep Sea Res.*, 20, 401-408.

———, D.H. Roemmich and J.A. Church, 1991: Ocean heat transport across $24°N$ in the Pacific. *Deep Sea Res.*, 38(3), 297-324.

Bunker, A.F., 1976: Computations of surface energy flux and annual air-sea interaction cycles of the North Atlantic Ocean.

Mon. Wea. Rev., 104, 1122-1140.

Cardone, V.J., J.G.Greenwood and M.Cane, 1990: On trends in historical marine wind data. *J. Climate*, 3, 113-127.

Cox, M.D., 1984: A primitive equation, 3-dimensional model of the ocean.

GFDL Ocean Group Technical Report No. 1,

GFDL/Princeton University,

Csanady, G. T., 1979: The pressure field along the western margin of the North Atlantic. *J. Geophys. Res.*, 84(C8), 4905-4915.

————, 1982: Circulation in the coastal ocean. Reidel, Holland, 279 pp.

Fanning, A.F., R.J. Greatbatch, A.M. da Silva and S. Levitus, 1992: Model-calculated seasonal transport variations through the Florida Straits: a comparison using different wind stress climatologies. To be submitted to *J. Phys. Oceanogr.*

Fuglister, F. C., 1963: Gulf Stream '60. *Prog. in Oceanogr.*, 1, 265-383.

Ghil, M. and R. Vautard, 1991: Interdecadal oscillations and the warming trend in global temperature time series. *Nature*, 350, 324-327.

Gill, A.E., 1982: Atmosphere-ocean dynamics. *Academic Press, 662 pp.*

Gordon, A. L., 1986: Interocean exchange of thermocline water.

J. Geophys. Res., 91(C4), 5037-5046.

Gordon, A. L., S. E. Zebiak, and K. Bryan, 1992: Climate variability and the Atlantic Ocean. *EOS, Trans. Amer. Geophys. Union*, Vol.73, No. 15: 161-164.

Greatbatch, R.J., A.F. Fanning, A.G. Goulding and S. Levitus, 1991: A diagnosis of interpentadal circulation changes in the North Atlantic. *J. Geophys. Res.*, 96(C12), 22009-22023.

———, and A. Goulding, 1992: A long-time-scale, density-stratified shelf circulation model. *Cont. Shelf Res.*, Vol.12, No. 1, 115-141.

Hall, M.M., and H.L. Bryden, 1982: Direct estimates and mechanisms of ocean heat transport. *J. Mar. Res.*, 29, 339-359.

Hastenrath, S., 1980: Heat budget of tropical ocean and atmosphere. *J. Phys. Oceanogr.*, 10(2), 159-170.

Helland-Hansen, B., 1934: The Sognefjord section : oceanographic observations in the northernmost part of the North Sea and the southern part of the Norwegian Sea. *James Johnstone Memorial Volume*, Proudman Oceanographic Lab., Bidston Observatory, Birkenhead, U.K..

Hellerman, S., and M. Rosenstein, 1983: Normal monthly wind stress over the world ocean with error estimates. *J. Phys. Oceanogr.*, 13, 1093-1104.

Hogg, N.G., R.S. Pickart, R.M. Hendry and W.J. Smethie, Jr., 1986:

The northern recirculation gyre of the Gulf Stream.

Deep Sea Res., 33(9), 1139-1165.

Holland, W.R., 1973: Baroclinic and topographic influences on the transport in western boundary currents. *Geophys. Fluid Dyn.*, 4, 187-210.

Kaufeld, L., The development of a new Beaufort equivalent scale.

Meteor. Rundsch., 34, 17-23.

Knauss, J. A., 1969: A note on the transport of the Gulf Stream.

Deep-Sea Res., 16, 117-123.

Larsen, J.C., 1992: Transport and heat flux of the Florida Current at 27°N derived from cross-stream voltages and profiling data: theory and observations. *Phil. Trans. R. Soc. Lond. A*, 338, 169-236.

Lazier, J.N. and D.G. Wright, 1992: Annual velocity variations in the Labrador Current. *J. Phys. Oceanogr.*, in press.

Leaman, K.D. and J.E. Harris, 1990: On the average absolute transport of the deep western boundary currents east of Abaco Island, the Bahamas. *J. Phys. Oceanogr.*, 20(3), 467-475.

Lee, T.N., W. Johns, F. Schott and R. Zantopp, 1990: Western boundary current structure and variability east of Abaco, Bahamas at 26.5°N. *J. Phys. Oceanogr.*, 20(3), 446-466.

Leetmaa, A., P. Niiler and H. Stommel, 1977: Does the Sverdrup Relation account for the Mid-Atlantic circulation ? *J. Mar. Res.*, 35, 1-10.

Levitus, S., 1982: Climatological Atlas of the World Ocean. *NOAA Prof.Pap.*, 13, Natl. Oceanic and Atmos. Admin., Washington D.C.

———, 1989a: Interpentadal variability of temperature and salinity at intermediate depths of the North Atlantic Ocean, 1970-1974 versus 1955-1959. *J. Geophys. Res.*, 94(C5), 6091-6131.

———, 1989b: Interpentadal variability of salinity in the upper 150m of the North Atlantic Ocean, 1970-1974 versus 1955-1959. *J. Geophys. Res.*, 94(C7), 9679-9685.

———, 1989c: Interpentadal variability of temperature and salinity in the deep North Atlantic, 1970-1974 versus 1955-1959. *J. Geophys. Res.*, 94(C11), 16125-16131.

———, 1990: Interpentadal variability of steric sea level and geopotential thickness of the North Atlantic Ocean, 1970-1974 versus 1955-1959. *J. Geophys. Res.*, 95(C4), 5233-5238.

Lynch, D. R., F. E. Werner, D. A. Greenberg and J. W. Loder, 1992: Diagnostic model for baroclinic, wind-driven and tidal circulation in shallow seas. *Cont. Shelf Res.*, Vol.12, No. 1.

Mellor, G.L., C.R. Mechoso and E. Keto, 1982: A diagnostic model of the general circulation of the Atlantic Ocean. *Deep-Sea Res.*, 29, 1171-1192.

Molinari, R.L., E. Johns and J.F. Festa, 1990: The annual cycle of meridional

heat flux in the Atlantic Ocean at $26.5^{o}N$.

J. Phys. Oceanogr., 20(3), 476-482.

Montgomery R. B., 1974: Comments on "seasonal variability of the Florida Current", by Niiler and Richardson. *J. Mar. Res.*, 32, 533-535.

Munk, W. H., 1950: On the wind-driven ocean circulation.

J. Meteor., 7, 79-93.

Niiler, P.P., and W.S. Richardson, 1973: Seasonal variability of the Florida Current. *J. Mar. Res.*, 31, 144-167.

Olbers, D. J., et al. 1985: The inference of North Atlantic circulation patterns from climatological hydrographic data.

Rev. of Geophysics 23(4), 313-356

Oort, A. H. and Vonder Haar, T.H. 1976: On thr observed annual mean cycle in the ocean-atmosphere haet balance over the northern hemisphere. *J. Phys. Oceanogr.*, 6(6), 781-800

Richardson, P.L., 1985: Average velocity and transport of the Gulf Stream near $55^{0}W$. *J. Mar. Res.*, 43, 83-111.

Rintoul, S.R., and C. Wunsch, 1991: Mass, heat, oxygen and nutrient fluxes and budgets in the North Atlantic Ocean.

Deep Sea Res., 38(suppl.), S355-S377.

Robinson, A. R., et al. 1974: Transient Gulf Stream meandering. Part I: An observational experiment. *J. Phys. Oceanogr.*, 4, 237-255.

Roemmich, D., 1985: Sea level and the variability of the ocean, Glaciers, Ice Sheets, and Sea Level: Effect of a CO_2-induced climatic change. *Rep. DOE/ER/G0235-1*, 104-115, Dep. of Energy, Wash.

Roemmich, D., and C. Wunsch, 1985: Two transatlantic sections: meridional circulation and heat flux in the subtropical North Atlantic Ocean. *Deep Sea Res.*, 32(6), 619-664.

Rosenfeld, L., R.L. Molinari and K.D.Leaman, 1990: Observed and modelled annual cycle of transport in the Straits of Florida and east of Abaco Island, the Bahamas. *J. Geophys. Res.*, 94, 4867-4878.

Schmitz, W.J., 1980: Weakly depth-dependent segments of the North Atlantic circulation. *J. Mar. Res.*, 38, 111-133.

————, J.D. Thompson and J.R. Luyten, 1992: The Sverdrup circulation for the Atlantic along $24^{o}N$. *J. Geophys. Res.*, 97(C5), 7251-7256.

da Silva, A.M., 1991: Estimates of monthly mean wind stress from monthly mean pseudo-stress, winds and wind standard deviations. Dept. of Geophysics, University of Wisconsin, Milwaukee, USA.

----------, C.C. Young and S. Levitus, 1992: The sensitivity of climatological wind statistics on scientific Beaufort scales. Submitted to *J. Climate*.

Stommel, H, 1965: The Gulf Stream. *University of California Press*

————, 1948: The westward intensification of wind-driven ocean currents.

Trans. Amer. Geophys. Union, 29: 202-206

Sverdrup, H. U. et al., 1942: The oceans: their physics, chemistry and general biology. *New York: Prentice-Hall.*

Sverdrup, H. U., 1947: Wind-driven currents in a baroclinic ocean; with application to the bequatorial currents of the eastern Pacific. *Proc. Nat. Acad. Sci. Wash.*, 33, 318-326.

Vonder Harr, T.H., Oort, A. H. 1973: New estimate of annual poleward energy transport by northern hemisphere oceans. *J. Phys. Oceanogr.*, 3(2): 169-172.

Weaver, A.J., and E.S. Sarachik, 1991: Evidence for decadal variability in an ocean general circulation model: an advective mechanism. *Atmosphere-Ocean*, 29(2), 197-231.

————, and T.M.C. Hughes, 1992: Stability and variability of the thermohaline circulation and its link to climate. Centre for Climate and Global Change Research, Report #92 – 5, McGill University, Montreal, Quebec, Canada.

Worthington, L.V., 1976: On the North Atlantic Circulation. John Hopkins Univ. Press, Baltimore, MD, USA, 110 pp.

————, 1977: The intensification of the Gulf Stream after the winter of 1976-77. *Nature*, 270, 415-417.